Title
Discoveries in Human Biology Through Kinase Signaling

Author
Moss, Steven Michael

Publication Date
2019

Peer reviewed|Thesis/dissertation

Discoveries in Human Biology Through Kinase Signaling

by
Steven Michael Moss

DISSERTATION
Submitted in partial satisfaction of the requirements for degree of
DOCTOR OF PHILOSOPHY

in

Chemistry and Chemical Biology

in the

GRADUATE DIVISION
of the
UNIVERSITY OF CALIFORNIA, SAN FRANCISCO

Approved:

DocuSigned by:
Kevan Shokat
8FDF47C586EF40D...

Kevan Shokat
Chair

DocuSigned by:
Shaeri Mukherjee
DocuSigned by:
Jason Gestwicki
4909848DBB404E5...

Shaeri Mukherjee

Jason Gestwicki

Committee Members

Acknowledgements

This work would not have been possible without the support and mentorship from both Dr. Kevan Shokat and Dr. Shaeri Mukherjee. Both were instrumental in moving the project forward and helping me develop my own scientific ideas. I am very appreciative of the scientific help I received from Dr. Jason Gestwicki and Dr. Davide Ruggero, in addition to the people in their labs, particularly Dr. Isabelle Taylor from the Gestwicki lab, and Dr. Crystal Conn from the Ruggero lab. All of the members of the Shokat lab have helped move my project forward, and I am particularly grateful for the mentorship and guidance I received from Dr. Rebecca Levin and Dr. Daniel Gentile. I am equally grateful to the members of the Mukherjee lab as they helped me to navigate the unfamiliar worlds of microbiology and cell biology. I frequently received both scientific and emotional support from the other members of the 2014 UCSF Chemistry and Chemical Biology graduate class, as well as from members of the 2014 Biophysics class, which helped me to thrive during the most trying times of my research. A special thank you to my various communities of friends outside of the lab, particularly my friends who supported me from Washington, DC. I could not have completed my PhD without the encouragement and support of Mona Thompson, my partner and best friend. Finally, I want to thank my parents and sister who have been unwavering in their support of everything I do, and encouraged me to pursue my passions.

Contributions:

Chapter 2 is reproduced in part from:

Meyer, N.O., O'Donoghue, A.J., Schulze-Gahmen, U., Ravalin, M., Moss, S.M., Winter, M.B., Knudsen, G.M., Craik, C.S. "Multiplex Substrate Profiling by Mass Spectrometry for Kinases as a Method for Revealing Quantitative Substrate Motifs", *Anal Chem*, 2017, 89: 4550-4558.

Chapter 3 is reproduced in part from:

Moss, S.M., Taylor, I.R., Ruggero, D., Gestwicki, J.E., Shokat, K.M., Mukherjee, S. "A *Legionella pneumophila* Kinase Phosphorylates the Hsp70 Chaperone Family to Inhibit Eukaryotic Protein Synthesis", *Cell Host & Microbe*, 2019, 25: 454-462.

Chapter 4 is reproduced in part from:

Coles, G.L., Cristea, S., Webber, J.T., Levin, R.S., Moss, S.M., Sangodkar, J., Hwang, Y.H., Arand, J., Drainas, A.P., Spradlin, J.N., Mauch, B., Le, V., Kong, C., Nomura, D.K., Ohlmeyer, M., Swaney, D.L., Narla, G., Gordan, J.D., Shokat, K.M., Sage, J. "Unbiased Proteomic Profiling Uncovers a Targetable PKA/PP2A Axis in Neuroendocrine Lung Cancer", *In Review*.

Discoveries in Human Biology Through Kinase Signaling

By

Steven M. Moss

Abstract

Kinases are signaling proteins that are involved in many different cellular processes. There are over 500 different kinases to accomplish these various tasks. Abnormal kinase signaling can lead to severe disease outcomes. Studying these disruptions have led to fundamental discoveries about human and cellular biology. **Chapter 1** introduces a number of cases in both cancer and infectious disease where kinase signaling is disrupted. The subsequent studies used to elucidate why these disruptions occur have helped advance our current knowledge of human biology. In **Chapter 2** I describe about some of our studies with eukaryotic-like ser/thr protein kinases used as effector proteins by the bacteria *Legionella pneumophila*, the causative agent of Legionnaires' disease. This chapter explores *in vitro* and *in vivo* assays to characterize four of the known and conserved effector kinases from *Legionella*. **Chapter 3** takes a comprehensive look at *Legionella* kinase 4 (LegK4), one of the effector kinases that showed an interesting Golgi fragmentation phenotype. We discovered that LegK4 targets host Hsp70, reduced the chaperone's refolding activity, and subsequently reduced global translation of the host cell. Further work showed that phosphorylation of Hsp70 by LegK4 increases the amount of the chaperone present on highly translating polysomes. **Chapter 4** reviews the available kinase substrate identification techniques, and explain how we used one of them to explore substrates of Protein Kinase A (PKA) in cell lines of small cell lung cancer. While many substrates were found, a general theme emerged where a number

of the direct targets of PKA were involved in cell cycle and cell proliferation. Follow-up experiments performed by our collaborators showed that these results align well with a global phosphoproteomic analysis carried out for PKA in a small cell lung cancer setting. All of these examples show kinase signaling that helped to inform us about new human biology.

Table of Contents

Chapter 1 – Introduction: Studying kinases to advance human biology……1

Chapter 2 – Characterization of the eukaryotic-like effector kinases in *Legionella pneumophila*……13

Chapter 3 - A *Legionella pneumophila* Kinase Phosphorylates the Hsp70 Chaperone Family to Inhibit Eukaryotic Protein Synthesis……..…….27

Chapter 4 – Substrate Targets of PKA in Neuroendocrine Lung Cancer…….79

Appendix 1 – Substrates of PKA identified by covalent capture……..……94

List of Figures

Figure 1.1 – *Legionella pneumophila* life cycle within a human cell……..….4

Figure 2.1 – Genetic and structural analysis of *legk* genes……..…….16

Figure 2.2 – Phosphorylation activity of LegK2……19

Figure 2.3 – Example of phenotypic characterization of LegK proteins using immunofluorescence……..…20

Figure 2.4 – Multiplex substrate profiling mass spectrometry results for LegK1…….…22

Figure 3.1 – LegK4 causes Golgi fragmentation and inhibits yeast growth…….33

Figure 3.2 – Establishing specificity of LegK4 phosphorylation…….35

Figure 3.3 – Identification of Hsp70 as the substrate of LegK4…….37

Figure 3.4 – Identification and characterization of LegK4 phosphosite……39

Figure 3.5 – Phosphorylation of Hsp70 by LegK4 decreases activity and causes a reduction in global protein translation…….43

Figure 3.6 – JG-98 recapitulates results observed with LegK4…….47

Figure 3.7 – Characterization of LegK4 behavior during infection……49

Figure 3.8 – Interactions of phosphorylated Hsc70 with the ribosome…….51

Figure 3.9 – Diagram of LegK4 interactions in the host cell……..……53

Figure 4.1 – Methods of kinase substrate discovery using thiophosphorylation…….82

Figure 4.2 – Recombinant AS PKA phosphorylates lysates selectively……...85

Figure 4.3 – Analysis of PKA substrates from covalent capture screen……..……86

List of Tables

Table 2.1 – Results of phenotypic kinase analysis using Immunofluorescence……..21

Table 2.2 – Summary of information and experimentation on *L.p.* effector kinases…...24

Chapter 1

Introduction: Studying kinases to advance human biology

Kinases, and the chemical signaling that they accomplish through phosphorylation, are essential to many different processes in the human cell. The human genome encodes over 500 different protein kinases, many involved in diverse functions and pathways (1, 2). In contrast to their diversity, the protein structures of mammalian kinases are very similar, each with eleven defined structural components that constitute the canonical kinase fold (3). Despite the diversity of substrate targets, similarities in kinase structure makes kinase biology a challenging field. While many tools have been developed to circumvent this problem, including but not limited to, chemical tools (4, 5), protein engineering, and genetic knockouts, one of the best ways to glean information about human biology, is to use these tools in a context where normal signaling is disrupted, such as disease.

Many diseases are caused, or their physiological effects are enhanced, when the homeostasis of phosphorylation is disrupted. Cancer is a prominent example, as cancers are driven by activating mutations in kinases or the loss of tumor suppressive phosphatases (6). Disease and dysregulation of kinases help to highlight important biology that might be causing the disease. For example, the kinase BCR-Abl is a fusion of the tyrosine kinase Abl, and the *bcr* gene (7). The BCR-Abl protein is created by an abnormal translocation of chromosomes 9 and 22 (8). The fusion protein causes the kinase to be constitutively active and leads to uncontrolled cellular proliferation, and

eventually cancer (9, 10). This translocation was discovered when Nowell and Hungerford were studying the chromosomes of patients with Chronic Myeloid Leukemia (CML) (11), and noticed an abnormally small chromosome (named the Philadelphia chromosome) present in many patient samples (12). When the fusion gene product of BCR-Abl was discovered to be the cancer driver, it led researchers to elucidate the role of the tyrosine kinase Abl as a cellular proliferation checkpoint (13, 14). This is a case of kinase-driven biology revealing both genetic and biochemical information about the human cell.

Another kinase that has revealed important insights into human biology is v-Src. This kinase is one of four genes expressed by the Rous Sarcoma Virus (RSV), which causes cancer in chickens. The genes of RSV were dubbed “oncogenes,” due to their ability to cause cancer (15), and later, v-Src was found to be the specific cancer driver from RSV (16, 17). Characterization of this protein led to the discovery that it was a kinase (18), and further studies showed that the kinase was phosphorylating tyrosine residues, not serines or threonines as previously thought (19, 20). This was the first discovery of a kinase that phosphorylated tyrosine instead of serine or threonine. Further work showed a family of tyrosine kinases present in the human genome that are critical for a number of cellular processes including cellular proliferation (21). One member of this tyrosine kinase family includes a homologous gene to v-Src, first discovered in chickens as c-Src (22). This homologous kinase has lower kinase activity, and was termed a “proto-oncogene,” as a precursor to the more active viral version of the protein (22). This viral kinase helped researchers better understand mechanisms of

cancer pathogenicity, and has led to the discovery of a new and prevalent class of signaling molecule.

Similar to v-Src, kinases that are used by infectious diseases to help with host infection and pathogenicity have also helped teach us about human biology. Canonically, prokaryotes use histidine kinases as their predominant signaling molecules (23, 24). In addition to these histidine kinases, a number of intracellular bacterial pathogens have adopted eukaryotic-like ser-thr protein kinases (eSTPKs) as effector proteins that enhance the microbe's ability to survive in the host cell (25, 26). These eSTPKs have evolved to phosphorylate host proteins and tend to modify functionally important domains on host target protein (25, 27).

One such example is the eSTPK from various *Yersinia* bacteria called *Yersinia* protein kinase A (YpkA) (28). While YpkA performs a number of tasks, it importantly phosphorylates and deactivates $G\alpha_q$ by modifying the binding loop of the protein (29, 30). This PTM prevents RhoA mediated cellular processes such as phagocytosis by decreasing the GTPase's affinity for GTP. The kinase YpkA highlighted method of pathogenic phosphorylation and host substrate deactivation. In addition to the phosphorylation activity of YpkA, the kinase has a unique regulatory mechanism. In order to prevent phosphorylation of bacterial proteins, the kinase is autoinhibited until it binds to eukaryotic monomeric actin. This prevents off target phosphorylation prior to translocation, and reveals an interesting host recognition mechanism.

In addition to YpkA, there are a number of other eSTPKs that have been found in bacteria, however, only a small number of these are effector proteins. Effector proteins found in pathogenic bacteria are unique because they are evolved to serve a specific

and robust purpose upon infection. In identifying the target substrates of these proteins, such as $G\alpha_q$ for YpkA, researchers can learn about host-pathogen interactions in addition to general host biology (27).

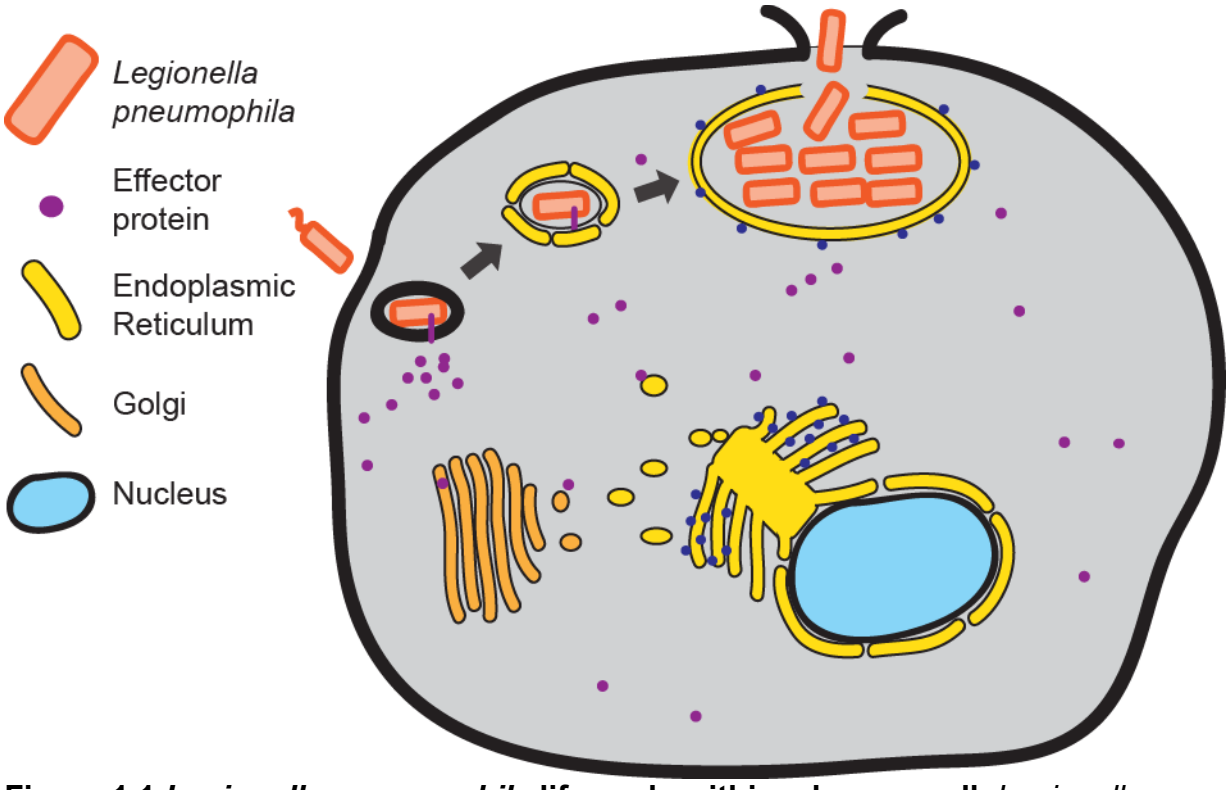

Figure 1.1 *Legionella pneumophila* life cycle within a human cell. *Legionella* uses over 300 different effector proteins to hijack various host processes so that the bacteria can survive and replicate. This figure show how the LCV uses host ER membrane to disguise itself and avoid destruction through the lysosome/endosome pathways.

A major focus of my thesis research has been using bacterial kinases to further understand cellular signaling in human biology. In order to accomplish this, I focused on *Legionella pneumophila* (*L.p.*), the causative agent of Legionnaires' disease. *Legionella* is a unique pathogen because it uses a large arsenal of 300 different effector proteins when infecting a cell (31). These effector proteins accomplish a number of different tasks, all toward the purpose of helping *L.p.* disguise itself from the host so that it can

survive and replicate (**Figure 1.1**). Many of the effectors hijack host processes such as innate immunity, autophagy, and vesicle transport, in order to accomplish this (32-34). One recurring theme amongst *L.p.* effectors, is that many of them use post-translational modifications (PTMs) of host proteins to accomplish a specific task upon infection (32). Furthermore, these PTMs are sometimes unique, and have revealed interesting human biology. For example, the effector protein AnkX performs a novel PTM known as a phosphocholination (35). Using CDP-choline as a substrate, AnkX modifies Rab1, a GTPase crucial in vesicle transport between the ER and the Golgi (35). The phosphocholination is performed by a Fic domain in AnkX. When the function of AnkX was discovered, Fic domains were thought to be involved in adenylylation modifications (addition of AMP), but following the discovery of phosphocholination by AnkX, Fic domain proteins from other species were observed to perform a number of other novel PTMs including phosphorylation and UMPylation (addition of UMP) (reviewed in 36).

In addition to novel PTMs, *Legionella* also has effectors that utilize canonical PTMs in unique ways. One of the best examples is SdeA, an effector protein that acts as an E3 ubiquitin ligase. This protein is unique because it does not need E1 or E2 to ubquitinate its substrate target (37). Instead, SdeA adds phoshoubiquitin to a Ser residue of the substrate. This is accomplished when SdeA ADP-ribsosylates ubiquitin. The ADP-ribosyl moiety is used to create the phosphodiester bond between the serine of the target protein and the phosphoubiquitin carried by SdeA (38, 39). This unique mechanism allows *Legionella* to use ubiquitin without the need for the mammalian enzymatic pathways. Additionally, this process sequesters the ubiquitin pools, as any ubiquitin that has been ADP-ribosylated cannot be used in the canonical E1-E2-E3

pathway (38). This is one example where a canonical PTM has taught us about the bacteria's reliance on the ubiquitination pathway and the unique mechanisms *Legionella* uses to control it.

Legionella also relies heavily on phosphorylation as it uses a set of 5 conserved effector eSTPKs (LegK1-4 and LegK7). In the next two chapters, I will delve more deeply into the exploration of these kinases and their function. I became especially interested in LegK4 after we discovered that the kinase targets the 70kDa heat shock protein (HSP70) family of enzymes. This was particularly striking because Hsp70s are involved in a number of crucial cellular processes. Hsp70s are typically referred to as chaperone proteins due to their canonical role in helping other proteins fold. Chaperones help misfolded proteins find their proper structure in addition to providing assistance to nascent polypeptide chains with a large number of hydrophobic residues on their N-terminus. These proteins are involved in many other crucial processes within the cell, but due to their role in helping newly translated polypeptides, we took a special interest in Hsp70s as a potential substrate target. *Legionella* was already known to block host translation upon infection. There are 5 *Legionella* effectors that are known to accomplish this, four of which are well characterized (40, 41). These previously known methods of host translation inhibition all target the host's translation initiation complex in some way. We found that by targeting Hsp70, *Legionella* uses a unique method of host translation inhibition to compliment the previously discovered mechanisms. I will delve more deeply into the discoveries made toward this story in **Chapter 3**.

In the final chapter I will explore some cancer related kinases, including protein kinase A (PKA), and how the different context that we study these kinases is important

to discovering unique signaling partners. Additionally, **Chapter 4** will include a summary of some of the substrate identification tools I utilized throughout my work, and explain how these tools have become essential in understanding biology.

References

1. Hornbeck PV, et al. (2015) PhosphoSitePlus, 2014: mutations, PTMs and recalibrations. *Nucleic Acids Research* 43(D1):D512–20.

2. Manning G, Whyte DB, Martinez R, Hunter T, Sudarsanam S (2002) The protein kinase complement of the human genome. *Science* 298(5600):1912–1934.

3. Hanks SK, Hunter T (1995) Protein kinases 6. The eukaryotic protein kinase superfamily: kinase (catalytic) domain structure and classification. *FASEB J* 9(8):576–596.

4. H S Lu C, Liu K, Tan LP, Yao SQ (2012) Current chemical biology tools for studying protein phosphorylation and dephosphorylation. *Chemistry* 18(1):28–39.

5. Knight ZA, Shokat KM (2005) Features of selective kinase inhibitors. *Chemistry & Biology* 12(6):621–637.

6. Bailey MH, et al. (2018) Comprehensive Characterization of Cancer Driver Genes and Mutations. *Cell* 173(2):371–385.e18.

7. Shtivelman E, Lifshitz B, Gale RP, Canaani E (1985) Fused transcript of abl and bcr genes in chronic myelogenous leukaemia. *Nature* 315(6020):550–554.

8. de Klein A, et al. (1982) A cellular oncogene is translocated to the Philadelphia chromosome in chronic myelocytic leukaemia. *Nature* 300(5894):765–767.

9. Heisterkamp N, et al. (1983) Localization of the c-ab1 oncogene adjacent to a translocation break point in chronic myelocytic leukaemia. *Nature* 306(5940):239–

242.

10. Groffen J, et al. (1984) Philadelphia chromosomal breakpoints are clustered within a limited region, bcr, on chromosome 22. *Cell* 36(1):93–99.

11. Stam K, et al. (1985) Evidence of a new chimeric bcr/c-abl mRNA in patients with chronic myelocytic leukemia and the Philadelphia chromosome. *N Engl J Med* 313(23):1429–1433.

12. NOWELL PC (1962) The minute chromosome (Phl) in chronic granulocytic leukemia. *Blut* 8:65–66.

13. Witte ON, Dasgupta A, Baltimore D (1980) Abelson murine leukaemia virus protein is phosphorylated in vitro to form phosphotyrosine. *Nature* 283(5750):826–831.

14. Konopka JB, Watanabe SM, Witte ON (1984) An alteration of the human c-abl protein in K562 leukemia cells unmasks associated tyrosine kinase activity. *Cell* 37(3):1035–1042.

15. Huebner RJ, Todaro GJ (1969) Oncogenes of RNA tumor viruses as determinants of cancer. *Proc Natl Acad Sci USA* 64(3):1087–1094.

16. Martin GS (2001) The hunting of the Src. *Nat Rev Mol Cell Biol* 2(6):467–475.

17. Brugge JS, Erikson RL (1977) Identification of a transformation-specific antigen induced by an avian sarcoma virus. *Nature* 269(5626):346–348.

18. Collett MS, Erikson RL (1978) Protein kinase activity associated with the avian

sarcoma virus src gene product. *Proc Natl Acad Sci USA* 75(4):2021–2024.

19. Eckhart W, Hutchinson MA, Hunter T (1979) An activity phosphorylating tyrosine in polyoma T antigen immunoprecipitates. *Cell* 18(4):925–933.

20. Hunter T, Sefton BM (1980) Transforming gene product of Rous sarcoma virus phosphorylates tyrosine. *Proc Natl Acad Sci USA* 77(3):1311–1315.

21. Thomas SM, Brugge JS (1997) Cellular functions regulated by Src family kinases. *Annu Rev Cell Dev Biol* 13(1):513–609.

22. Stehelin D, Varmus HE, Bishop JM, Vogt PK (1976) DNA related to the transforming gene(s) of avian sarcoma viruses is present in normal avian DNA. *Nature* 260(5547):170–173.

23. Pirrung MC (1999) Histidine kinases and two-component signal transduction systems. *Chemistry & Biology* 6(6):R167–75.

24. Krell T, et al. (2010) Bacterial sensor kinases: diversity in the recognition of environmental signals. *Annu Rev Microbiol* 64(1):539–559.

25. Canova MJ, Molle V (2014) Bacterial serine/threonine protein kinases in host-pathogen interactions. *J Biol Chem* 289(14):9473–9479.

26. Pereira SFF, Goss L, Dworkin J (2011) Eukaryote-Like Serine/Threonine Kinases and Phosphatases in Bacteria. *Microbiology and Molecular Biology Reviews* 75(1):192–212.

27. Salomon D, Orth K (2013) What pathogens have taught us about posttranslational

modifications. *Cell Host Microbe* 14(3):269–279.

28. Galyov EE, Håkansson S, Forsberg A, Wolf-Watz H (1993) A secreted protein kinase of Yersinia pseudotuberculosis is an indispensable virulence determinant. *Nature* 361(6414):730–732.

29. Juris SJ, Shah K, Shokat K, Dixon JE, Vacratsis PO (2006) Identification of otubain 1 as a novel substrate for the Yersinia protein kinase using chemical genetics and mass spectrometry. *FEBS Letters* 580(1):179–183.

30. Navarro L, et al. (2007) Identification of a molecular target for the Yersinia protein kinase A. *Mol Cell* 26(4):465–477.

31. Zhu W, et al. (2011) Comprehensive identification of protein substrates of the Dot/Icm type IV transporter of Legionella pneumophila. *PLoS ONE* 6(3):e17638.

32. Cornejo E, Schlaermann P, Mukherjee S (2017) How to rewire the host cell: A home improvement guide for intracellular bacteria. *The Journal of Cell Biology* 216(12):3931–3948.

33. Finlay BB, McFadden G (2006) Anti-immunology: evasion of the host immune system by bacterial and viral pathogens. *Cell* 124(4):767–782.

34. Mohr I, Sonenberg N (2012) Host translation at the nexus of infection and immunity. *Cell Host Microbe* 12(4):470–483.

35. Mukherjee S, et al. (2011) Modulation of Rab GTPase function by a protein phosphocholine transferase. *Nature* 477(7362):103–106.

36. Roy CR, Cherfils J (2015) Structure and function of Fic proteins. *Nat Rev Microbiol* 13(10):631–640.

37. Qiu J, et al. (2016) Ubiquitination independent of E1 and E2 enzymes by bacterial effectors. *Nature* 533(7601):120–124.

38. Bhogaraju S, et al. (2016) Phosphoribosylation of Ubiquitin Promotes Serine Ubiquitination and Impairs Conventional Ubiquitination. *Cell* 167(6):1636–1649.e13.

39. Kotewicz KM, et al. (2017) A Single Legionella Effector Catalyzes a Multistep Ubiquitination Pathway to Rearrange Tubular Endoplasmic Reticulum for Replication. *Cell Host Microbe* 21(2):169–181.

40. Belyi Y, et al. (2006) Legionella pneumophila glucosyltransferase inhibits host elongation factor 1A. *Proc Natl Acad Sci USA* 103(45):16953–16958.

41. Belyi Y, Tabakova I, Stahl M, Aktories K (2008) Lgt: a family of cytotoxic glucosyltransferases produced by Legionella pneumophila. *Journal of Bacteriology* 190(8):3026–3035.

Chapter 2

Characterization of the eukaryotic-like effector kinases in *Legionella pneumophila*

Introduction

Of the 300 effector proteins translocated by *Legionella pneumophila* (*L.p.*), many of those with characterized functions use post-translational modifications (PTMs) as their mode of action (1). The previous chapter discusses some examples of both canonical and non-canonical effector PTMs used by *L.p.*, but there is a series of eukaryotic-like ser/thr protein kinases (eSTPKs) used as effector protein by *L.p.*, whose functions are relatively unexplored. Of the effector kinases present in the *L.p.* genome, 5 are conserved over all strains of *L.p.*, which are dubbed *Legionella* kinase 1-4 and 7 (LegK1-4 and LegK7) (2, 3). There is an additional Legk5, but it is only present in some strains of *L.p.* and was therefore omitted from all further studies (4). It is important to note that LegK7 has a noncanonical amino acid kinase sequence, and was not originally picked up by traditional sequence alignment searches (3). While a substrate target of LegK7 has been identified (MOB1, discussed later in detail), it was omitted from our original characterization due to the lack of sequence recognition on our part.

While most of these eSTPKs do not have identified substrates, some work has been done on their characterization. LegK1 is one of the most well characterized eSTPKs from *L.p.* LegK1 was found to stimulate the NF-κB pathway in a kinase-dependent manner (5). Activation of innate immunity signaling through NF-κB is a known effect of *L.p.* infection, and LegK1 was one of the few effectors found to

accomplish this (5). Through careful dissection of the NF-κB pathway, Ge and colleagues found that LegK1 was imitating the activity of the host IKK kinases and directly phosphorylating IκBα on the Ser-32 and Ser-36 endogenous phosphorylation sites. These phosphorylation events allow for the NF-κB complex to enter the nuclear pore and initiate transcription of innate immunity mRNAs. In addition, LegK1 was found to phosphorylate p100, an inhibitor in the non-canonical NF-κB pathway (5). Phosphorylation of p100 allows for another pathway of NF-κB activation. Disruption of these two pathways show that LegK1 gives *L.p.* control over the host cell's inflammatory response.

LegK7 was well-characterized in a recent paper by Lee and Machner. The group first identified that LegK7 had structural homology to a canonical kinase using *in silico* screening (3). The primary amino acid sequence homology of the kinase domain is below 12% and was not detected in original kinase sequence alignments of *L.p.* effector proteins (3). Following this discovery substrates were screened to identify MOB1 as the primary substrate of LegK7. MOB1 is a scaffolding protein involved in the Hippo signaling pathway. Following phosphorylation of MOB1, the Hippo transcription factors YAP and TAZ are degraded which alters the transcription profile of the host cell and regulates the cell's innate immunity pathways. LegK7 has revealed new and exciting host-pathogen biology as this is the first case of a microbial pathogen targeting the Hippo pathway directly (3).

Some of the other LegK effectors have been studied, but nothing about their activity is conclusive. For example, an isogenic Δ*legK2* strain of *L.p.* exhibits delayed intracellular replication in amoebae due to the kinase's ability to disrupt actin

polymerization (2). Later work suggested that this disruption was due to legK2 phosphorylating the ARP2/3 complex (6). Another paper elucidated the x-ray crystal structure of the kinase domain of LegK4 (7). While no substrate was identified, the researchers were able to show that LegK4 adopts a fold very similar to a eukaryotic protein kinase (**Figure 2.1**). Additionally, when comparing the ATP-bound and apo structures of LegK4 they showed little change in the position of the active site. This indicates that LegK4 might be a constitutively active kinase that does not depend of phosphorylation of the activation loop (7). The LegK4 structure also showed a novel dimeric interface mediated by the αF and αG helices (**Figure 2.1**) (7). The authors suggest that this novel dimer might stabilize and contribute to constitutive kinase activity. With all of this information, we were interested in learning more about the specific host substrates of *L.p.* kinases.

Genetic and *in vitro* Characterization of LegK1-4

There was only one kinase, LegK1, with both primary sequence homology and a known substrate. This led us to take an unbiased approach when characterizing the kinases from *L.p.* I first performed a primary amino acid sequence alignment to look for common kinase motifs amongst the four eSTPKs. Using ClustalOmega, I aligned the sequences of LegK1-4 from three different *L.p.* strains (Philadelphia, Lens, and Alcoy) (**Figure 2.1**). Prominently, all kinases contained some homolog of the classic HRD and DFG motifs important in the phosphorylation activity of most kinases (**Figure 2.1**). Using these motifs as reference points, the 11 structural elements of the kinase domains were easily

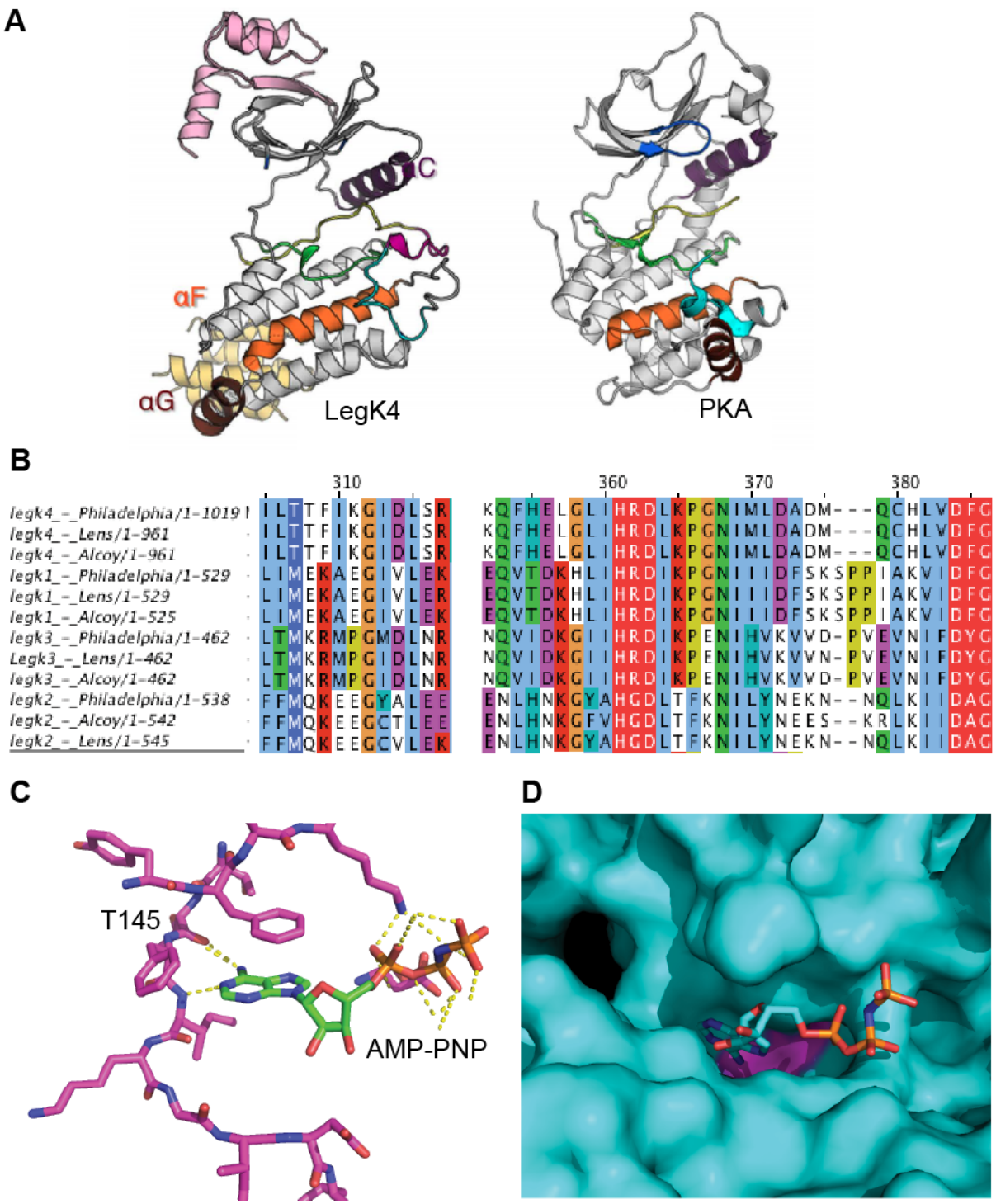

Figure 2.1 Genetic and structural analysis of *legk* genes. (**A**) Figure adopted from (7). Comparison of the LegK4 kinase structure (PDB code 5CLR) to the mammalian Protein Kinase A (PKA) (PDB code 4DFY). (**B**) Amino acid sequence alignements of *legk1-4* from 3 different strains (*Lens, Alcoy,* and *Philadelphia*). The label to the left is Gene name_strain/# of amino acids. The residue highlighted in blue with white text is the gatekeeper residue based on sequence and structural alignments. The "HRD" and "DFG" motifs are highlighted in red with white text. (**C**) The ATP binding pocket of

LegK4 (PDB code 5CKW). The structure includes AMP-PNP in green and orange. The protein structure is in purple, and the gatekeeper residue is labeled (T145) and shows interaction with the N6 of the adenosine ring. (**D**) Globular display of the LegK4 structure (PDB code 5CKW) showing the gatekeeper in purple at the back of the ATP binding pocket.

identifiable. One noticeable difference from the kinase alignments is the fact that LegK4 was approximately double the size of all the other LegKs (**Figure 2.1**). The kinase domain is on the N-terminus of LegK4, and the amino acid sequence following this has high homology to a conserved effector that is immediately downstream of LegK4 (*lpg0209* in *L.p.*-Philadelphia). While there is no known regulatory role between the two proteins, the sequence homology and genomic proximity is striking.

We decided to use a chemical genetic approach previously developed by the Shokat lab to specifically label the substrate targets of specific kinases (described in detail in Chapter 4). In brief, a space-creating mutation is made in the kinase's ATP-binding site by mutating the large hydrophobic gatekeeper residue to either a Gly or Ala. This mutated protein is the Analog Sensitive (AS) version of the kinase. The space in the ATP binding pocket is subsequently filled with an ATP-analog containing a bulky substitution on N^6 of the adenine ring (8). This ATP analog contains a γ-thio-phosphate that can be used by the kinase in the place of a normal phosphate and provides a reactive thiol (9). In order to use this methodology, we used sequence alignments and the solved crystal structure of LegK4 to find the gatekeeper residue on LegK4 (**Figure 2.1**). As shown in the structure, LegK4 contains a Thr gatekeeper that aligns with other large hydrophobic residues in the other LegKs (**Figure 2.1**).

To proceed with the substrate identification, we use recombinantly expressed protein that can be used in an *in vitro* assay setting. Once the identity of the gatekeeper

residues were established, we attempted purification of all WT and AS LegK proteins using the sequences from the *L.p.*-Philadelphia strain. In the initial round of purifications, LegK1 and its mutants purified with very low yields, LegK2 purified in high yields, and LegK3 and LegK4 never expressed in *E. coli*. We later discovered how to purify high yields of LegK4, which is discussed further in Chapter 3.

With LegK1 and LegK2 available and recombinantly purified, I tested the kinase activity of the WT and AS proteins. Initial assays were done using the model kinase substrate myelin-basic protein (MBP) and the previously mentioned thiophosphorylation system (described in detail in chapter 3). Neither LegK1 nor LegK2 were able to noticeably thiophosphorylate MBP under any of the conditions tested (**Figure 2.2 & Table 2.2**). We decided to test kinase activity in cell lysate to determine if there was a cellular factor that was missing in our *in vitro* MBP system. Similar to the experience with purified MBP, there was no observable phosphorylation of the cell lysate with LegK1 or LegK2 or their gatekeeper mutant isoforms (**Figure 2.2 and Table 2.2**). This lack of activity was discouraging due to previous reports of LegK1 and LegK2 phosphorylating MBP *in vitro* as well as the reported cellular targets of LegK1. Our results taken together with previous groups who were able to see activity in these kinases, led us to explore the phenotypic activity of these kinases, as well as the *in vitro* activity of LegK1 using a novel peptide based system discussed later.

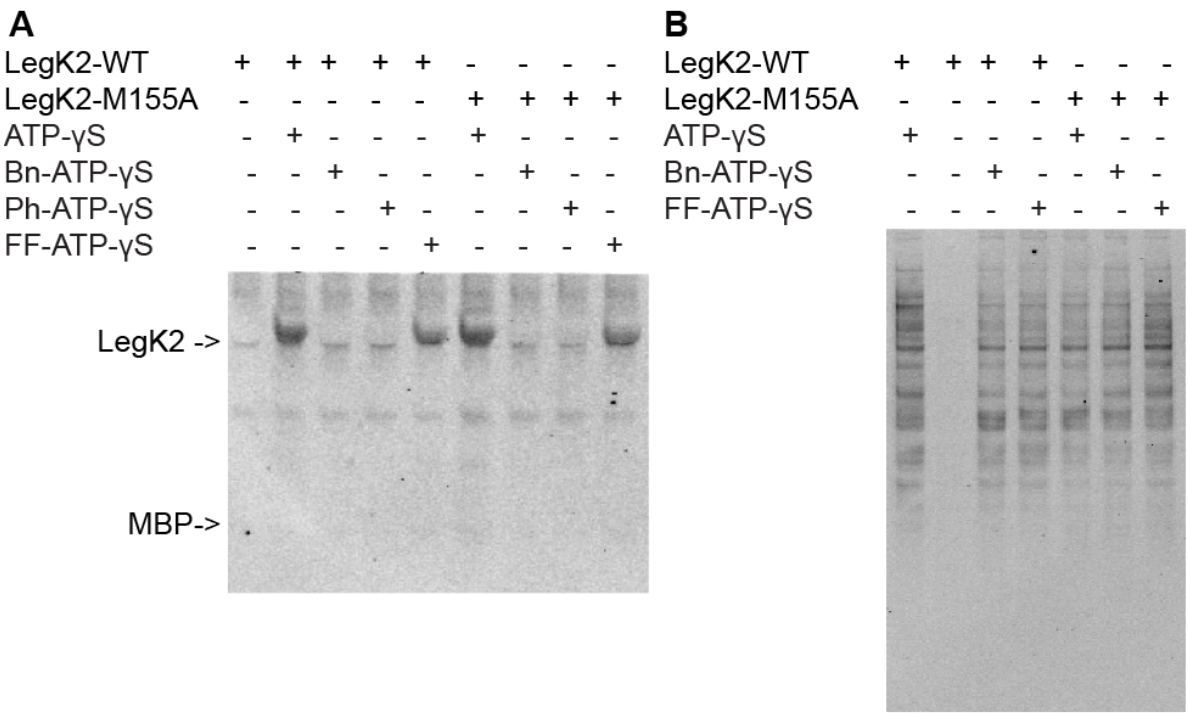

Figure 2.2 Phosphorylation activity of LegK2. Example of negative phosphorylation results using the kinase LegK2. LegK2-M155A is the gatekeeper mutation. Three versions of the N6-substituted ATP analog were used (Bn-Benzyl, Ph-Phenethyl, FF-Furfuryl). (**A**) Labeling of Myelin Basic Protein (MBP) as an ideal substrate for kinases. While some mild autophosphorylation is observed for LegK2, there is no discernable phosphorylation of the MBP substrate. (**B**) Labeling of HEK-293T cell lysate. There is no observable phosphorylation patterns with the AS kinase and the N6-substituted ATP analogs as expected.

Phenotypic Characterization of LegK1-4

Concurrently with attempts at sequence alignment and recombinant purification, we tested for different cellular phenotypes. We used a cellular overexpression system where the kinases tagged with GFP were transiently transfected into HeLa cells, and the cells were stained for cellular markers, including Golgi, ER, lysosome, and actin, that are known to be important to *L.p.* The first cellular marker tested was GM130 that stains the Golgi (**Figure 2.3 & Table 2.1**). *L.p*. is known to disrupt vesicle trafficking between in the ER and the Golgi in order to transform the membrane of the *Legionella* containing vacuole (LCV) to a more ER membrane-like structure (10). Additionally, we

looked at markers for the lysosome because *L.p.* is known to prevent the LCV from maturing into an endosome or lysosome via autophagy (**Table 2.1**). Finally, we looked at markers for actin (**Table 2.1**). This was particularly important because LegK2 was

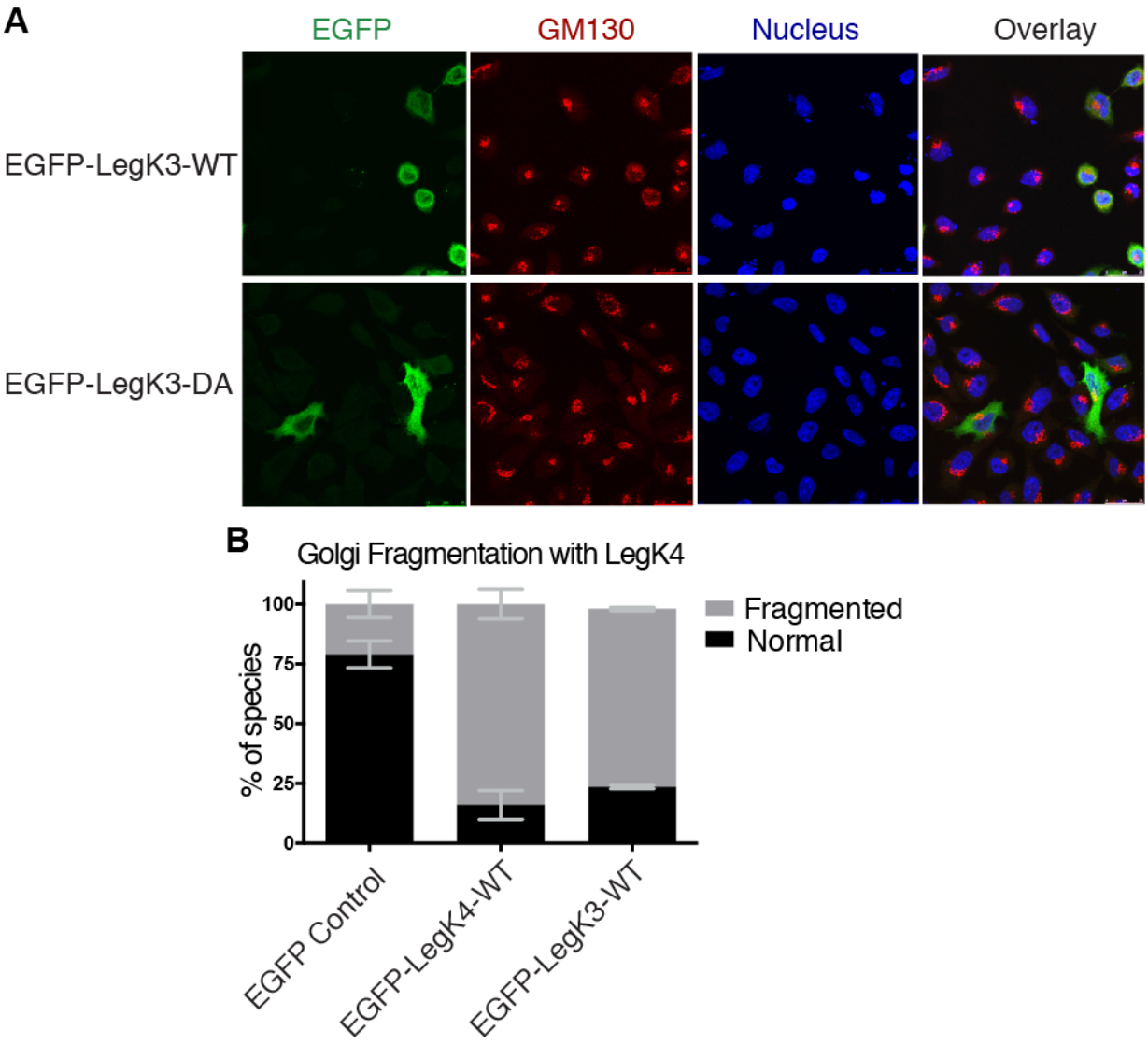

Figure 2.3 Example of phenotypic characterization of LegK proteins using immunofluorescence. (**A**) Labeling of Golgi using GM130 following overexpression of EGFP-LegK3. LegK3 is shown in green, Golgi is shown in Red, and the nucleus is shown in blue. A healthy Golgi should be compact while an unhealthy Golgi is fragmented throughout the cell. (**B**) Phenotypic analysis of Golgi health in LegK3 and LegK4 overexpression samples. Both LegK3 and LegK4 showed a large amount of phenotypic Golgi fragmentation (images: **A** and **Figure 3.1**).

reported to phosphorylate the Arp2/3, a protein complex involved in actin dynamics (6). Therefore, the overexpression of LegK2 should disrupt typical actin formation.

Of all the cellular markers we looked at in our overexpression system, GM130 was the only one that showed a distinct phenotype with some of the kinases (**Figure 2.3 & Table 2.1**). Phalloidin showed no noticeable phenotype with any of the kinases (**Table 1**). This was surprising because of the previously reported LegK2 result. However, we were encouraged by the ability of LegK3 and LegK4 to disrupt the Golgi and cause Golgi fragmentation (**Figure 2.3**). The effect was observed in both proteins, but was more pronounced in LegK4.

Table 2.1 Results of phenotypic kinase analysis using Immunofluorescence.

Phenotype / Marker	Golgi / GM130	ER / PDI	Lysosome / LAMP1	Actin / Phalloidin
LegK1	No	No	No	No
LegK2	No	No	No	No
LegK3	Yes	No	No	No
LegK4	Yes	No	No	No

Analysis of LegK1 using Multiplex Substrate Profiling by Mass Spectrometry

We became interested in exploring alternative methods of *in vitro* analysis of these kinases. A collaborator in Charles Craik's lab was using the Multiplex Substrate Profiling by Mass Spectrometry (MSP-MS) to look at the specificity profiles of kinase substrates. This method was originally developed to look at the amino acid sequence specificity of different proteases using a uniquely designed library of peptides (11). The technique uses a 228-member amino acid library designed to maximize sequence diversity in this set of tetradecameric peptides (11). Purified proteases are added to the library, and the proteolytic products are read and quantified by LC-MS/MS (**Figure 2.4**). This gives an

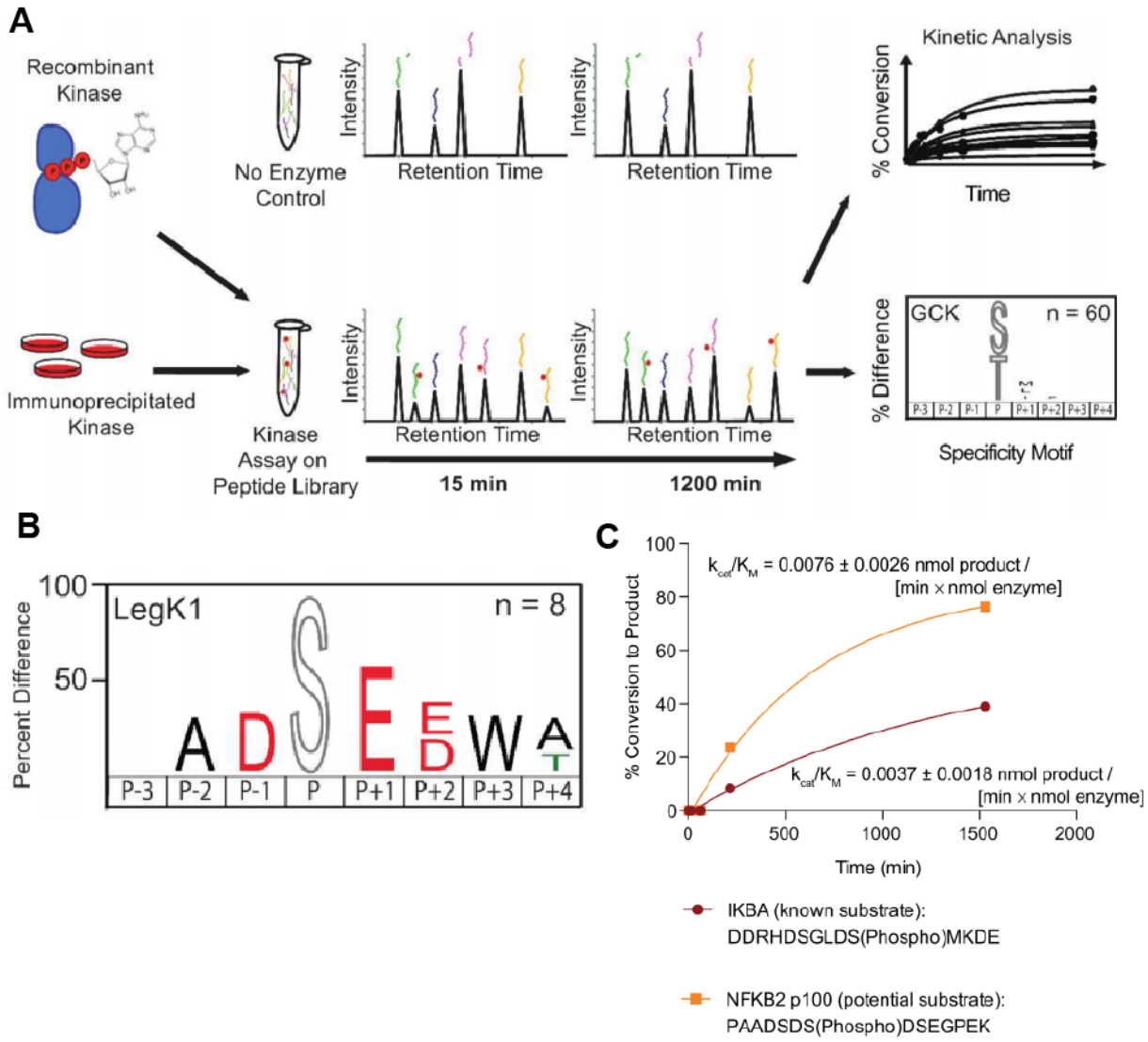

Figure 2.4 Multiplex substrate profiling mass spectrometry results of LegK1. (**A**) Depiction of the MSP-MS assay for kinases. Recombinant or immunoprecipitated kinases are added to the peptide library. Aliquots are removed from the reaction at several time points, quenched, and then analyzed by LC−MS/MS. Phosphopeptides were identified and quantified at each time point, then used to develop specificity motifs and generate catalytic efficiency values for each peptide in the multiplex assay. (**B**) Characterization of LegK1. Substrate signature was developed using the phosphopeptides identified after 1200 min of kinase reaction with the peptide library. (**C**) Time course experiment using peptides synthesized based on the sequences of candidate LegK1 substrates. Peak area values for the substrate and product at each time point were measured and used to calculate percent conversion to the phosphorylated product. These values were fit to a first order rate equation. k_{cat}/K_M values were be extracted for each peptide, resulting in values of 0.0037 ± 0.0018 nmol product / [min × nmol enzyme] for IKBA and 0.0076 ± 0.0026 nmol product / [min × nmol enzyme] for NFKB2.

amino acid specificity profile for the protease around the proteolytic cleavage. This information can then be used to determine potential proteolytic targets, or for uncharacterized proteases, help determine which class the protein falls into.

Further work was done to optimize this methodology for use in determining kinase substrates. The peptide library was optimized throughout the process of phosphorylation identification, and can be used on a diverse array of kinases to help determine substrate specificity. The technique can be used to determine specificity in the N-terminal (P – #) and C-terminal (P + #) directions. Additionally, due to the quantitative properties of this mass spectrometry method, it can be used to determine kinetic values of the kinase for specific peptides (**Figure 2.4**).

We profiled both LegK1 and LegK4 using MSP-MS. For LegK1, eight phosphopeptides were identified. An iceLogo generated from these phosphopeptides revealed a strong preference for acidic amino acids at P − 1, P + 1, and P + 2. The P − 1 specificity aligned with the phosphorylation sites within the known substrate IκBα, at Ser32 (RHDS(Phospho)GLD) and Ser36 (GLDS(Phospho)-MKDE). The P − 1 and P + 1 specificity also aligned with the phosphorylation sites within a suggested substrate p100 at Ser713, Ser715, and Ser717 (PPTSDS$_{713}$DS$_{715}$DS$_{717}$-EGP) (**Figure 2.4**). Peptides from the sequences of IκBα and p100 were synthesized and used in *in vitro* kinase assays with LegK1. LegK1 phosphorylated both peptides, with k_{cat}/K_M values of 0.0037 ± 0.0018 nmol product/[min × nmol enzyme] for IκBα and 0.0076 ± 0.0026 nmol product/[min × nmol enzyme] for p100 (**Figure 2.4**). Interestingly, no phosphopeptides were identified from the library for LegK4. While this was disheartening at the time, we

now believe this is due to the extraordinary specificity of the kinase for a highly-conserved sequence in Hsp70.

Discussion

The cumulative effort of this characterization work showed that these kinases all have different experimental challenges. When deciding which kinase(s) to move forward with in performing substrate identification, we considered several factors. First we prioritized the ability to observable a strong cellular phenotype when the active kinase was expressed in mammalian cells. Second, we required recombinantly active kinase so it would be used in *in vitro* cell lysate phosphorylation experiments. We took other factors into account such as any previous work that had been done to characterize the kinase and/or its substrates. The observed Golgi fragmentation, ease of purification, and accompanying crystal structure led us to further study and characterize the substrates and role of LegK4 (Chapter 3).

Table 2.2 Summary of information and experimentation on *L.p.* effector kinases.

Kinase	Known substrate?	Recombinant purification?	Phosphorylate MBP?	Phosphorylate lysate?	Phenotype?
LegK1	IκBα and p100	Low yields	No	No	No
LegK2	ARP2/3?	High yields	No	No	No
LegK3	N/A	No	No	No	Fragmented Golgi
LegK4	N/A but structure is solved	High yields	No	Yes (Ch. 3)	Fragmented Golgi
LegK7	MOB1	N/A	N/A	N/A	N/A

References

1. Doublet P, Michard C (2015) Post-translational modifications are key players of the Legionella pneumophila infection strategy. *Frontiers in Microbiology* 6(87):1–12.

2. Hervet E, et al. (2011) Protein Kinase LegK2 Is a Type IV Secretion System Effector Involved in Endoplasmic Reticulum Recruitment and Intracellular Replication of Legionella pneumophila. *Infection and Immunity* 79(5):1936–1950.

3. Lee P-C, Machner MP (2018) The Legionella Effector Kinase LegK7 Hijacks the Host Hippo Pathway to Promote Infection. *Cell Host Microbe* 24(3):429–438.e6.

4. Hervet E, et al. (2011) Protein Kinase LegK2 Is a Type IV Secretion System Effector Involved in Endoplasmic Reticulum Recruitment and Intracellular Replication of Legionella pneumophila. *Infection and Immunity* 79(5):1936–1950.

5. Ge J, et al. (2009) A Legionella type IV effector activates the NF-kappaB pathway by phosphorylating the IkappaB family of inhibitors. *Proc Natl Acad Sci USA* 106(33):13725–13730.

6. Michard C, et al. (2015) The LegionellaKinase LegK2 Targets the ARP2/3 Complex To Inhibit Actin Nucleation on Phagosomes and Allow Bacterial Evasion of the Late Endocytic Pathway. *mBio* 6(3):e00354–15–14.

7. Flayhan A, et al. (2015) The structure of Legionella pneumophila LegK4 type four secretion system (T4SS) effector reveals a novel dimeric eukaryotic-like kinase.

Nature Publishing Group:1–13.

8. Blethrow JD, Glavy JS, Morgan DO, Shokat KM (2008) Covalent capture of kinase-specific phosphopeptides reveals Cdk1-cyclin B substrates. *Proc Natl Acad Sci USA* 105(5):1442–1447.

9. Allen JJ, et al. (2007) A semisynthetic epitope for kinase substrates. *Nat Meth* 4(6):511–516.

10. Bärlocher K, Welin A, Hilbi H (2017) Formation of the Legionella Replicative Compartment at the Crossroads of Retrograde Trafficking. *Front Cell Infect Microbiol* 7:482.

11. O'Donoghue AJ, et al. (2012) Global identification of peptidase specificity by multiplex substrate profiling. *Nat Meth* 9(11):1095–1100.

Chapter 3

A bacterial kinase phosphorylates the Hsp70 chaperone family to inhibit eukaryotic protein synthesis

Steven M. Moss[1], Isabelle R. Taylor[2], Davide Ruggero[1,3,4], Jason E. Gestwicki[2], Kevan M. Shokat[1,5,6,*], and Shaeri Mukherjee[7,8,*]

[1]Department of Cellular and Molecular Pharmacology, University of California, San Francisco, CA 94158; [2]Department of Pharmaceutical Chemistry, University of California, San Francisco, CA 94158; [3]Hellen Diller Family Comprehensive Cancer Center, University of California, San Francisco, CA 94158; [4]Department of Urology, University of California, San Francisco, CA 94158; [5]Howard Hughes Medical Institute, University of California, San Francisco, CA 94158; [6]Department of Chemistry, University of California, Berkeley, Berkeley, CA 94720; [7]Department of Microbiology and Immunology, University of California, San Francisco, CA 94143; [8]George Williams Hooper Foundation, University of California, San Francisco, CA 94143.

Summary

Legionella pneumophila (*L.p.*), the microbe responsible for Legionnaires' disease, secretes ~300 bacterial proteins into the host cell cytosol. A subset of these proteins cause a wide range of post-translational modifications (PTMs) to disrupt cellular mechanisms of its host. We employed a chemical genetic screen to identify the Hsp70 chaperone family as the direct target of LegK4, one of four eukaryotic-like Ser/Thr effector kinases. Phosphorylation of Hsp70s at T495 in the substrate-binding domain disrupted the Hsp70's ATPase activity and greatly inhibited its protein folding capacity. Phosphorylation of cytosolic Hsp70s by LegK4 resulted in global translation inhibition and an observable increase in the amount of Hsp70 on highly translating polysomes. LegK4's ability to inhibit host translation via a single modification uncovers a previously uncharacterized role for Hsp70 in protein synthesis.

Keywords

kinase; host-pathogen interaction; Hsp70; phosphorylation; Legionella pneumophila; translation.

Introduction

Intracellular pathogens are successful because they manipulate multiple host processes to escape immune detection and enable their own survival; thus, studying these pathogens has facilitated our understanding of the intricate regulation of fundamental host pathways(1, 2). Targeting eukaryotic mRNA translation is one such pathway, and is a common mechanism by which pathogens regulate their hosts. Work on Diphtheria toxin (3) and Shiga toxin (4) have identified fascinating mechanisms for blocking host protein synthesis (2). Almost all cases of translation inhibition are a result of targeting the translation machinery itself such as inhibiting elongation factors (e.g. Diphtheria toxin) (3) or inhibiting the 28S rRNA (Shiga toxin) (5).

The bacterial pathogen *Legionella pneumophila* (*L.p.*) has emerged as a model organism for studying host-pathogen interactions given its expert manipulation of many key regulatory pathways including host translation and eukaryotic vesicle transport. To control these host processes, *L.p.* uses a type IV secretion system called Dot/Icm that functions to translocate an astonishing ~300 bacterial effector proteins directly into infected host cells(6, 7). Studying the mechanisms of *L.p.* effectors has not only uncovered fascinating aspects of the host-pathogen arms race, it has also led to the identification of important regulators of host cell processes (2, 8, 9). A subset of these effectors hijack the host transport machinery to establish an Endoplasmic Reticulum (ER)-derived *Legionella* containing vacuole (LCV) in which the pathogen replicates. This is partially accomplished through targeting Rab proteins with a suite of post-translational modifications (PTMs) that redirect the subcellular localization of these proteins to the LCV (10, 11). While some effectors are involved in creating a replicative niche, others

work to inhibit protein synthesis by manipulating the host translational machinery (12-14). Three of these proteins are a set of glucosyltransferases (Lgt1-3) that glucosylate and inhibit eukaryotic elongation factor1A (eEF1A) (12, 13). A fourth effector protein SidI binds to eEF1A and another elongation factor eEF1Bγ to block mRNA translation (14). In addition to these four proteins, there are several other *L.p.* effectors that have been suggested to block host translation, but lack mechanistic detail or extensive characterization (15).

With the important role that PTM's play in *L.p.*'s survival and replication, its effector eukaryotic-like Ser/Thr protein kinases (eSTPKs) are emerging as important drivers of pathogenicity. *L.p.* has 5 conserved eSTPKs designated as *Legionella* kinase 1-4 and 7 (LegK1-4 and LegK7)(16, 17), that are translocated during infection. Many of these kinases were evolved to target functionally important domains of host proteins. Previous research has shown that some eSTPKs of *L.p.* modify important cellular pathways such as innate immunity, actin polymerization pathways, and the Hippo pathway (1, 17-19). Characterization of LegK1 revealed its role in altering innate immunity by modifying the endogenous site of phosphorylation, Ser32, on IκBα (20). Ser32 is typically phosphorylated by the mammalian kinases IKKα or IKKβ, an event that activates the canonical NF-κB pathway. In another example, an isogenic Δ*legK2* strain of *L.p.* exhibits delayed intracellular replication in amoebae due to the kinase's ability to disrupt actin polymerization (16, 21). Recently, LegK7 was shown to mimic Hippo kinase activity and phosphorylate MOB1(17). This is the first known interaction of *L.p*. and the host Hippo pathway, paving the way to future research in understanding the Hippo pathway's role in innate immunity(17).

Through studying the cellular phenotypes of known eSTPKs in *L.p.*, we identified a novel mechanism of pathogenic translation inhibition in which LegK4 phosphorylates the Hsp70 chaperone family. The effector LegK4 phosphorylates cytosolic Hsp70s at a highly conserved Thr residue. This is the first identification of a bacterial effector directly targeting Hsp70 with a PTM, and a unique mechanism of controlling host translation that does not act directly through the translational machinery. Hsp70 was identified as a substrate of LegK4 through a chemical genetic screen. A single site of phosphorylation on the Hsp70 family of chaperones, particularly the 71 kDa heat shock cognate (Hsc70) and 70 kDa heat shock protein 1A, (Hsp72) is targeted by LegK4. Phosphorylation of cytosolic Hsp70s by LegK4 at a highly conserved Thr site reduced the chaperone's ATPase activity and subsequently decreased its overall protein refolding capacity. LegK4's phosphorylation of Hsp70 blocked protein synthesis and caused an increase in the Hsp70 load on highly translating polysomes. Thus, this work directly links Hsp70 to the translational machinery via a bacterially programmed PTM.

Results

Expression of LegK4 causes Golgi fragmentation and yeast lethality

L.p. is known to interact with the Golgi during infection (22). To look at any effects the conserved eSTPKs from *L.p.* might have on Golgi morphology, we transiently transfected these effectors into HeLa cells for 24 hours. LegK4 overexpression, but none of the other kinases, caused Golgi fragmentation in 90% of transfected cells (**Figure 3.1**). The LegK4-Δ1-58 construct in this data represents the recombinantly purified version of LegK4 that was used in all *in vitro* phosphorylation

assays. In many *L.p.* strains, including the *Corby* strain used to obtain the LegK4 crystal structure (23), the *legK4* gene sequence begins at the conserved M59 of LegK4 from the *Philadelphia* strain. Based on this analysis, we modified the *legk4* gene from the *Philadelphia* strain of *L.p.* by truncating the first 58 amino acids (LegK4-Δ1-58). This LegK4 truncation was successfully expressed and purified from *E. coli* while the full length LegK4-wt protein was not. Both full length LegK4 and LegK4-Δ1-58 showed a similar Golgi fragmentation phenotype (**Figure 3.1**). A kinase dead construct of LegK4 (**Figure 3.2**), in which the Mg^{2+} coordinating aspartate of the DFG motif is mutated to an alanine (D271A, “LegK4-DA” for remainder of manuscript), did not show Golgi disruption (**Figure 3.1**). This indicates that the kinase activity of LegK4 is responsible for the Golgi fragmentation phenotype. This is the first description of a cellular phenotype for LegK4.

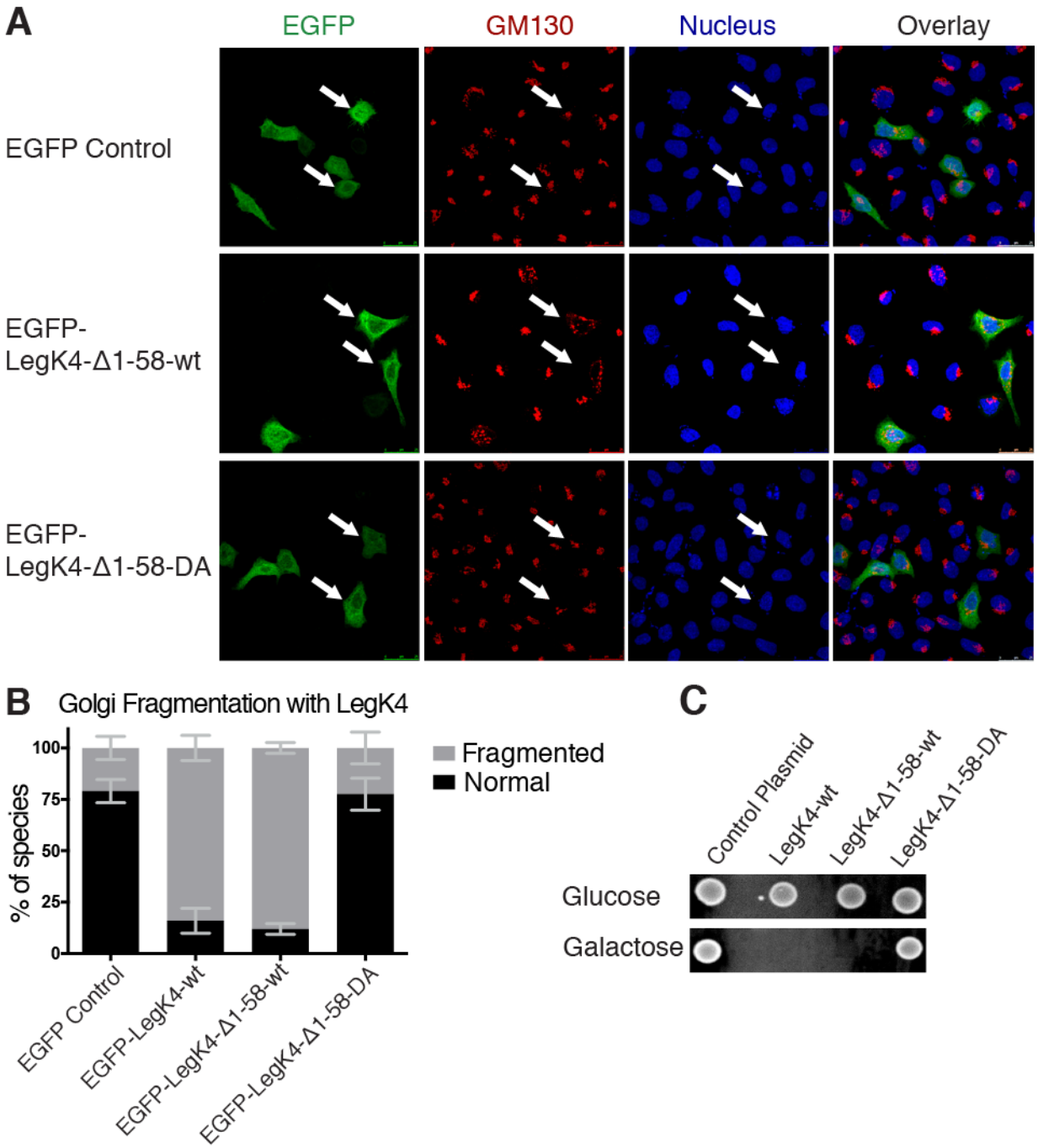

Figure 3.1 LegK4 causes Golgi fragmentation and inhibits yeast growth. (**A**) HeLa cells were transiently transfected with an EGFP tagged LegK4-Δ1-58-wt, as well as EGFP control, and the D271A kinase dead construct of LegK4. Golgi was stained with GM130 in red, and nuclei were stained with blue. Fragmented Golgi were observed in many of the LegK4Δ1-58-wt expressing cells, while the Golgi remained punctate in the kinase dead control. (**B**) Amount of Golgi fragmentation was quantified by counting 100 EGFP positive cells per experimental condition. Counts for the EGFP control, Full length LegK4 (LegK4-wt), truncated LegK4Δ1-58-wt, and LegK4Δ1-58-DA are shown. Each condition was done in triplicate. (**C**) LegK4-wt as well as LegK4-Δ1-58-wt were

transformed into yeast behind a galactose promoter. Yeast growth was inhibited with both of the wt constructs but unaffected with the kinase dead and plasmid control constructs. Shown is a representative of the experiment which was confirmed in 3 separate biological replicates.

Several *L.p.* proteins are known to cause yeast lethality when exogenously expressed. We tested our LegK4 constructs for yeast lethality and showed that they prevented yeast growth when expressed under a Galactose inducible promoter (**Fig. 3.1**). There was no difference in yeast growth between the full length and the truncated versions of LegK4. The D271A mutant exhibited no yeast lethality phenotype, showing that the kinase activity of LegK4 is essential to inhibit yeast growth.

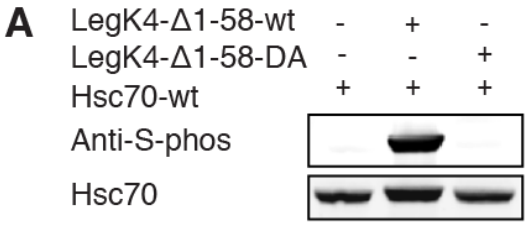

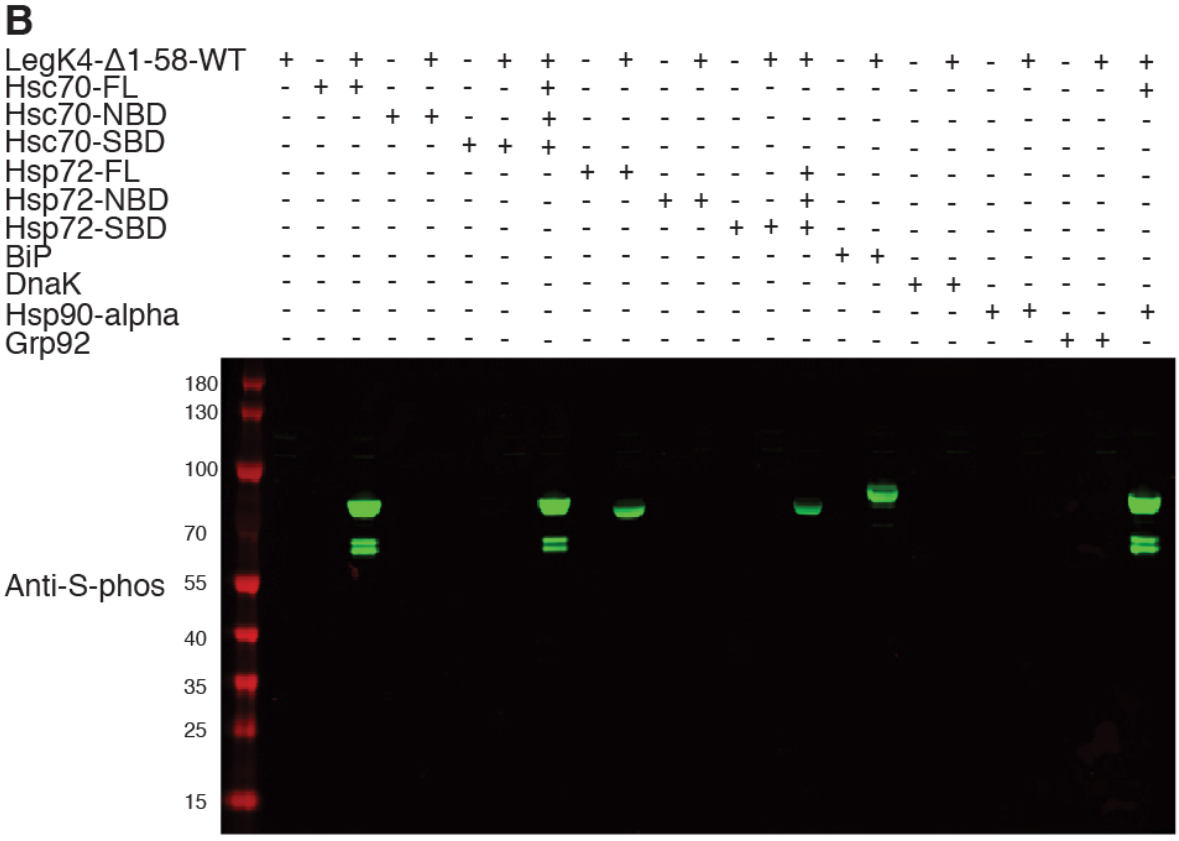

Protein name	Hsp type	Species	Phosphorylated
Hsc70	Hsp70	*Homo sapien*	Yes
Hsp72	Hsp70	*Homo sapien*	Yes
Grp78/BiP	Hsp70	*Cricetulus barabensis*	Yes
DnaK	Hsp70	*Escherichia coli*	No
Hsp90α	Hsp90	*Homo sapien*	No
Grp92	Hsp90	*Homo sapien*	No

Figure 3.2 Establishing specificity of LegK4 phosphorylation. (**A**) Kinase activity of the kinase dead LegK4-D271A (LegK4-Δ1-58-DA) was tested by incubating either the wt kinase (LegK4-Δ1-58-wt) or the DA version with purified Hsc70. Experiment was performed with ATP-γ-S-phos, and anti-S-phos was blotted for. (**B**) Various chaperones were incubated with purified LegK4 and ATP-γ-S-phos *in vitro* to determine the specificity of the kinase. The only proteins that exhibited phosphorylation were full

length Hsc70, Hsp72, and BiP. The separate N-terminal nucleotide binding domain (NBD) and C-terminal substrate binding domain (SBD) of Hsc70 and Hsp72 were incubated to determine specificity of phosphorylation. However, neither were phosphorylated on their own by LegK4. Additionally, DnaK, the Hsp70 from E. coli, and several Hsp90s could not be phosphorylated by LegK4. Shown is a representative of three biological replicates.

LegK4 phosphorylates the Hsp70 chaperone family

We conducted a chemical genetic screen to identify substrates phosphorylated by LegK4. We used an ATP analog that has a benzyl (Bn) group at the N6 position of the adenine ring. These ATP analogs possess a γ-thio-phosphate group that is then differentiated from endogenous kinase phosphorylation sites (24-26). Chemical genetic substrate identification typically requires a space-creating mutation at the gatekeeper position of the kinase of interest in order to accommodate the bulky N6-substituted ATP analogs. Surprisingly, purified LegK4-Δ1-58-wt was able to use N6-substituted analogs of ATP to thio-phosphorylate substrate proteins in HEK-293T cell lysate without the need for a gatekeeper mutation (**Figure 3.3**). Several other kinases are known to accept N6 substituted ATP analogs without a gatekeeper mutation, including CDPK1 from the pathogen *Toxoplasma gondii* (27).

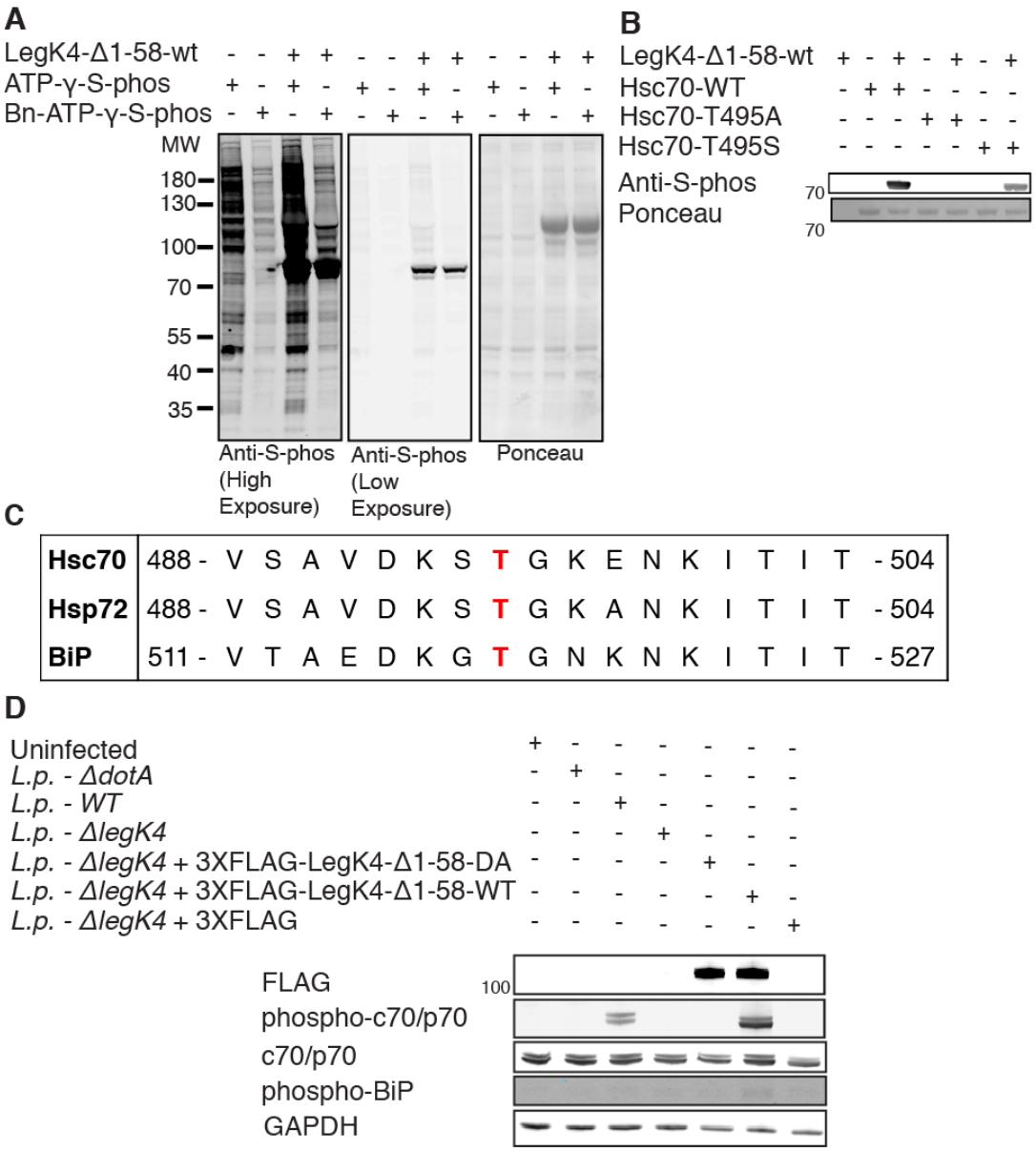

Figure 3.3 Identification of Hsp70 as the substrate of LegK4. (**A**) Purified LegK4-Δ1-58-wt was added to HEK-293T cell lysate along with ATP-γ-thiophosphate (ATP-γ-S-phos) or the corresponding Benzyl-N6-substitued ATP derivative (Bn-ATP-γ-S-phos). (**B**) Following identification of the phosphorylated residue in Hsp70, Hsc70-T495A and T495S constructs were purified. Mutation to alanine completely abrogated phosphorylation, while the serine mutation greatly reduces signal. (**C**) Amino acid sequence of the identified phosphosites. (**D**) The targeted threonine is in bold red. HEK-293T-FCγIII cells were infected for 4 hours with various strains of L.p. including the Dot-Icm secretion system knockout (ΔdotA) as well as the LegK4 knockout. Cells were additionally infected with strains transformed with 3XFLAG-LegK4. Lysates were blotted for phospho-Hsc70/Hsp72 as well as phospho-BiP using custom antibodies.

When HEK-293T cell lysate was incubated with purified LegK4-Δ1-58 and N6-substituted ATP-γ-thio-phos, a striking banding pattern was observed. A minor population of LegK4-Δ1-58-wt autophosphorylation was observed at 110kDa, but there were also two or more strong bands between 70 and 80 kDa (**Figure 3.3**). It is unusual for a purified kinase incubated with cell lysate to phosphorylate a small number of proteins so specifically and robustly (24). We immunoprecipitated all thio-phosphorylated proteins followed by LC MS/MS identification and found 52 unique peptides from a cytosolic Hsp70 (HSPA8). This result, and the relative molecular weight and abundance of the phosphorylated proteins made Hsp70s stand out as the likely substrates of LegK4. Hsp70s are a family of abundant molecular chaperones whose members include Hsc70 (HSPA8) and Hsp72 (HSPA1A) of the cytosol and BiP (HSPA5) of the endoplasmic reticulum. Using purified human Hsc70, we confirmed that this protein is phosphorylated by LegK4 *in vitro* (**Figure 3.3**). We tested if other chaperones were phosphorylated by LegK4 to explore the kinase's specificity. LegK4 showed robust phosphorylation of Hsc70, Hsp72, and BiP, but not the closely related Hsp70 from *Escherichia coli*, DnaK, or 90 kDa heat shock proteins (**Figure 3.2**).

We determined the sites of phosphorylation using LC MS/MS. There was only a single observed phosphorylation at a conserved Thr in the substrate-binding domain (SBD) of the Hsp70s (T495 in Hsc70 and Hsp72, and T518 in BiP) (**Figure 3.3 and Figure 3.4**). Removal of the T495 phosphorylation site in Hsc70 abrogated LegK4-mediated phosphorylation, suggesting high specificity for a single site of phosphorylation (**Figure 3.3**). As all three Hsp70 family members have a highly conserved Thr at this position, we constructed an Hsc70-T495S mutant which showed a

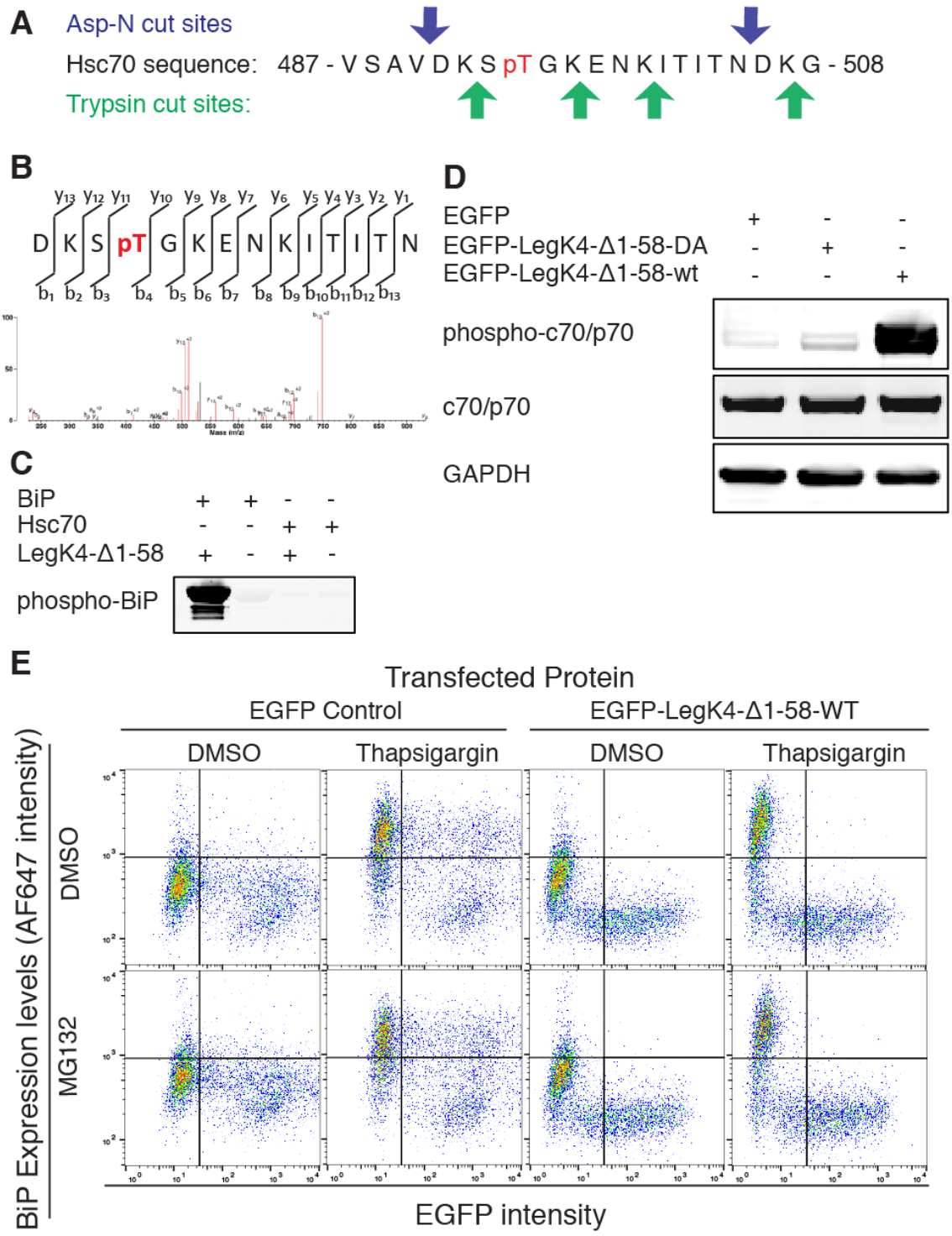

Figure 3.4 Identification and characterization of LegK4 phosphosite. (**A**) The figure represents the peptide containing the phosphorylated threonine, and the various sites where trypsin and Asp-N would cut the peptide. Using trypsin would make the peptide too small and unable to be identified by mass spec. (**B**) After Asp-N cleavage the mass spec results showed T495 in Hsc70 as the phophosite of LegK4. (**C**) the phospho-T518 BiP antibody specificity was confirmed by comparing labeling for phosphorylated and

nonphosphorylated BiP and Hsc70 using purified proteins. (**D**) HEK-293T cells were transiently transfected with LegK4-Δ1-58-wt or LegK4-Δ1-58-DA attached to EGFP, or an EGFP control construct. Lysates were tested for phosphorylation of Hsc70 and Hsp72 via western blot. (**E**) Cells were pretreated with MG-132 for 1 hour and then the UPR was induced with thapsigargin for 5 hours. The presence of MG-132 had no effect on the suppression of BiP overexpression observed in cells transfected with LegK4. Both experiments show a representative of three biological replicates.

noticeable reduction in LegK4 phosphorylation revealing modest selectivity for Thr over Ser phosphorylation (**Figure 3.2 and Figure 3.3**).

LegK4 phosphorylates cytosolic Hsp70s during *L.p.* infection

We generated phospho-specific antibodies to Hsc70/Hsp72-pT495 and BiP-pT518 (**Figure 3.4)** to determine which Hsp70 isoforms were phosphorylated during infection. We also generated an isogenic *ΔlegK4* strain of *L.p* and complemented the strain with a plasmid encoding either a WT 3XFLAG-tagged LegK4-Δ1-58 or a kinase dead LegK4-Δ1-58-DA mutant. Cells stably expressing the FC-γ receptor (to allow opsonization of *L.p*. with a *L.p.* specific antibody) were infected for one hour. The infection produced a strong phosphorylation signal of Hsc70/Hsp72 in the *L.p.*-WT but not in the *L.p.-ΔlegK4* or *L.p.-ΔdotA* strains (**Figure 3.3**). There was no noticeable phosphorylation of ER-resident BiP upon infection (**Figure 3.3**), consistent with the cytosolic localization of *L.p.* effectors. The complemented *L.p.-Δlegk4* strain containing 3X-FLAG-LegK4-Δ1-58-WT showed an enhanced phosphorylation of Hsc70/Hsp72 while the kinase dead strain did not (**Figure 3.3**).

Hsc70 phosphorylation reduces its J-protein stimulated ATPase activity

Hsp70s are ATPases known to play key roles in protein folding and homeostasis (28). The identified LegK4 phosphorylation site on Hsp70's substrate-binding domain was previously shown to be an important phosphoregulon in yeast Hsp70s (29). Additionally, T518 in the endoplasmic reticulum (ER) resident Hsp70, BiP, is adenylylated by the human Fic protein HYPE (30, 31). Previous research showed that his modification reduced ATPase activity *in vitro*, but had no noticeable effect on the ability of BiP to refold model proteins (30). To test if LegK4-mediated phosphorylation might likewise impact ATPase activity or refolding functions, we used LegK4-Δ1-58-wt to phosphorylate recombinant Hsc70. We compared the ATPase activity of this modified chaperone to Hsc70-wt using an malachite green-based *in vitro* ATPase assay. Because the rate of ATP hydrolysis by Hsc70 is normally low, a stimulatory co-chaperone, DnaJA2 (DJA2), was added to improve signal intensity (32). Using this assay format, we found that the DRA2-stimulates ATPase activity of phosphorylated Hsc70 (+LegK4) was decreased (V_{max} of 24.2 ± 0.9 pmol/min) when compared to Hsc70-wt (-LegK4), (V_{max} of 33.4 ± 0.8 pmol/min (**Figure 3.5**).

To understand the functional consequences of this reduced DJA2-stimulated ATPase activity, we compared the ability of phospho-Hsc70 to refold the model substrate firefly luciferase *in vitro*. Denatured luciferase was incubated with Hsc70, ATP and DJA2 and luminescence was used to measure the chaperone's ability to restore native folding. As the concentration of DJA2 was increased in these reactions, luminescence signal was first increased, followed by a characteristic decrease after reaching an optimal ratio of Hsc70:DJA2 (**Figure 3.5**). In contrast, we found that

phosphorylated Hsc70 had reduced refolding capacity as compared to the Hsc70-wt (**Figure 3.5**). Interestingly, this finding suggests that the effects of phosphorylation are different than what was reported for adenylylation of BiP (30). Specifically, the maximum amount of folded luciferase was decreased and the modified chaperone showed decreased stimulation by DJA2. Thus, LegK4 phosphorylation of Hsc70 decreased both its DJA2-stimulated ATPase activity and its protein refolding function.

Using a phos-tag gel, we quantified the amount of Hsc70 that had been phosphorylated by LegK4. We observed two distinct species, of which 53.4 ± 1.5% was phosphorylated (**Figure 3.5**). The sub-stoichiometric phosphorylation of Hsc70 may explain the modest reduction in ATPase activity.

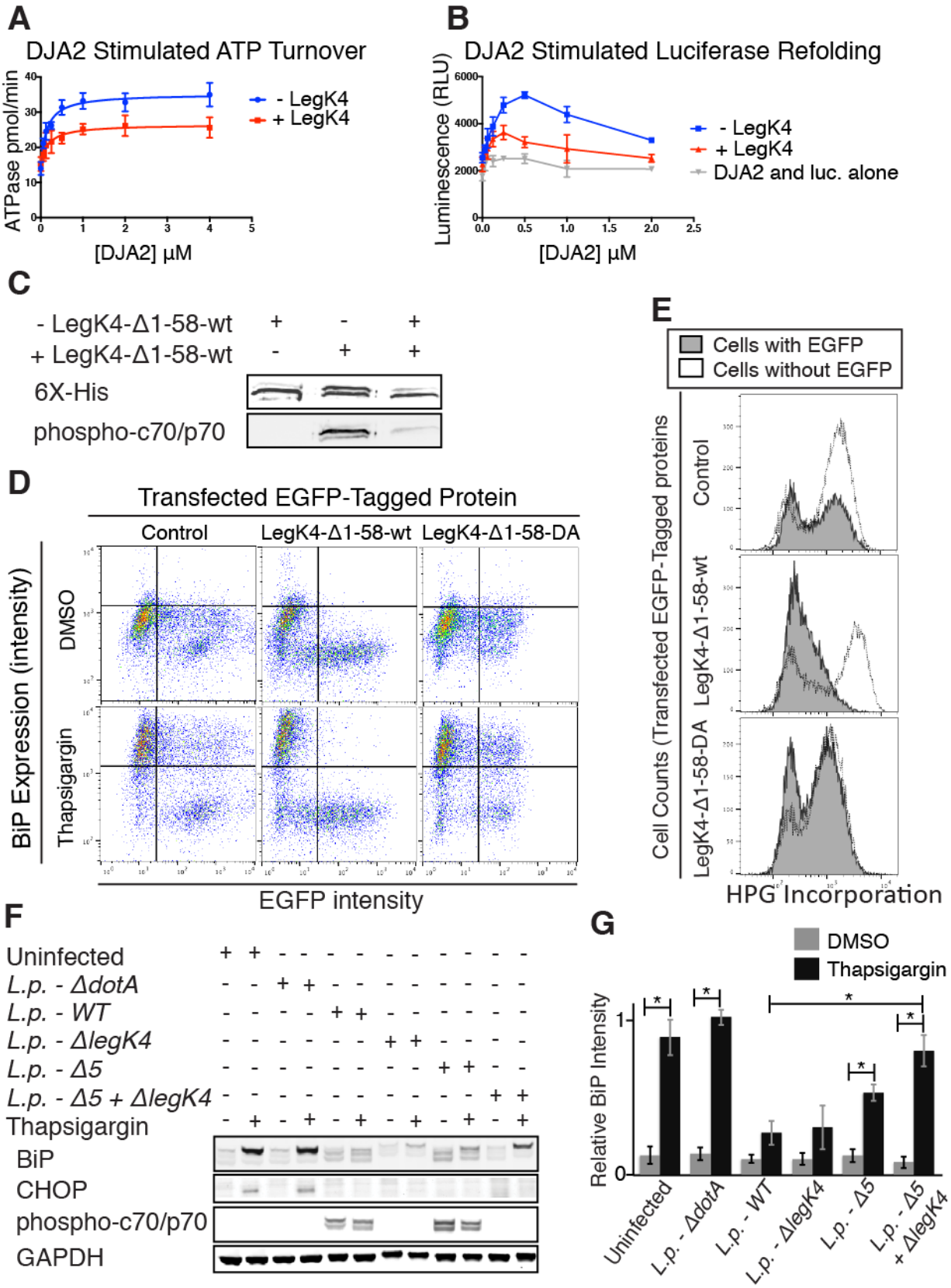

Figure 3.5 Phosphorylation of Hsp70 by LegK4 decreases activity and causes a

reduction in global protein translation. (**A** & **B**) *In vitro* analysis of phosphorylated Hsc70 using purified protein. (**A**) ATPase activity was tested using a malachite green assay with DNAJ2 to stimulate ATPase activity. (**B**) The refolding activity of Hsc70 was determined using a luciferase assay. Luminescence signal was read upon luciferase refolding by Hsc70 in the presence of DNAJ2 to stimulate ATPase activity and refolding. Data analysis for was done using Prism 6 software. ATPase activity was determined using a nonlinear fit and Michaelis-Menten graphical analysis. Each graph represents 6 experimental replicates. (**C**) The amount of phosphorylated Hsc70 after incubation with LegK4 was quantified using Phos-Tag SDS-Page gels. The two distinct bands in lanes containing the phosphorylated Hsc70 were quantified in triplicate to show that 53.4 ± 1.5% of the Hsc70 was phosphorylated. All recombinant Hsc70 was purified with a 6XHis tag, as represented by the western blot. (**D**) BiP levels were tested following transient transfection with EGFP tagged LegK4-Δ1-58-wt, LegK4-Δ1-58-DA, or EGFP control plasmid. After 24 hours of transfection, HEK-293T cells were treated with DMSO or 1uM Thapsigargin for 6 hours. Cells were then analyzed by FACS based on expression of transfected protein (EGFP) and levels of BiP (AF647). (**E**) Global translation was tested using a HPG assay. Cells were pulsed with HPG for 1 hour after transient transfection. EGFP expressing and nonexpressing cells were gated and are shown in grey and white respectively. (**F**) HEK-293T-FCγIII cells were infected with L.p. for 1 hour followed by 5 hour treatment with 1uM thapsigargin. Blotting was done for the UPR stress markers BiP and CHOP. L.p. infections suppress BiP and CHOP overexpression in *WT*, *ΔlegK4*, and *Δ5* strains but allow the expression of higher levels of BiP in the *Δ5 + ΔlegK4* strain. (**G**) BiP levels were quantified from 3 biological replicates using the same experimental conditions. Individual data points were normalized to GAPDH, and all the data was then normalized to the uninfected condition. The values in graphs are mean ± s.e.m. *P<0.05, Student's t-test.

LegK4 suppresses the unfolded protein response

Hsp70 family members are critical effectors of the unfolded protein response. Our previous research showed that *L.p.* has the ability to suppress certain arms of the UPR (33). Following *L.p.* infection and UPR induction with Thapsigargin, there was no upregulation of the canonical UPR targets BiP and CHOP (33). Our work showed that while UPR induction still showed elevated mRNA levels of BiP and CHOP, no protein was produced, indicating that *L.p.* was suppressing the UPR at the level of protein synthesis (33).

We wondered whether the phosphorylation of Hsc70 might be involved in this process. After transient transfection of EGFP-LegK4-Δ1-58-wt, but not EGFP or EGFP-LegK4-Δ1-58-DA, into HEK-293T cells, we observed robust levels of Hsc70 phosphorylation (**Figure 3.4**). We examined the UPR using fluorescence-activated cell sorting (FACS) to distinguish between EGFP-expressing and untransfected cells and then measured levels of the UPR biomarker, BiP, in both cell populations. There was a noticeable increase in the production of BiP after treatment with Thapsigargin in cells transfected with the EGFP control plasmid (**Figure 3.5**). In contrast, cells expressing the EGFP-LegK4-Δ1-58-wt construct did not show increased BiP expression in response to Thapsigargin treatment (**Figure 3.5**). The population of cells in the EGFP-LegK4-Δ1-58-wt experimental sample that were not transfected had a normal response to Thapsigargin treatment (**Figure 3.5**). Interestingly, cells that were not treated with Thapsigargin but were transfected with EGFP-LegK4-Δ1-58-wt also showed a modest decrease in basal levels of BiP as compared to untransfected cells in the same experiment (**Figure 3.5**). The kinase activity of LegK4 is critical, as the kinase dead mutant showed a normal upregulation of BiP after UPR induction (**Figure 3.5**). Transfected HEK-293T cells were pretreated with the proteasome inhibitor MG-132 before Thapsigargin treatment to assess whether the lack of BiP observed in LegK4 expressing cells was due to proteasomal degradation of BiP. BiP suppression by EGFP-LegK4-Δ1-58-wt was unchanged in the presence of the proteasome inhibitor (**Figure 3.4**).

LegK4 expression reduces host global protein synthesis

One role that Hsc70 plays in the cell is to assist in folding of nascent polypeptides during translation (34). Hsp70's dissociation from the ribosome during extreme heat shock leads to an inhibition of global protein synthesis (35). LegK4's phosphorylation and subsequent inactivation of Hsc70 led us to test whether this modification was causing inhibition of global protein synthesis. We used a homopropargylglycine (HPG) assay in which HPG is incorporated into newly synthesized proteins and can act as a reporter of translation (36). Cells were first transiently transfected with the conditions described above. HPG was then pulsed into the media for 1 hour, and newly synthesized proteins were reacted with an azide-fluorophore (AF-647) for analysis with FACS. Cells were sorted into EGFP expressing and EGFP negative (untransfected) populations. We observed a high translation and low translation population of cells in all conditions (**Figure 3.5**). However, the cells that were transfected with EGFP-LegK4-Δ1-58-wt fell exclusively into the low translation population indicating suppression of global translation (**Figure 3.5)**. The cells transfected with EGFP as well as the kinase dead EGFP-LegK4-Δ1-58-DA were observed in both the high and low translating populations (**Figure 3.5**). A previous screen for *L.p.* effectors that block host translation identified Lpg0208 (Pkn5) as a hit (15). We have now confirmed that LegK4 and Pkn5 are the same effectors.

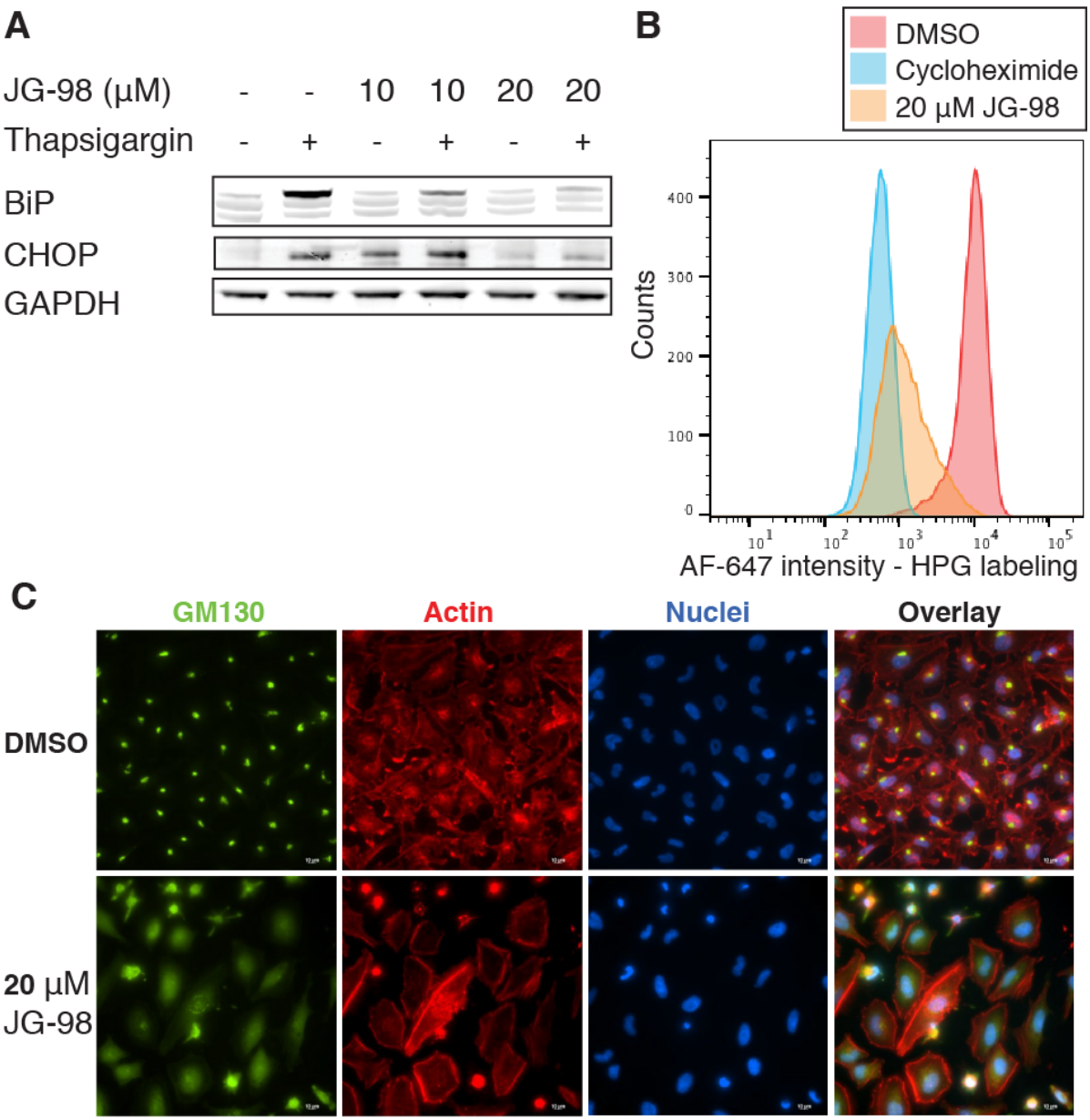

Figure 3.6 JG-98 recapitulates results observed with LegK4. (**A**) HEK-293T cells were pre-treated with JG-98 at indicated concentrations for 1 hour. This was followed by 5 hour treatment with thapsigargin. Levels of BiP and CHOP were determined by western blotting. BiP overexpression appears to be suppressed, while CHOP overexpression was suppressed at a higher dose of JG-98, but not at the lower dose. This experiment was done in biological triplicate (**B**) HEK-293T cells were treated for 2 hours with either JG-98, cycloheximide, or DMSO, followed by a 1 hour pulse with HPG. FACS was used to determine HPG incorporation. Both JG-98 and cycloheximide treatment decreased translation below DMSO control levels. Shown is a representative of the three biological replicates. (**C**) Cells were treated with JG-98 for 24 hours followed by fixing and staining for Golgi and actin. JG-98 treatment showed a clear Golgi fragmentation phenotype while DMSO did not. Shown is a representative of three biological replicates.

We pharmacologically tested whether the disruption of Hsp70 is responsible for the observed reduction in translation by inhibiting Hsp70's ATPase activity with the chemical inhibitor JG-98 (37). Cells pre-treated with JG-98 (20 μM) showed a modest suppression of UPR induction by Thapsigargin, as measured by reduced upregulation of BiP and CHOP (**Figure 3.6**). Treatment with JG-98 (20 μM) also showed a reduction in global protein synthesis using the HPG assay (**Figure 3.6**). We then used JG-98 to test whether the LegK4-mediated Golgi fragmentation phenotype was also produced by inhibition of Hsp70 activity. Cells were treated with JG-98 (20 μM) for six hrs, and stained with phalloidin and GM130 to label actin and Golgi respectively. While the Golgi appeared healthy and perinuclear in the DMSO treated samples, it was difficult to observe any Golgi staining in the JG-98 treated cells due to the robust Golgi fragmentation (**Figure 3.6**). These results corroborated the genetic and biochemical studies, suggesting that Hsc70 may be an important biological target of LegK4.

LegK4 knockout in *L.p.* releases translational suppression of BiP

The functional redundancy between the ~300 effectors of *L.p.* causes very few single effectors to show any growth defect in macrophages. A strain of *L.p.* lacking roughly one third of the entire genome showed no growth defect (38). Instead of looking at growth, we decided to test translation inhibition during infection. First, we tracked levels of phosphorylated Hsp70 during an infection time course to gain a better temporal understanding of the translational control related to LegK4. Phosphorylation of Hsp70 appears to peak at 4 hours, but some phosphorylation is maintained throughout an 8 hour infection time course (**Figure 3.7**).

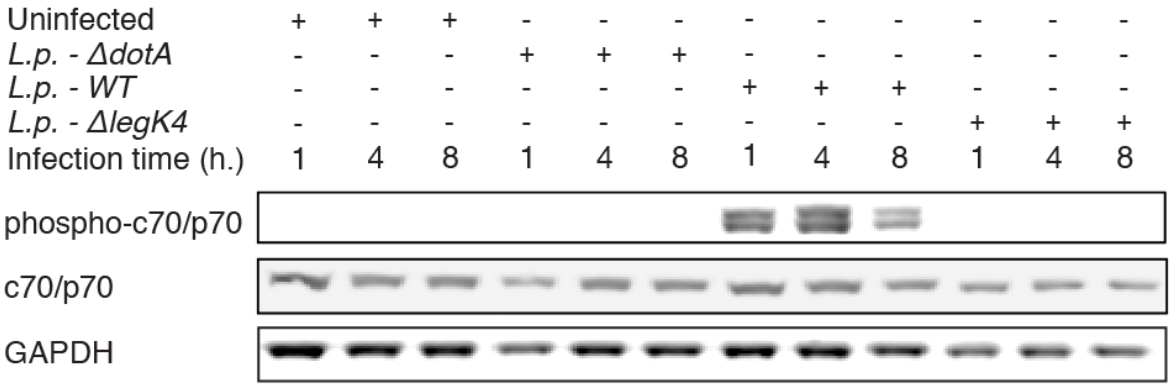

Figure 3.7 Characterization of LegK4 behavior during infection. HEK-293T cells constitutively expressing the FcγRIII receptor were infected with L.p. to determine the temporal activity of LegK4. Phosphorylation of Hsp70 peaks after 4 hours of infection and seems to decrease 8 hour after infection. Shown is a representative of three biological replicates.

We then focused on LegK4 in the context of other *L.p.* effectors that were also shown to block translation. We made use of the Δ5 strain of *L.p*. that lacked the 5 previously identified effectors known to inhibit protein synthesis (39), and tested expression of the UPR marker BiP. The Δ*legk4* and Δ*5* strains both showed similar suppression of BiP after UPR induction with Thapsigargin as compared to WT (**Figure 3.5**). However, the Δ*5* + Δ*legk4* strain showed an upregulation in BiP after Thapsigargin induction (**Figure 3.5**). Interestingly, there was a small but noticeable increase in the amount of BiP expressed in the *L.p.*-Δ*5* (**Figure 3.5**), but it was not significant when compared to the Thapsigargin-induced increase in BiP from *L.p.*-*WT*. There was no noticeable increase in CHOP with the Δ*5* + Δ*legk4* strain. We believe this is because BiP is rapidly and robustly upregulated in response to the UPR. Therefore, it is easier to observe small changes in the amount of newly synthesized protein. This is in contrast to CHOP, which is a low abundance transcription factor.

Transient transfection of LegK4 increases the Hsp70 load on ribosomes

We transiently transfected LegK4 into HEK-293T cells to see if the observed reduction in global translation could be directly linked to Hsp70's association with the ribosome. The cell lysates of LegK4-Δ1-58-wt and LegK4-Δ1-58-DA transfected cells were fractionated with a sucrose gradient. The UV traces of the gradient showed that LegK4-Δ1-58-wt transfected cells had an increased 80S monosome peak while the heavier polysome peaks were decreased as compared to the kinase dead LegK4-Δ1-58-DA transfected cells (**Figure 3.8**). This result confirms our previous finding that LegK4-Δ1-58-wt decreases global translation, as there are less of the highly translating polysomes present in the UV trace. To validate the possibility that the observed changes in the ratio between polysomes and monosomes was due to Hsp70, we fractionated the lysate of HEK-293T cells treated with JG-98 for 3 hours. An increase in the 80S monosome peak and subsequent decrease in the heavy polysomes was also observed in these samples, as compared to the DMSO treated sample (**Figure 3.8**).

To explore the interaction between phosphorylated Hsp70 and the translating ribosome, we precipitated Hsp70 from each fraction of a sucrose gradient in LegK4-Δ1-58-wt and LegK4-Δ1-58-DA transfected cells. Surprisingly, we noticed that wt LegK4 caused a higher load of Hsp70 in the fractions containing ribosomes compared to the catalytic dead mutant (**Figure 3.8**). As heavier polysome fractions started to emerge, the difference in the amount of Hsp70 between LegK4-Δ1-58-wt and LegK4-Δ1-58-DA transfected cells, became more pronounced.

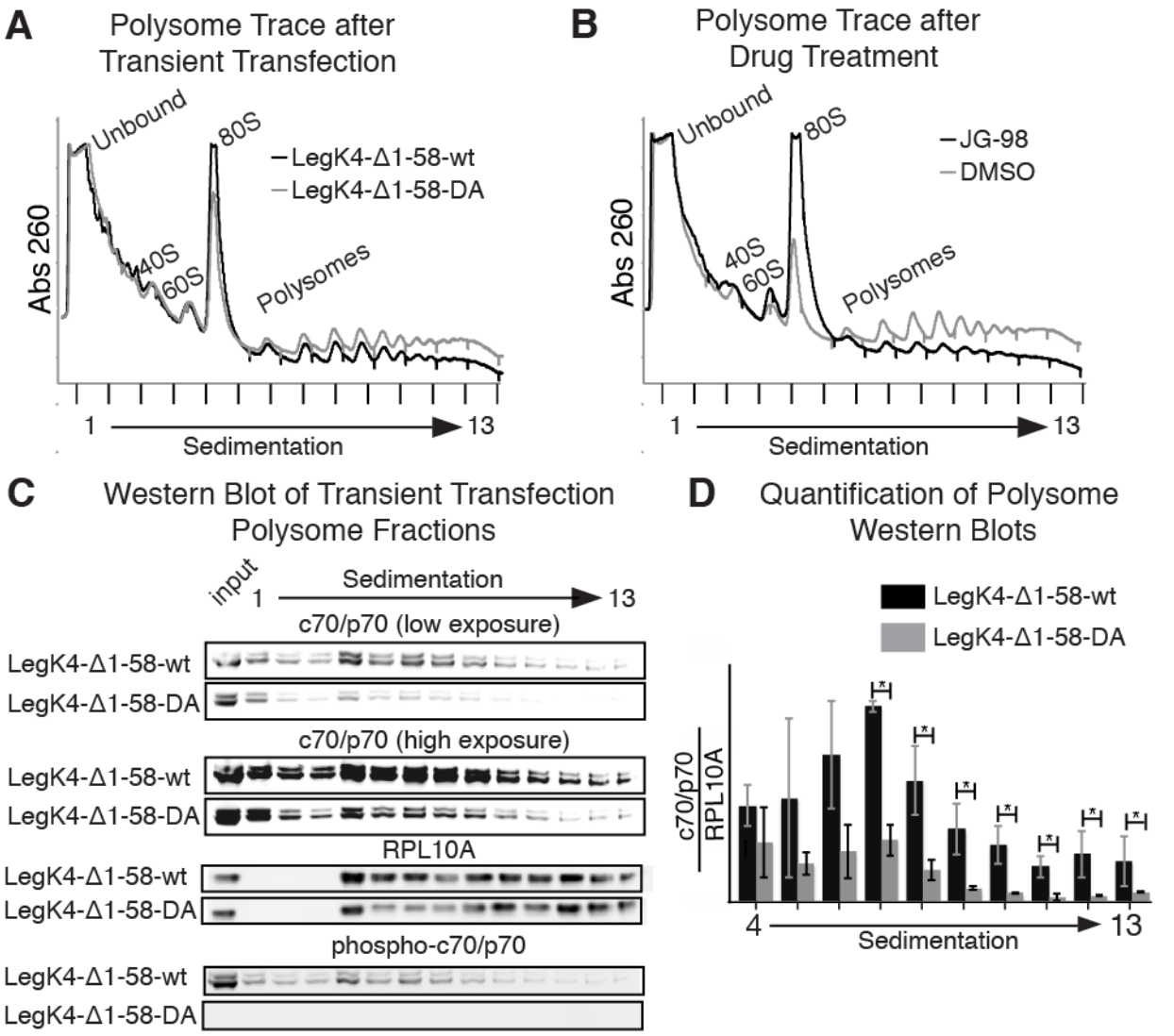

Figure 3.8 Interactions of phosphorylated Hsc70 with the ribosome. (**A & B**) HEK-293T cells were transiently transfected with LegK4-Δ1-58-wt or LegK4-Δ1-58-DA (**A**), or treated with DMSO or JG-98 for 3 hours (**B**), and the lysates were loaded onto a sucrose gradient and fractionated into polysomes. Protein levels were monitored at a 240 nm absorbance until the entire gradient ran. The graph is a representative of the polysome UV trace which were done in triplicate. (**C**) The protein was precipitated and western blots were run on all fractions from the transient transfection experiment in (**A**) to determine amount of cytosolic Hsp70 (c70/p70) associated with the polysomes. (**D**) c70/p70 levels of each fraction containing RPL10A were quantified from 3 biological replicates using the same experimental conditions. Individual data points were gathered by dividing the raw quantitation of c70/p70 by the amount of RPL10A. The data was then normalized to the input. The values in graphs are mean ± s.e.m. *P<0.05, Student's t-test.

Discussion:

Several potent bacterial toxins have been previously shown to target host protein synthesis. From the earliest discovery of Diphtheria toxin (3) to more recent advances in Shiga toxin (4), and several translocated effectors of the Type III and Type IV secretion systems, researchers have identified fascinating mechanisms for blocking host protein synthesis (2). Conversely, some pathogens, such as Herpesvirus, produce effectors that play a role in stimulating mRNA translation (40). Almost all cases of translation inhibition are a result of targeting the translation machinery itself such as inhibiting elongation or initiation factors (e.g. Diphtheria toxin or Lgt effectors from *L.p*.) (3, 12, 13). We have identified a novel method of translation suppression and have characterized a highly specific and functionally important target of the *L.p.* eSTPK LegK4. The most prominent previous research done on LegK4 was limited to a crystal structure of the kinase domain showing that it does indeed adopt the fold of a eukaryotic-like kinase, and contains a novel dimeric interface not observed in any eukaryotic protein kinases (23). Through the phosphorylation of Hsp70, LegK4 is able to reduce global translation (**Figure 3.9**). To our knowledge, this is the first description of a bacteria using a PTM to directly target Hsp70 during infection.

Hsp70 is an essential protein and serves a large number of functions in the host cell. Our results show that one of the primary reasons *L.p.* targets Hsp70 is to reduce host translation. We have not excluded the fact that Hsp70 phosphorylation could serve to help *L.p.* infections in other ways, and this is a subject of ongoing investigation.

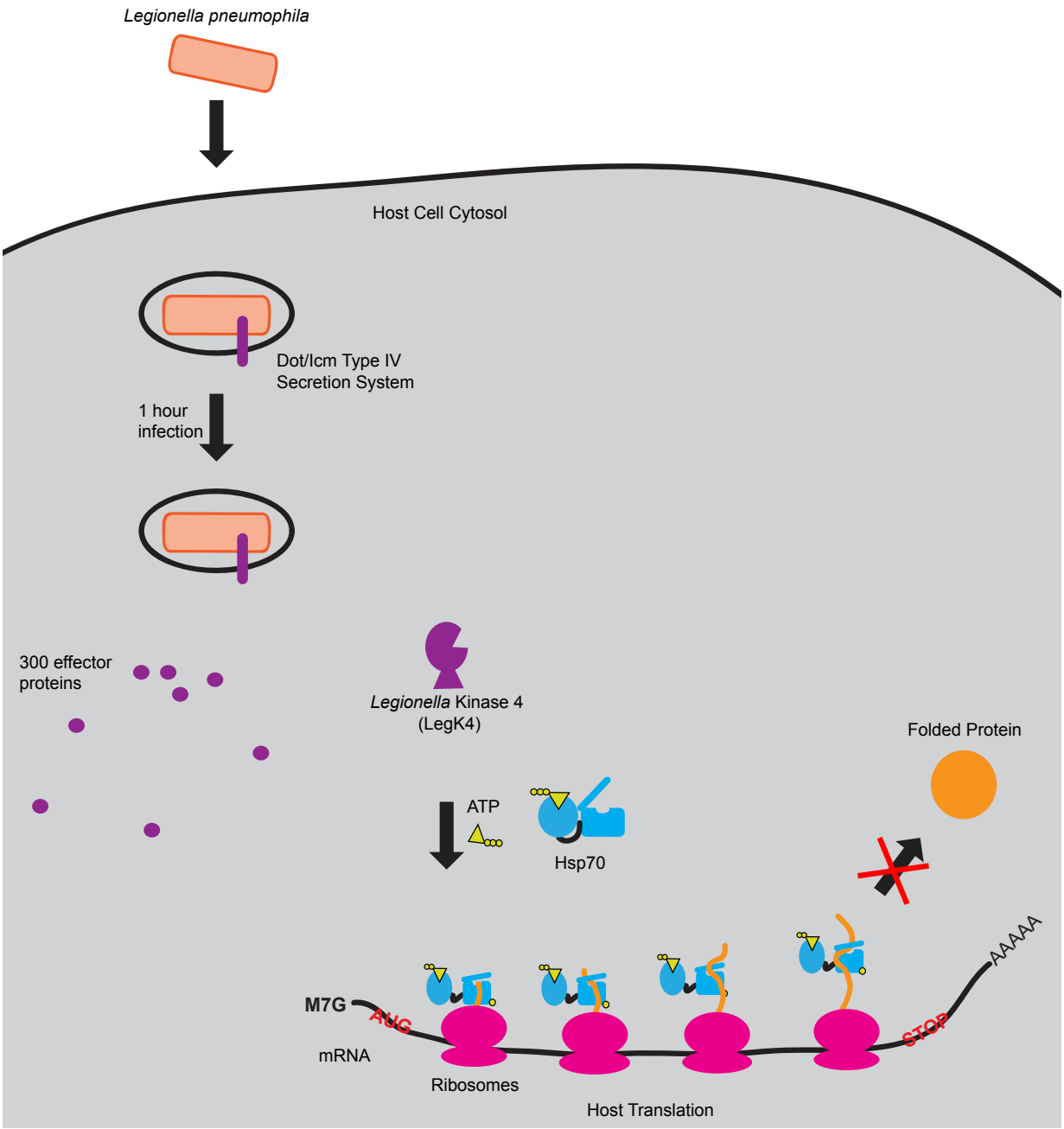

Figure 3.9 Diagram of LegK4 interactions in the host cell. The diagram shows *Legionella* entering the host cell and releasing effector proteins that include LegK4. LegK4 then targets Hsp70 which resides on the ribosome and prevents protein synthesis and reduces global translation.

L.p. tightly controls host translation and the UPR. While many pathogens control host protein synthesis, *L.p.* is thought to use this mechanism to increase the available amino acid pool, which the pathogen then uses for its own survival (41). The

complimentary inhibition of the UPR is a common mechanism by which many bacteria promote their own survival inside of a host cell (42). Even in cases where multiple *L.p.* effectors that control protein synthesis are removed, such as *L.p.*-Δ*5*, there are mixed results in recovering host translation (15). Monitoring BiP, which is produced rapidly and robustly following induction of the UPR, provides a more sensitive method for observing the recovery of host translation. The *L.p.*-Δ*5*+Δ*legk4* showed a recovery of BiP expression that has not previously been seen in *L.p.* infection. This further implicates LegK4's role in suppressing translation, and subsequently UPR signaling (33).

We also describe the first PTM of Hsp70 that is directly linked to protein synthesis. There is a large body of work characterizing the endogenous adenylylation of BiP at a homologous site to the phosphorylation that we observed (30, 31, 43, 44). These studies have shown an important role of adenylylation regulating BiP activity during the UPR cycle. Phosphorylation of this site in cytosolic Hsp70s imparts an increased association with the ribosome. There are many possible explanations as to why an increase in Hsp70 on ribosomes can cause a decrease in protein synthesis. Taken together, our data suggests that a LegK4 mediated block in protein synthesis raises the possibility that phosphorylated Hsp70 is unable to fold nascent polypeptides correctly and thus remains associated with the polysomes longer than usual. Ongoing future work will look to address the details of the mechanism by which phosphorylated Hsp70 remains on the ribosome.

Prolonged exposure to LegK4 and the subsequent reduction in global translation, is toxic to mammalian cells. To temper individual effectors in *L.p.* that are toxic, the bacterium frequently uses a counter-measure to ensure that the host cell does not

induce apoptosis (45). We postulate two possible explanations for how *L.p.* manages LegK4-associated toxicity and allows the host cell to continue living. First, it is possible that, similar to other PTMs performed by *L.p.*, there is a eukaryotic-like phosphatase co-effector that is secreted to prevent over-stimulation by phospho-Hsp70. Alternatively, because phosphorylations are endogenous PTMs, it is possible that *L.p.* exhibits temporal control and secretes LegK4 at the beginning of its lifecycle while mammalian phosphatases are able to remove the PTM over the course of the infection. Our experiments suggest that phosphorylation peaks after 4 hours of infection and then is reduced 8 hours into infection (**Figure 3.7**). Determining the cause of this reduction is an ongoing area of research. Previous work using a yeast lethality screening assay claimed that LegK4 yeast toxicity was abrogated by the uncharacterized effectors RavO (lpg1129) and MavM (lpg2577) (46).

LegK4's phosphorylation of Hsp70 at a site that reduced global translation also indicates the possibility of an endogenous mammalian kinase that is capable of causing Hsp70 phosphorylation. Many PTMs observed during *L.p.* infection mimic mammalian signaling. There are also scenarios in which a cell reduces or alters global translation, particularly under stress (47, 48). Interestingly, the phosphosite database on protein PTMs reports a possible phosphorylation of Thr 518 in the Hsp70 chaperone, BiP, the analogous site of Hsp70 phosphorylation mediated by LegK4 (49). Future work holds promise in identifying an endogenous kinase as well as further characterizing the phosphorylation at this site in relevance to other diseased or stressed conditions.

Materials and Methods

Experimental Model and Subject Details

All HEK-293T (Female) and HeLa (Female) cell lines were grown at 37°C and 5% CO_2 in DMEM (Gibco) containing 10% (vol/vol) FBS (Axenia BioLogix). HeLa cells were authenticated through the UCSF Cell Culture Facility.

All *L.p.* proteins were cloned from genomic DNA prepared from the Philadelphia strain of WT *L.p.* (LP01) and cloned into their respective vectors. The LP02 thymidine auxotrophy strain of *L.p.* (LP02) was used in all cases of infection. All strains were grown on charcoal-yeast extract (CYE) plates for 48 hours. These plates were supplemented with the appropriate antibiotic when plasmids were introduced, and thymidine (100 µg/mL) for all LP02 growth. The *ΔlegK4* and *Δ5 + ΔlegK4* strains were constructed by allelic exchange (50) using the gene replacement vector pSR47S as previously described (51). Plasmids for *L.p.* transformation were made by cloning the specified DNA into pJB1806 (52), a kind gift from the lab of Dr. Craig Roy, behind an introduced 3x FLAG tag. *L.p.* strains that were overexpressing 3X-Flag epitope tagged proteins were transformed with a pJB1806 plasmid containing an IPTG inducible tac promoter. The transformation was done by electroporation as previously described (53). The recovery was done on CYE plates containing chloramphenicol (10ug/mL).

Hsc70 proteins and vectors (pMCSG7) were gifts from J.E.G. and they were cloned from the *Homo sapien* Hsc70 and included a 6XHis tag followed by a TEV cleavage site. Protein purifications for *L.p.* proteins used a pPROEX HTb vector that included a 6XHis tag followed by a TEV cleavage site.

All yeast experiments were done with the with the BY4741 strain. For yeast overexpression experiments, proteins were cloned into a pCH043 plasmid, a kind gift from the lab of Dr. Jaime Fraser at UCSF. For mammalian transfection, all proteins were cloned into a pEGFP-C2 plasmid. All point mutants were generated by site directed

Method Details

Transfections and Western Blotting

Fugene HD (Promega) and opti-MEM (Gibco) were used for all transfections of HeLa and HEK-293T cells. Cells were transfected (conditions based on manufacturers recommendations) once the cells reached 60% confluency, for 24 hours. Cells were harvested at 75-85% confluency. Mammalian cell lysis was performed in cell lysis buffer (20 mM Tris at pH 7.6, 100 mM NaCl, 1 mM MgCl2, 1 mM DTT, 1% Triton, 1x Roche EDTA-free Complete protease inhibitor mixture, and 1x PhosStop phosphatase inhibitor (Roche)) unless otherwise specified. For western blotting, cells were washed once with ice cold PBS, and lysed in cell lysis buffer for 30 minutes on ice. Protein concentrations were measured using a Bio-Rad Protein Assay Dye (procedure based on factory recommendations).

After this, 10-20 µg of protein were separated by SDS/PAGE using pre-cast 4-12% Bis-Tris gels (Thermo-Fischer) and run in MOPS (Invitrogen) buffer at 200V for 1 hour. Following this, gels were transferred to 0.45µM nitrocellulose paper (Bio-Rad) in transfer buffer (1X TOWBIN, 10% v/v MeOH) at 90V for 35 minutes. Membranes were blocked for 1 hour, and then incubated with antibody concentrations based on the

manufacturer's guidelines in all cases except the pT495-Hsc70/Hsp70 and the pT518-BiP antibodies from GenScript, which were used at 1:10,000. All blocking and primaries were done in a 5% bovine serum albumin (BSA) (Sigma-Aldrich) in TBST solution containing 0.02% (w/vol) sodium azide. Blots were imaged on a Licor system. All biological experiments were performed in triplicate and a representative blot was chosen for publication.

Immunofluorescence

HeLa cells were plated on glass coverslips and grown to 60% confluency. Cells were then transfected, grown for 24 h, and fixed. For Hsp70 drug treatment, cells were grown to 60% confluency, treated with JG-98 (Gifted from J.E.G.) for 6 hours at indicated concentrations, and then fixed. Fixing was done with 4% paraformaldehyde, followed by permeabilization with 0.1% saponin (Sigma Aldrich), and staining. Transient transfection staining included rabbit anti-GFP and mouse anti-GM130 (Invitrogen) for 1 hour, followed by washing, then anti-rabbit and anti-mouse antibodies conjugated to Alexa-488 and Alexa-568, respectively. Drug treated cells were stained with rhodamine-phalloidin (Invitrogen) and mouse anti-GM130 followed by anti-mouse Alexa-488. Coverslips were then stained with Hoeschst reagent, fixed to slides, imaged, and quantified manually.

Quantification for transient transfection was performed by randomizing samples with numbers assigned by labmate that were hidden to experimenter. One-hundred EGFP positive cells were counted and the Golgi were observed for fragmentation. Following quantification, the identity of samples was revealed to the experimenter.

Yeast Growth Assay

Handling and transformations were done based on previously published methodologies (54). Following transformations, each yeast strain was streaked on SD –URA. A single colony was grown overnight in SD –URA media with shaking. In the morning, a new liquid culture was started at OD_{600}=0.25. When cultures reach an OD_{600}=1.0, 5 mL was collected, washed in sterile ddH_2O, and resuspended in 500uL of ddH_2O. Five µL of each condition was plated on SD –URA and Gal/Raf –URA plates, and grown for 3 days to analyze growth. Experiment was done in biological triplicate and a representative image is shown in the figure.

Purification of LegK4 and Hsp70s

LegK4-Δ1-58-wt was purified as previously described (23). Hsc70, Hsp72, BiP, and all point mutations of these proteins were purified as previously described (55). Briefly, plasmids containing His-tagged proteins were transformed into *E. coli* BL21 (DE3). Following transformation, Bacteria were grown in TB broth at 37°C to an OD_{600}=0.6. Protein expression was induced by adding 1mM Isopropyl β-D-1-thiogalactopyranoside (IPTG), and the bacteria grew at 18°C for 16 hours. Selection antibiotic concentrations used for respective plasmids are as follows: ampicillin – 100 µg/mL, kanamycin – 50 µg/mL, chloramphenicol – 10 µg/mL (GoldBio). The cells were harvested by centrifugation and then mechanically lysed with a microfluidizer in lysis buffer (50 mM Tris at pH 8.0, 500 mM NaCl, 10% glycerol (vol/vol), 20 mM Imidazole, and 1x Roche Complete protease inhibitor mixture). The cleared lysate was incubated with 1mL/L

Ni/NTA agarose resin (Qiagen) for 1 hour at 4°C. Bound proteins were washed with lysis buffer and eluted in buffer containing 300 mM imidazole. LegK4-Δ1-58-wt was further purified by size-exclusion chromatography on a Superdex 200 column (Amersham Biotech) and concentrated. In cases where the His tag needed to be cleaved, The purified LegK4-Δ1-58 was mixed with 6x-His tagged TEV protease at a 1:40 (w/w) ratio in the presence of 0.5 mM EDTA and 0.5 mM DTT. The mixture was dialyzed against 20 mM Tris at pH 8.0, 150 mM NaCl, and 5% glycerol (vol/vol) at 4°C. Cleaved LegK4-Δ1-58-wt was separated from uncleaved protein by reloading dialyzed protein onto Ni/NTA agarose resin. This was incubated for 1 hour at 4°C, and initial flow through was collected and concentrated. All Hsp70s were further purified by an ATP-agarose column using previously established protocols (56). Purified DnaK, Hsc70-NBD, Hsc70-SBD, Hsp72-NBD, and Hsp72-SBD were acquired from J.E.G. Purified Grp92 and Hsp90α were gifts from the lab of Dr. Jack Taunton at UCSF.

Thiophosphorylation assays and immunoprecipitations.

Thiophosphorylation assays were performed as previously described (57). In brief, assays for cell lysates and purified Hsp70s with purified LegK4-Δ1-58-wt were performed in buffer containing 50 mM Tris at pH 7.5, 150 mM NaCl, and 10 mM $MgCl_2$. For experiments with purified substrate, the buffer was supplemented with 1 µg of purified Hsp70 per condition, 0.1 µg of purified LegK4-Δ1-58-wt per condition, and ATP-γ-thiophosphate (Axxora) at 250 µM. Cell lysate labeling experiments were done with HEK-293T at a concentration such that there was 20 µg of protein per condition. Lysate was incubated with buffer supplemented with 250 µM of the designated ATP-γ-

thiophosphate analog (6-Benzyl-ATP-γ-S (Bn) Axxora) 250 μM ATP, 3 mM GTP, and 1% (w/w) purified LegK4-Δ1-58-wt. Labeling reactions were left at room temperature for 1 h before quenching with 25 mM EDTA. Thirty μL aliquots of each reaction were alkylated with 2 uL of 100 mM p-nitro benzyl-mesylate (PNBM) for 30 minutes at room temperature. Thiophosphorylation was detected by western blot with the antithiophosphate antibody. Immunoprecipitations of thio-phosphorylated substrates were performed using Bn-ATP-γ-S as previously described (26).

LC-MS/MS Phosphosite Identification

Purified Hsc70-wt was phosphorylated with LegK4 as described for the thiophosphorylation assay, with the exception that ATP-γ-thiophosphate was replace with 1 mM ATP. Mass Spectrometry was performed as previously described (57) with some modifications. After the 1 hour incubation at room temperature, ammonium bicarbonate and DTT were added to the reaction to reach final concentrations of 50 mM and 5 mM, respectively. The proteins were denatured at 55°C for 30 min. Denatured proteins were alkylated with Iodoacetamide that was added to 10 mM, and the solution was incubated at room temperature for 30 min. Samples were digested overnight at 37°C with trypsin or Asp-N (Promega) at a 1:20 (w/w) ratio. Peptides were acidified with 2% (vol/vol) formic acid, desalted with ZipTips (Millipore), and speed-vacuumed to dryness.

Desalted peptides were resuspended in 0.1% formic acid and diluted so that only 0.1 μg of peptides were analyzed per LC-MS/MS run. Peptides were loaded onto a nanoACQUITY (Waters) UPLC instrument for reversed-phase chromatography with a

C18 column (BEH130, 1.7-μM bead size, 100 μm x 100 mm) in front of an LTQ Orbitrap Velos. The LC was operated at a 600-nL/min flow rate and peptides were separated over a 60-min gradient from 2 to 50% buffer B (Buffer A: water and 0.1% formic acid; buffer B: acetonitrile and 0.1% formic acid). Survey scans were recorded over a 350-1,800 *m/z* range and MS/MS fragmentation was performed using HCD on the top eight peaks. Peak lists were generated with an in-house software called PAVA and searched against the SwissProt *Homo sapien* database (downloaded June 27, 2013; 20,264 entries), as well as a manual user input of the LegK4 amino acid sequence, using Protein Prospector (v5.21.2). Data were searched with a 20-ppm tolerance for parent and fragment ions allowing for standard variable modifications and S/T/Y phosphorylation.

***L.p.* Infections.**

HEK-293 cells expressing FCγRIII (Gift from the lab of Dr. Craig Roy) cells were infected as described previously (10). Cells were grown to 80% confluency and infected with the designated *L.p.* strain or isogenic mutant at an MOI of 100. Following a 48 hour heavy patch, *L.p.* was grown in ACES buffered yeast extract (AYE) supplemented with 0.33 mM $Fe(NO_3)_2$, 3.3 mM L-cysteine, and any necessary antibiotics or auxotrophy supplements. In any 3X-Flag overexpressing strains, AYE broth included 0.5 mM IPTG to induce protein production. Liquid cultures were grown overnight and collected at an OD_{600} of 3.0-3.5. HEK-293 cells require opsonization which uses a lab-generated anti *L.p.* antibody at 1:2000 for a 20 min incubation with *L.p.* before infection. For the 3X-Flag overexpressing strains of *L.p.*, all media used during infection included 0.5mM

IPTG. Infection was initiated with a centrifugation spin at 1000xg. Treatment of cells with thapsigargin (Enzo) was done as described previously (33). Briefly, cells were washed once with PBS after 1 hour of infection followed by the addition of either thapsigargin at 1uM or DMSO for 5 hours. All infected cells were harvested after infection, and snap frozen at specified time points.

Isolation of purified phosphoT495-Hsc70

The Hsc70 purification process started as described above. Following the lysis with a microfluidizer and clearing of the lysate by centrifugation, the protein concentration of the crude cellular supernatant was measured using a Bio-Rad protein assay dye. The lysate was split into two even aliquots (phosphorylated and nonphosphorylated samples). Both samples were treated with $MgCl_2$ to a final concentration of 10mM and ATP to a final concentration of 1 mM. Purified LegK4-Δ1-58-wt without a 6x-His tag, was added to one of the samples (phosphorylated) at 1% (w/w) of total protein concentration. The samples were both incubated at room temperature for 2 hours with gentle rotation. Following this, the samples were purified in the same way as other Hsp70s starting with Ni/NTA-agarose resin.

ATPase assays with Malachite Green

The ATPase activity of phosphorylated and non-phosphorylated Hsc70 was done with malachite green (MG) (Sigma Aldrich) as described previously (56). Briefly, in a clear 96-well plate, phosphorylated or non-phosphorylated Hsc70 were incubated with human DnaJA2 (DJA2) in 25 µL total volume. The assay buffer was 100 mM Tris at pH 7.4, 20

mM KCl, 6 mM $MgCl_2$, and 0.01% Triton. The reaction was initiated by the addition of ATP at a final concentration of 1 mM and incubated at 37 °C for 1 hour. After incubation, 80 µL of MG reagent was added, followed by 10 µL of saturated sodium citrate to quench the reaction. Absorbance was measured at 620 nm on a SpectraMax M5 plate reader (Molecular Devices). ATP hydrolysis rates were calculated by comparison to a phosphate standard. Displayed curves are a combination of 6 replicates.

Luciferase Refolding

Luciferase refolding assays were preformed as previously described (58). Briefly, native firefly luciferase (Promega) was denatured in 6 M guanidinium hydrochloride for 1 h at room temperature and then diluted into assay buffer (28 mM HEPES at pH 7.6, 120 mM potassium acetate, 12 mM magnesium acetate, 2.2 mM DTT, 8.8 mM creatine phosphate, and 35 U/mL creatine kinase). Solutions were prepared of phosphorylated and nonphosphorylated Hsc70, denatured luciferase (at 0.1 µM), DnaJA2 (DJA2) and 1 mM ATP. Total volume was 25 µL and incubation time was 1 hour at 37 °C. Steady Glo reagent was prepared fresh and added to the plate immediately prior to reading luminescence. Displayed curves are a combination of 6 replicates.

SDS-PAGE Phos-Tag Gels

Hsc70 that was phosphorylated by LegK4 during the purification process was separated into phosphorylated and nonphosphorylated species using 8% SDS-PAGE gels with 100µM Phos-tag™(Wako Chemicals) acrylamide and 200µM $MnCl_2$. Gels were run under standard electrophoresis conditions. Gels were then incubated in

transfer buffer containing 1 mM EDTA for 20 minutes, followed by incubation in transfer buffer for another 20 minutes. Gels were transferred and treated as described above. This experiment was repeated in triplicate and then quantified to obtain the ratio of phosphorylated vs. nonphosphorylated Hsc70 in the sample.

Flow Cytometry Experimentation and Analysis

All flow cytometry experiments were performed on a FACSCantoII (BD Biosciences) using 405 nm, 488 nm, and 635 nm lasers, and the software analysis was done using FlowJo (v. 10.3.0). Cells were first gated for singlets by graphing forward scatter height vs. forward scatter area and excluding any outliers. These cells were then gated for viability by removing any cells above background control of the Zombie Aqua dye with 405 nm laser. Any further analysis was done only on this population of cells.

BiP Expression Assay for FACS

HEK-293T cells were grown and transiently transfected in 6-well plates, as described above. For experiments with MG-132, cells were pretreated with 10 μM MG-132 (Selleckchem) or DMSO for 1 hour. All cells were treated with 1 μM Thapsigargin or DMSO for 6 hours. Cells were removed from the plate, washed 2x with phosphate buffered saline (PBS), and stained with Zombie Aqua (BioLegend) at 1:1000 in PBS to test for viability. Cells were washed 2x with PBS, fixed with 4% paraformaldehyde, washed once with PBS, washed once with permeabilization buffer (3% (w/vol) BSA, 0.5% saponin (w/vol), and PBS), and incubated in permeabilization buffer for 30 min at room temperature. Cells were spun down and resuspended in permeabilization buffer

containing BiP antibody at 1:100 (manufacturer recommended conditions for fixing, permeabilization, and antibody concentrations) for 30 min at room temperature. Cells were washed 3 times with permeabilization buffer and resuspended in permeabilization buffer, with anti-rabbit Alexa-647 (Invitrogen) at 1:1000, for 30 min at room temperature. Cells were washed twice with permeabilization buffer and twice with FACS buffer (1% BSA (w/vol) in PBS) and then resuspended in FACS buffer for analysis by flow cytometry.

Measuring Translation with Homopropargylglycine

Homopropargylglycine (HPG) labeling was performed as described previously (59), with some modifications. HEK-293T cells were grown on 6-well plates and were either transiently transfected as described above, or grown to 80% confluency and treated with drug for 1 hour (JG-98 at 20 μM and cyclohexamide (Cell Signaling Technologies) at 100 μg/mL). Media was removed and cells were washed with PBS. HPG was pulsed for one hour at 37°C and 5% CO_2, by adding cys/met-free DMEM (Thermo Fisher - 21013024) supplemented with 10% dialyzed FBS (Thermo Fisher), 200 μM cys (Sigma Aldrich), and 1 mM HPG (ClickChemistryTools) or 1 mM Methionine (Sigma Aldrich) as a negative control. Cells were washed once with PBS, then removed from plates with 250 μL of 0.25% Trypsin-EDTA solution (LifeTechnologies). Cells were washed twice with PBS and stained with Zombie Aqua at 1:1000 in PBS. Cells were washed 2x with PBS, then fixed with 4% paraformaldehyde. Fixed cells were washed twice with PBS, and twice with permeabilization buffer. Cells were resuspended in 25 μL of permeabilization buffer and 100 μL of azide click mixture (50 mM HEPES at pH 7.5, 150

mM NaCl, 400 µM Tris(2-carboxyethyl)phosphine hydrochloride (TCEP) (Pierce), 250 µM Tris[(1-benzyl-1*H*-1,2,3-triazol-4-yl)methyl]amine (TBTA) (ClickChemistryTools), 5 µM AlexaFluor-647 azide (Thermo Fisher), and 200 µM $CuSO_4$ (Sigma Aldrich)) was added. This was gently mixed and incubated overnight in the dark. The cells were washed three times with permeabilization buffer, twice with FACS buffer, and then analyzed via flow cytometry.

Polysome Fractionation and Protein Precipitation for Western Blotting

Polysome profiling was performed as previously described (60). In brief, 5 X 10 cm plates of transiently transfected or drug treated (JG-98 or DMSO at 20µM for 3 hours) cells were treated with 100 µg/mL cyclohexamide for 5 min at 37°C and 5% CO_2. Cells were collected, washed with PBS containing 100 µg/mL cyclohexamide, then lysed in polysome buffer (10 mM HEPES at pH 7.4, 100 mM KCl, 5 mM $MgCl_2$, 100 µg/mL cyclohexamide, and 2 mM DTT) supplemented with 1% Triton, 1x Roche EDTA-free Complete protease inhibitor mixture, 1x PhosStop phosphatase inhibitor (Roche), and 100 U/mL of RNaseOUT (Invitrogen). Lysates were cleared by centrifugation for 10 min at 9300xg and supernatants were loaded onto a 10-50% sucrose gradient. Sucrose gradients were made by diluting 60% Sucrose solution (60% w/v sucrose in polysome buffer) to 10% and 50% sucrose solutions with polysome buffer. Each centrifuge tube was filled half-way with 10% and then 50% sucrose solutions, and a Gradient Master 108 (BIOCOMP) was used to make the gradients.

Samples were spun at 37,000rpm for 2.5 h at 4°C in a Beckman L8-70M ultracentrifuge using a Beckman SW-40 rotor, and then separated on an ISCO gradient

fractionation system to evaluate polysome profiles and collect polysome fractions. Protein was precipitated from each individual fraction using a trichloroacetic acid (TCA) (Fisher) - acetone precipitation. A 6M stock solution of TCA was added to each fraction to reach a final concentration of 20% (vol/vol). This was incubated on ice for 30 min, followed by centrifugation at 20,000xg for 30 min. The pellet that formed was washed twice with ice-cold acetone and then air dried for 2 min. The protein pellet is dissolved in Laemmli buffer at pH 8.8 to neutralize any remaining TCA. Samples were denatured at 95°C for 10 min and then used in western blotting.

Antibodies used were as follows, with product number in parenthesis: Abcam: Antithiophosphate ester (Ab92570); proteintech: BiP (11587-1-AP), CHOP (15204-1-AP); Enzo: HSC70/HSP70 (ADI-SPA-820); NovusBio: RPL10A (NBP2-47298); Cell Signaling Technology: GAPDH (2118); Invitrogen: FLAG (MA1-91878-D680); BD: GM-130 (610823). Both the pT495 HSC70/HSP72 rabbit polyclonal antibody and the pT518 Grp78/BiP mouse monoclonal antibody were raised by GenScript and are available upon request.

Quantification and Statistical Analysis

Quantification of the transient transfection immunofluorescence images was graphed using Prism 6.0. error bars in **Figure 3.1** represent s.e.m. and the data is pooled from 3 biological replicates that included the counting of 100 EGFP positive cells for all conditions.

The *In vitro* Hsc70 assays in **Figure 3.5** were analyzed using Prism 6.0. Each line represents the averages of 6 replicates. The data in **Figure 3.5** was fit to a Michaelis-Menten curve and the error bars for both Figures represent s.e.m. for each data point. The acquired V_{max} was determined with the same analysis and represents V_{max} ± s.e.m.

Quantification of western blots was performed using ImageJ64. Raw quantifications were used for analysis and standardization as specified in the figure legends for **Figure 3.5 and Figure 3.8**. Error bars in these graphs represent s.e.m. Significance indicated by "*" in the text is designated at $P<0.05$ using a Student's t-test. Each experiment was done in biological triplicate.

Acknowledgements

We thank members of the Ruggero lab at UCSF (especially Dr. Crystal Conn, Dr. Xiaming Pang, and Dr. Duygu Kuzuoglu) for helpful discussions, protocols, and use of the ISCO purification system; Dr. Jack Taunton at UCSF and his lab (especially Dr. Jordan Carelli) for helpful discussion, protocols, and reagents for HPG assays; members of J.E.G.'s lab for reagents and plasmids; Dr. Rebecca Levin for helpful discussions and protocols; Dr. Alma Burlingame for use of the mass spectrometry; Sarah Elmes for help and access to the flow cytometry instruments. This work was funded by RO1 CA190409, RO1 AI1099245, and U19 AI109622 (K.M.S.); RO1 AI118974, and A129837 from the pew charitable trust (S.M.); RO1 NS059690 (J.E.G.); R01CA140456, R01CA184624, and R01CA154916 (D.R.); NSF-GRFP award 2015204830 (S.M.M.); the facilities at UCSF National Institutes of Health shared

instrumentation program grant 1S10OD016229-0 (Dr. Alma Burlingame). K.M.S. is an Investigator of the Howard Hughes Medical Institute.

References:

1. Salomon D, Orth K (2013) What pathogens have taught us about posttranslational modifications. *Cell Host Microbe* 14(3):269–279.

2. Mohr I, Sonenberg N (2012) Host translation at the nexus of infection and immunity. *Cell Host Microbe* 12(4):470–483.

3. Collier JR (1975) Diphtheria Toxin: Mode of Action and Structure. *Bacteriological Reviews* 39(1):54–85.

4. Brown JE, Rothman SW, Doctor BP (1980) Inhibition of Protein Synthesis in Intact HeLa Cells by Shigella dysenteriae 1 Toxin. *Infection and Immunity* 29(1):98–107.

5. Tumer NE, Li X-P (2012) Interaction of ricin and Shiga toxins with ribosomes. *Curr Top Microbiol Immunol* 357(Chapter 174):1–18.

6. Zhu W, et al. (2011) Comprehensive identification of protein substrates of the Dot/Icm type IV transporter of Legionella pneumophila. *PLoS ONE* 6(3):e17638.

7. Finsel I, Hilbi H (2015) Formation of a pathogen vacuole according to Legionella pneumophila: how to kill one bird with many stones. *Cellular Microbiology* 17(7):935–950.

8. Cornejo E, Schlaermann P, Mukherjee S (2017) How to rewire the host cell: A home improvement guide for intracellular bacteria. *The Journal of Cell Biology* 216(12):3931–3948.

9. Finlay BB, McFadden G (2006) Anti-immunology: evasion of the host immune

system by bacterial and viral pathogens. *Cell* 124(4):767–782.

10. Mukherjee S, et al. (2011) Modulation of Rab GTPase function by a protein phosphocholine transferase. *Nature* 477(7362):103–106.

11. Müller MP, et al. (2010) The Legionella effector protein DrrA AMPylates the membrane traffic regulator Rab1b. *Science* 329(5994):946–949.

12. Belyi Y, et al. (2006) Legionella pneumophila glucosyltransferase inhibits host elongation factor 1A. *Proc Natl Acad Sci USA* 103(45):16953–16958.

13. Belyi Y, Tabakova I, Stahl M, Aktories K (2008) Lgt: a family of cytotoxic glucosyltransferases produced by Legionella pneumophila. *Journal of Bacteriology* 190(8):3026–3035.

14. Shen X, et al. (2009) Targeting eEF1A by a Legionella pneumophila effector leads to inhibition of protein synthesis and induction of host stress response. *Cellular Microbiology* 11(6):911–926.

15. Barry KC, Fontana MF, Portman JL, Dugan AS, Vance RE (2013) IL-1α signaling initiates the inflammatory response to virulent Legionella pneumophila in vivo. *J Immunol* 190(12):6329–6339.

16. Hervet E, et al. (2011) Protein Kinase LegK2 Is a Type IV Secretion System Effector Involved in Endoplasmic Reticulum Recruitment and Intracellular Replication of Legionella pneumophila. *Infection and Immunity* 79(5):1936–1950.

17. Lee P-C, Machner MP (2018) The Legionella Effector Kinase LegK7 Hijacks the

Host Hippo Pathway to Promote Infection. *Cell Host Microbe* 24(3):429–438.e6.

18. Canova MJ, Molle V (2014) Bacterial serine/threonine protein kinases in host-pathogen interactions. *J Biol Chem* 289(14):9473–9479.

19. Pereira SFF, Goss L, Dworkin J (2011) Eukaryote-Like Serine/Threonine Kinases and Phosphatases in Bacteria. *Microbiology and Molecular Biology Reviews* 75(1):192–212.

20. Ge J, et al. (2009) A Legionella type IV effector activates the NF-kappaB pathway by phosphorylating the IkappaB family of inhibitors. *Proc Natl Acad Sci USA* 106(33):13725–13730.

21. Michard C, et al. (2015) The LegionellaKinase LegK2 Targets the ARP2/3 Complex To Inhibit Actin Nucleation on Phagosomes and Allow Bacterial Evasion of the Late Endocytic Pathway. *mBio* 6(3):e00354–15–14.

22. Bärlocher K, Welin A, Hilbi H (2017) Formation of the Legionella Replicative Compartment at the Crossroads of Retrograde Trafficking. *Front Cell Infect Microbiol* 7:482.

23. Flayhan A, et al. (2015) The structure of Legionella pneumophila LegK4 type four secretion system (T4SS) effector reveals a novel dimeric eukaryotic-like kinase. *Nature Publishing Group*:1–13.

24. Blethrow JD, Glavy JS, Morgan DO, Shokat KM (2008) Covalent capture of kinase-specific phosphopeptides reveals Cdk1-cyclin B substrates. *Proc Natl*

Acad Sci USA 105(5):1442–1447.

25. Hertz NT, et al. (2010) Chemical genetic approach for kinase-substrate mapping by covalent capture of thiophosphopeptides and analysis by mass spectrometry. *Curr Protoc Chem Biol* 2(1):15–36.

26. Allen JJ, et al. (2007) A semisynthetic epitope for kinase substrates. *Nat Meth* 4(6):511–516.

27. Lourido S, Jeschke GR, Turk BE, Sibley LD (2013) Exploiting the unique ATP-binding pocket of toxoplasma calcium-dependent protein kinase 1 to identify its substrates. *ACS Chem Biol* 8(6):1155–1162.

28. Zuiderweg ERP, Hightower LE, Gestwicki JE (2017) The remarkable multivalency of the Hsp70 chaperones. *Cell Stress Chaperones* 22(2):173–189.

29. Beltrao P, et al. (2012) Systematic functional prioritization of protein posttranslational modifications. *Cell* 150(2):413–425.

30. Preissler S, et al. (2015) AMPylation matches BiP activity to client protein load in the endoplasmic reticulum. *Elife* 4:337.

31. Sanyal A, et al. (2015) A novel link between Fic (filamentation induced by cAMP)-mediated adenylylation/AMPylation and the unfolded protein response. *J Biol Chem* 290(13):8482–8499.

32. Rauch JN, Gestwicki JE (2014) Binding of human nucleotide exchange factors to heat shock protein 70 (Hsp70) generates functionally distinct complexes in vitro. *J*

Biol Chem 289(3):1402–1414.

33. Treacy-Abarca S, Mukherjee S (2015) Legionella suppresses the host unfolded protein response via multiple mechanisms. *Nature Communications* 6:7887.

34. Nelson RJ, Ziegelhoffer T, Nicolet C, Werner-Washburne M, Craig EA (1992) The translation machinery and 70 kd heat shock protein cooperate in protein synthesis. *Cell* 71(1):97–105.

35. Shalgi R, et al. (2013) Widespread regulation of translation by elongation pausing in heat shock. *Mol Cell* 49(3):439–452.

36. Beatty KE, Xie F, Wang Q, Tirrell DA (2005) Selective dye-labeling of newly synthesized proteins in bacterial cells. *J Am Chem Soc* 127(41):14150–14151.

37. Li X, et al. (2013) Analogues of the Allosteric Heat Shock Protein 70 (Hsp70) Inhibitor, MKT-077, As Anti-Cancer Agents. *ACS Med Chem Lett* 4(11):1042–1047.

38. O'Connor TJ, Adepoju Y, Boyd D, Isberg RR (2011) Minimization of the Legionella pneumophila genome reveals chromosomal regions involved in host range expansion. *Proc Natl Acad Sci USA* 108(36):14733–14740.

39. Fontana MF, et al. (2011) Secreted bacterial effectors that inhibit host protein synthesis are critical for induction of the innate immune response to virulent Legionella pneumophila. *PLoS Pathogens* 7(2):e1001289.

40. Chuluunbaatar U, et al. (2010) Constitutive mTORC1 activation by a herpesvirus

Akt surrogate stimulates mRNA translation and viral replication. *Genes & Development* 24(23):2627–2639.

41. De Leon JA, et al. (2017) Positive and Negative Regulation of the Master Metabolic Regulator mTORC1 by Two Families of Legionella pneumophila Effectors. *CELREP* 21(8):2031–2038.

42. Celli J, Tsolis RM (2014) Bacteria, the endoplasmic reticulum and the unfolded protein response: friends or foes? *Nat Rev Microbiol* 13(2):71–82.

43. Preissler S, Rato C, Perera LA, Saudek V, Ron D (2017) FICD acts bifunctionally to AMPylate and de-AMPylate the endoplasmic reticulum chaperone BiP. *Nature Structural & Molecular Biology* 24(1):23–29.

44. Ham H, et al. (2014) Unfolded protein response-regulated Drosophila Fic (dFic) protein reversibly AMPylates BiP chaperone during endoplasmic reticulum homeostasis. *J Biol Chem* 289(52):36059–36069.

45. Doublet P, Michard C (2015) Post-translational modifications are key players of the Legionella pneumophila infection strategy. *Frontiers in Microbiology* 6(87):1–12.

46. Havey JC, Roy CR (2015) Toxicity and SidJ-Mediated Suppression of Toxicity Require Distinct Regions in the SidE Family of Legionella pneumophila Effectors. *Infection and Immunity* 83(9):3506–3514.

47. Bouche G, Amalric F, Caizergues-Ferrer M, Zalta JP (1979) Effects of heat shock

on gene expression and subcellular protein distribution in Chinese hamster ovary cells. *Nucleic Acids Research* 7(7):1739–1747.

48. Lindquist S (1980) Varying patterns of protein synthesis in Drosophila during heat shock: implications for regulation. *Dev Biol* 77(2):463–479.

49. Hornbeck PV, et al. (2015) PhosphoSitePlus, 2014: mutations, PTMs and recalibrations. *Nucleic Acids Research* 43(D1):D512–20.

50. Campodonico EM, Chesnel L, Roy CR (2005) A yeast genetic system for the identification and characterization of substrate proteins transferred into host cells by the Legionella pneumophila Dot/Icm system. *Mol Microbiol* 56(4):918–933.

51. Merriam JJ, Mathur R, Maxfield-Boumil R, Isberg RR (1997) Analysis of the Legionella pneumophila flil gene: intracellular growth of a defined mutant defective for flagellum biosynthesis. *Infection and Immunity* 65(6):2497–2501.

52. Bardill JP, Miller JL, Vogel JP (2005) IcmS-dependent translocation of SdeA into macrophages by the Legionella pneumophila type IV secretion system. *Mol Microbiol* 56(1):90–103.

53. Berger KH, Isberg RR (1993) Two distinct defects in intracellular growth complemented by a single genetic locus in Legionella pneumophila. *Mol Microbiol* 7(1):7–19.

54. Lundblad V, Struhl K (2001) *Yeast* (John Wiley & Sons, Inc., Hoboken, NJ, USA).

55. Chang L, Thompson AD, Ung P, Carlson HA, Gestwicki JE (2010) Mutagenesis

Reveals the Complex Relationships between ATPase Rate and the Chaperone Activities of Escherichia coliHeat Shock Protein 70 (Hsp70/DnaK). *Journal of Biological Chemistry* 285(28):21282–21291.

56. Chang L, et al. (2008) High-throughput screen for small molecules that modulate the ATPase activity of the molecular chaperone DnaK. *Anal Biochem* 372(2):167–176.

57. Levin RS, Hertz NT, Burlingame AL, Shokat KM, Mukherjee S (2016) Innate immunity kinase TAK1 phosphorylates Rab1 on a hotspot for posttranslational modifications by host and pathogen. *Proc Natl Acad Sci USA* 113(33):E4776–83.

58. Wisén S, Gestwicki JE (2008) Identification of small molecules that modify the protein folding activity of heat shock protein 70. *Anal Biochem* 374(2):371–377.

59. Beatty KE, Tirrell DA (2008) Two-color labeling of temporally defined protein populations in mammalian cells. *Bioorganic & Medicinal Chemistry Letters* 18(22):5995–5999.

60. Truitt ML, et al. (2015) Differential Requirements for eIF4E Dose in Normal Development and Cancer. *Cell* 162(1):59–71.

Chapter 4

Substrate Targets of PKA in Neuroendocrine Lung Cancer

Introduction

Discovering the important substrate targets of kinases is a continually evolving field of study with a large number of methodologies. There are over 800,000 identified phosphorylations in the phosphoproteome (1), the overwhelming majority of which have no known function. With a little over 500 kinases present in the human genome (2), each kinase is responsible for 1,600 of these phosphorylations on average. This makes screening for phosphorylation events challenging, as you need many layers of specificity and enrichment to ensure that a given substrate identification is logical (3).

To accomplish this, there are a number of methods used to identify the substrate targets of a particular kinase. One strategy for substrate identification is the use of *in vitro* kinase assays. This strategy takes on a number of different forms, including individual assays with substrate kinase pairs and peptide or protein arrays for screening (4, 5). These methods are good for showing a kinase's ability to phosphorylate a substrate, but have the major disadvantage of not recapitulating a cellular context (4, 5). In order to solve this problem, many researchers turn to the identification of kinase interacting partners. Methodologies that use proximity-based ligation can identify proteins the kinase is interacting with, but typically do a poor job of discovering transient interactions (6). This method becomes difficult to use for phosphorylation substrates, as transient interactions are a hallmark of the phosphorylation reaction.

One way to circumvent many of the problems with artificial systems is to simply look at the entire phosphoproteomic landscape. This method provides the most *in situ* look into the activity of the cell. These experiments are set up by introducing a cellular perturbation, followed by a comparison of the phosphoproteomes to the perturbation vs. control using quantitative tracking methods such as stable isotope labeling by amino acids in cell culture (SILAC) or isobaric tag for relative and absolute quantification (iTRAQ) (7-9). The outstanding issue with this methodology is that it is difficult to attribute specific phosphorylation events to the kinase of interest. Global phosphoproteomic methods provide a wealth of information, but require carefully designed follow-up experiments or complimentary screens (3).

Multiple techniques have been developed to address the challenge of identifying the substrates of a kinase in a relevant biological setting. Previous members of the Shokat lab developed a chemical biology approach, termed the “bump-hole” method, to create specificity within a substrate identification screen (Mentioned in **Chapter 2** and **3**). This method utilizes a large hydrophobic residue that is present in the ATP binding pocket of a majority of kinases called the gatekeeper residue. This large hydrophobic residue is mutated to a smaller Ala or Gly to create space in the ATP-biding pocket of the kinase (**Figure 4.1**) (10, 11). The mutated kinase is called an analog-specific (AS) kinase. This space is then filled with an ATP analog with a bulky N6 substitution such as furan or benzene. This analog of ATP also contains a γ-thiophosphate group. This thiophosphate can be transferred to a target protein similarly to a normal γ-phosphate group, except the thiol allows for additional functionalization (**Figure 4.1**) (12, 13). The developed system allows for a mutated kinase to specifically accept a bulky ATP analog

and then chemically add a functionalized PTM onto its target. The thiophosphate tagged proteins can be pulled down or detected in various ways.

When performing a substrate screen with an AS kinase, the preferred method uses cellular lysate and a recombinantly purified version of the AS kinase. While this is a more artificial *in vitro* system, it provides the most comprehensive list of substrate targets (14). This is due to the low activity of endogenous kinases. The opportunity to increase the proportion of kinase to lysate allows for the identity of minor substrates that might have otherwise been missed. Another way to carry out the screen is to overexpress the AS kinase in cells and permeabilize the cells to introduce the N^6-substituted-ATP-γS, although the results tend to be less robust (13). Once the substrates have been thiophosphorylated, there are two approaches used to enrich your samples prior to proteomic analysis on LC-MS/MS. The more robust method is dubbed "covalent capture" and involves trypsinizing the cell lysate sample, and then enriching for thiophosphorylated peptides by reacting them with iodoacetimide beads (**Figure 4.1**). The thiophosphorylated peptides are then selectively eluted from the beads in a reaction that replaces the thiophosphorylation with a phosphorylation, and all phosphopeptides are analyzed by LC-MS/MS. In another method, the thiophosphorylated proteins are reacted with *para*-nitrobenzylmesylate (pNBM), and the attached moiety is recognized by an antibody. Using this method, a researcher can immunoprecipitate all proteins that have been thio-phosphorylated. From here, the

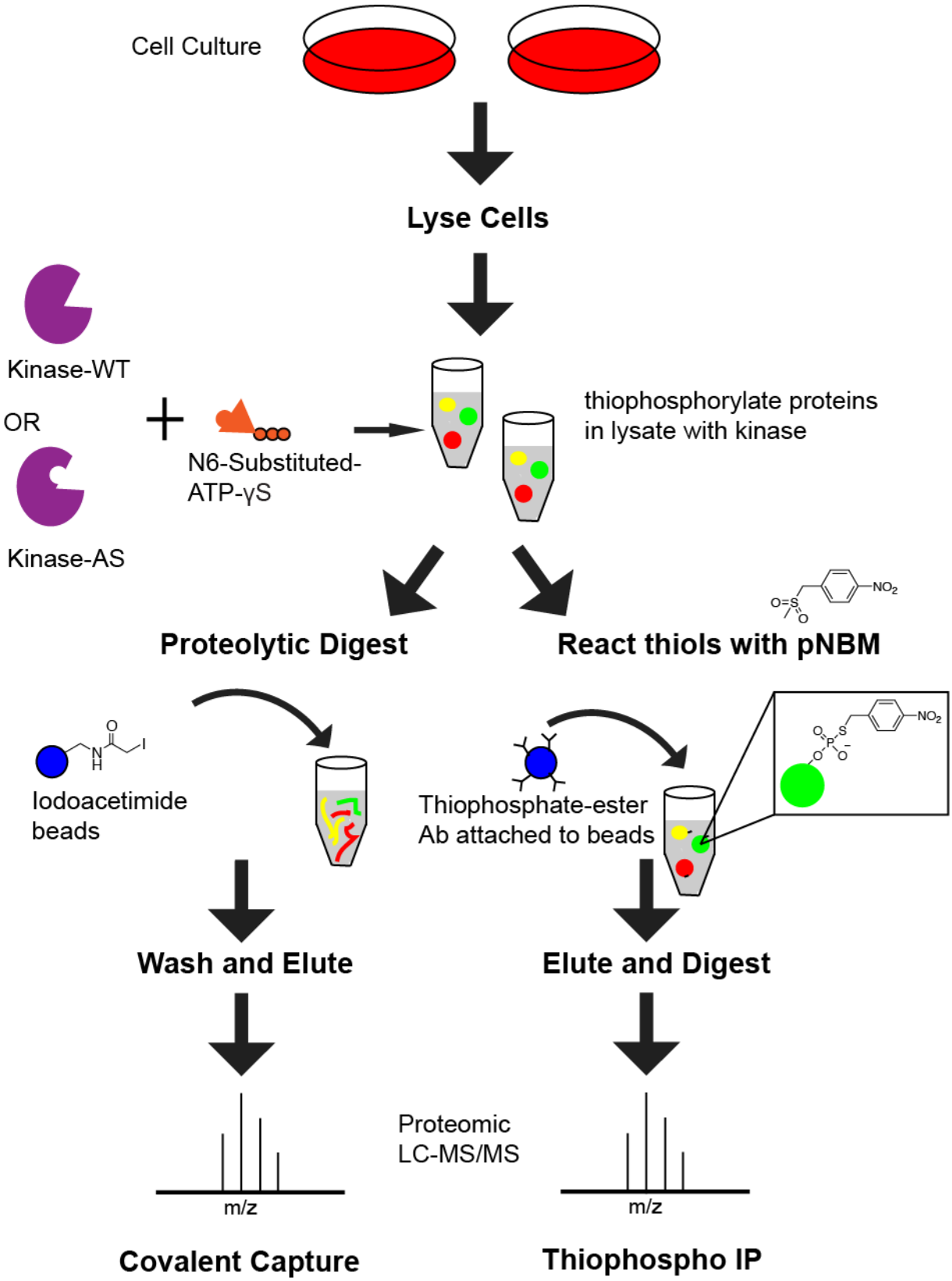

Figure 4.1 Methods of kinase substrate discovery using thiophosphorylation. The graphic description of the two main methods used for substrate discovery with AS-

kinases. Both methods start with the culture and lysis of cells. Following this, the lysate is treated with WT or AS kinase and the N6-substituted ATP with a γ-thiophosphate group. The thiol functionalizes the tagged substrate. For covalent capture (left), the proteins are digested with trypsin, and the individual peptides are reacted with iodoacetimide beads. The thiophosphorylated peptides are then eluted and analyzed. For immunoprecipitation with the thiophosphate-ester antibody (right), the proteins are pulled-down with beads containing the antibody. These proteins are then eluted, digested, and analyzed by mass spectrometry.

protein samples are trypsinized, and the general abundance of proteins is compared following LC-MS/MS (**Figure 4.1**).

These methodologies have been used in a number of different biological settings, and for a variety of different kinases. This includes kinases from bacteria, such as LegK4 from *Legionella pneumophila* described in Chapter 3. Additionally, the method has widely been applied to a number of cancer cell lines, and the kinases that drive those cancers (12). One particular case that this chapter will focus on, is the use of covalent capture in small cell lung cancer (SCLC) to identify substrates of protein kinase A (PKA), a kinase discovered to be an important driver of SCLC.

Approximately 15% of lung cancers are SCLC, and the overall 5-year survival rate of inflicted patients is 5-10%. Treatments for SCLC tend to be ineffective, including immunotherapies (15) that have been promising for a number of other cancers with high mortality rates (reviewed in (16, 17)). In relation to many other kinases that are driven by signaling pathways, particularly phosphorylation, the lab of Julien Sage identified PKA as a kinase that is expressed in high levels in human SCLC. Additionally, they were able to show that decreased PKA activity inhibits tumor growth. Taken together, this information provides a promising avenue of treatment if the specific substrates and pathways can be elucidated and utilized to halt or even reverse tumorgenesis for SCLC.

The observations that PKA activity is necessary and sufficient to promote the growth of SCLC led to the investigation of molecular mechanisms of PKA action in SCLC cells. The transcription factor CREB (cAMP Response Binding Element factor) is a well-known target of PKA and CREB has been found to be transcriptionally active in a mouse model of SCLC (18). Our collaborators found that knocked down CREB in murine SCLC cells in the same conditions under which PKA knock-down significantly inhibits tumor growth, did not inhibit SCLC cell growth in culture or in mice. While these results do not exclude that CREB may play a role in SCLC cells in certain contexts, it suggested that PKA controls SCLC growth largely through other targets.

Covalent Capture for identification of PKA substrates in SCLC Cell Lines

To identify potential direct PKA substrates in SCLC cells, we used an AS kinase approach with the M120A form of PKA-Cα. The M120A mutation was tested to be the most efficient gatekeeper mutation for PKA. As previously described, the mutation enlarges the ATP binding pocket of PKA and results in a kinase that uses ATP less efficiently, but allows for the covalent incorporation of bulky ATP analogs such as Bn-ATPγS (14).

Our collaborators prepped two patient-derived xenograft (PDX) models (NJH29 and LX102), one allograft model (derived from a *Rb/p53/p130* triple knockout mouse, 5BI), and one human cell line (H82), which all have moderate expression and activity of PKA and were representative of the diversity of molecular phenotypes in human SCLC. They chose SCLC models with moderate PKA activity because high PKA activity may result in a high rate of intrinsic phosphorylation of PKA substrates, which may limit the

detection of thiophosphorylated proteins following *in vitro* kinase assays using PKA-Cα^{M120A}. They generated recombinant active PKA (rPKA) and PKA-Cα^{M120A} (rAS-PKA) using a bacterial co-expression system. As expected, rPKA was better able to phosphorylate substrates with ATP while rAS-PKA was better at using Bn-ATPγS **(Figure 4.2**).

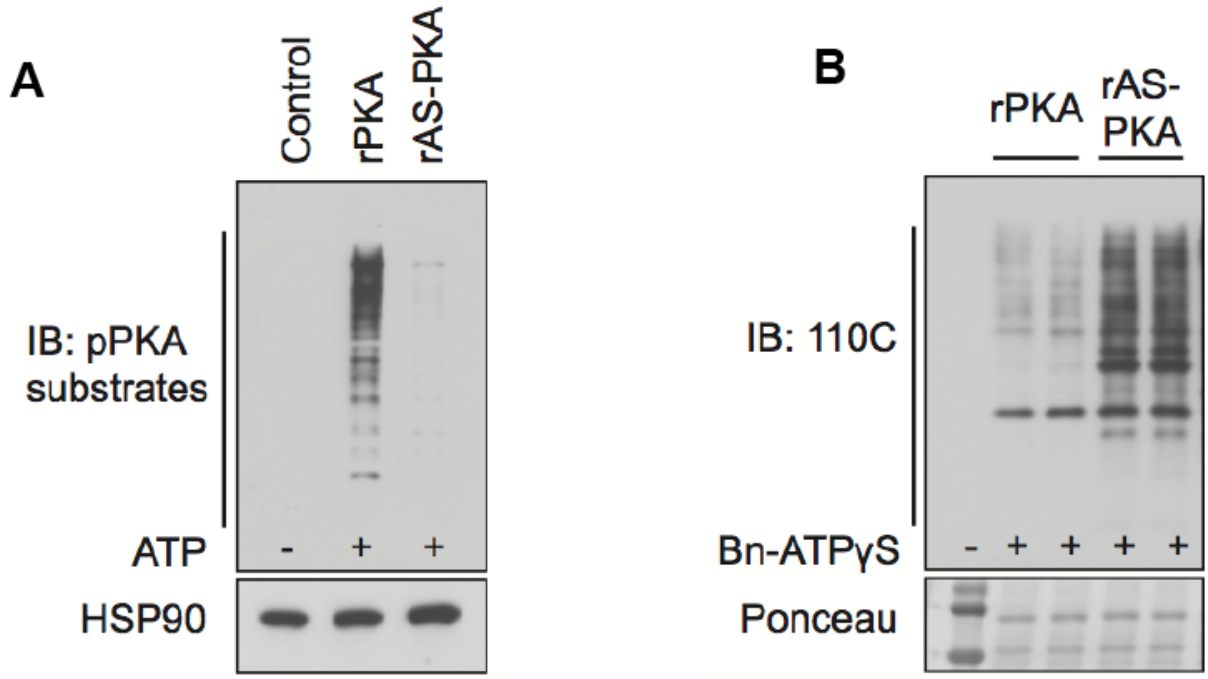

Figure 4.2 Recombinant AS PKA phosphorylates lysates selectively. (**A**) Immunoblot analysis of *in vitro* kinase assays performed with NJH29 tumor extracts using recombinant PKA (rPKA) or recombinant analog-sensitive PKA (rAS-PKA). The pPKA substrate antibody was used to identify phosphorylated PKA substrates. (**B**) Immunoblots of *in vitro* kinase assays performed as in (**B**) except that the bulky Bn-ATPγS analog was used as an ATP donor and the 110C antibody was used to detect thiophosphorylated proteins.

Once they were able to show a difference in labeling efficiency of the AS versus WT PKA using the Bn-ATPγS, they prepped a large-scale labeling reaction for covalent capture. We identified PKA phosphorylated peptides using covalent capture enrichment protocol, and the method identified ~200 substrates over the four different cell lines that were labeled by rAS-PKA and not wild-type rPKA (**Appendix A**). Despite the number of

substrates, there was little overlap in the identity of the substrates between the different cell lines used. Additionally, because some known substrates such as CREB and VASP were not found in this analysis, this number of substrates is likely to be an underestimate of the total number of PKA substrates in SCLC cells. Among the identified substrates, at least 31 have been described before (19-23), even though we did not always find the same site being phosphorylated as in previous reports.

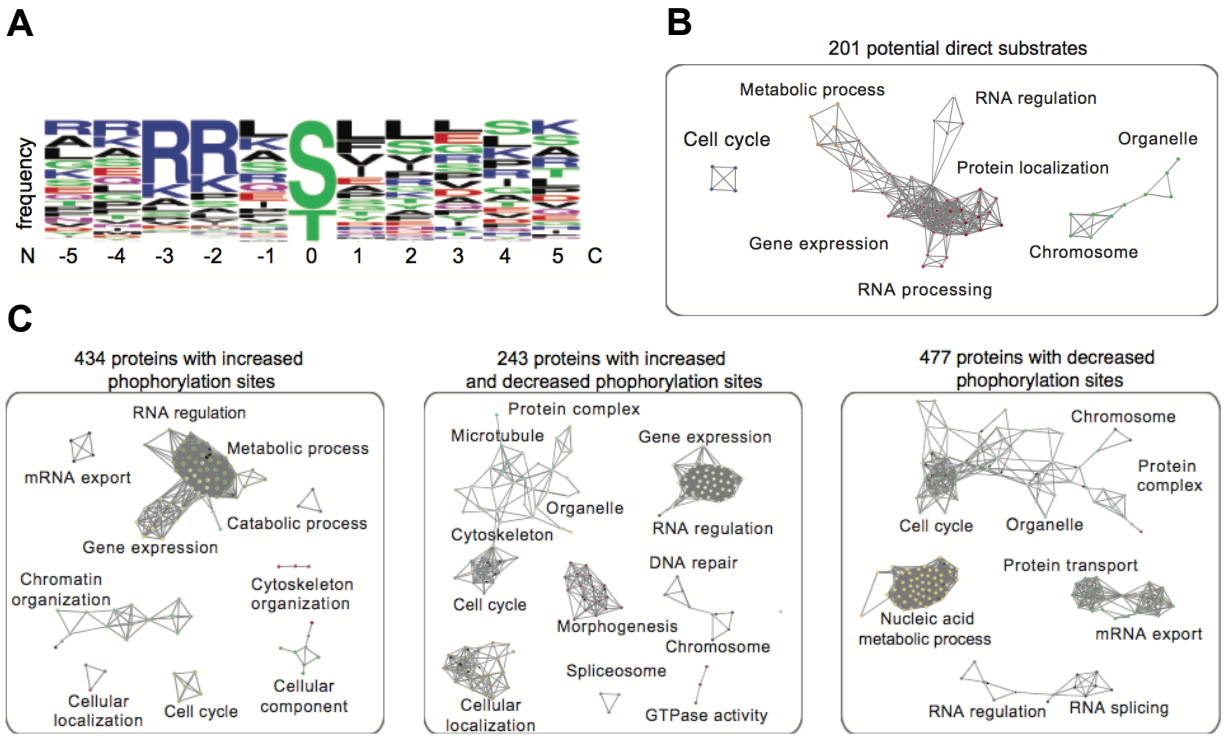

Figure 4.3 Analysis of PKA substrates from covalent capture screen. (**A**) Motif analysis for the candidate direct PKA-Cα substrates identified with the rAS-PKA enzyme following analysis. (**B**) Nodes of GO terms of the biological processes in which the candidate PKA substrates are implicated. (**C**) Nodes of GO terms of biological processes altered by activation of PKA in H69 SCLC cells after analysis of the global phosphoproteomic data.

Using the phosphorylation sites identified by the covalent capture screen, our collaborators used logo motif analysis and found that the majority of substrates had the canonical PKA motif RXXS/T (**Figure 4.3**). Additionally, a GO term analysis for the PKA

substrates identified showed enrichment in multiple signaling pathways involved in cell cycle, gene expression and metabolic processes (**Figure 4.3**). These data indicate that PKA probably phosphorylates hundreds of substrates in SCLC and identify a broad role for PKA in cell cycle and cell growth mechanisms that can promote SCLC expansion.

Conclusions and Future Work

Further work by our collaborators looked to validate the PKA results with a global phosphoproteomics screen. Using a SCLC cell line with a high expression of PKA, they found thousands of phosphosite changes (either up- or downregulated). The functional significance of these sites showed a similar GO term analysis that was enriched for cell proliferation (**Figure 4.3**). There were 80 overlapping phosphorylation sites between the global phosphoproteomic screen and the covalent capture screen. Further validation with RNAi of some of the direct PKA substrates showed their importance in SCLC cell expansion in culture, including some ribosomal subunits and replication machinery factors. These results taken together help to validate to the phosphoproteomic covalent capture screen, and the hits that were discovered for PKA in SCLC cell lines.

Materials and Methods

Covalent Capture Protocol (Modified from (14))

Labeling experiments for covalent capture enrichment were performed on 2 mg of protein lysate per sample (N=2/line). Samples were incubated in lysis buffer supplemented with 250 μM Bn-ATPγS, 250 μM ATP, 5 mM GTP, 10 mM $MgCl_2$, and 20 μg of purified PKA as indicated. Labeling reactions were performed at 37°C for 60 min

before quenching with 50 mM EDTA. Thirty-microliter aliquots of each reaction were alkylated with 2 µL of 100 mM p-nitro mesylate (PNBM) for 30 min at room temperature. Thiophosporylation was detected by immunoblot with the antithiophosphate ester antibody (110C).

Covalent capture of thiophosphorylated proteins was performed as described previously (Hertz et al., 2010). Briefly, lysates were denatured by adding 60% (wt/vol) solid urea, 10 mM final TCEP, and incubating at 55 °C for 30 min. Samples were diluted to 2 M urea with 50 mM ammonium bicarbonate, brought to a pH of 8, and digested overnight at 37 °C with trypsin (Promega) at a 1:20 ratio. Peptides were acidified with trifluoroacetic acid, desalted on a SepPak C18 column (Waters), and speed-vacuumed to dryness. Peptides were resuspended in 50 mM HEPES and 50% (vol/vol) acetonitrile and adjusted to pH 7. The peptide solution was incubated overnight rocking with 100 µL of iodoacetyl Sepharose resin in the dark (Thermo Fisher Scientific). Beads were washed by gravity flow with water, 5 M NaCl, 50% (vol/vol) acetonitrile, 5% (vol/vol) formic acid, and 10 mM DTT followed by elution with 1 mg/mL oxone (Sigma). Peptides were desalted with ZipTips (Millipore) and speed-vacuumed until dry.

LC-MS/MS Analysis and Data Processing

All desalted peptides were resuspended into 10 µL of 0.1% formic acid. Peptides were loaded on to a nanoACQUITY (Waters) UPLC instrument for reversed-phase chromatography with a C18 column (BEH130, 1.7-µm bead size, 100 µm × 100 mm) in front of an LTQ Orbitrap Velos. The LC was operated at a 600-nL/min flow rate and peptides were separated over an 80-min gradient from 2 to 50% buffer B (buffer A:

water and 0.1% formic acid; buffer B: acetonitrile and 0.1% formic acid). Survey scans were recorded over a 350–1,800 m/z range and MS/MS fragmentation was performed using HCD on the top eight peaks. A second injection (i.e., technical replicate) of each sample was performed using ETD fragmentation on the top six peaks. Peak lists were generated with an in-house software called PAVA and searched against the SwissProt Homo sapiens database (downloaded June 27, 2013; 20,264 entries) using Protein Prospector (v5.10.10). Data were searched with a 20-ppm tolerance for parent and fragment ions (HCD or 20 ppm/0.6 Da ETD), allowing for standard variable modifications and S/T/Y phosphorylation. Filtering of background peptides and phosphopeptides was accomplished using an in-house R script described previously (24). The AS-PKA logo motif was generated using the Berkley Berkeley's WebLogo generator (25).

References:

1. Hornbeck PV, et al. (2015) PhosphoSitePlus, 2014: mutations, PTMs and recalibrations. *Nucleic Acids Research* 43(D1):D512–20.

2. Manning G, Whyte DB, Martinez R, Hunter T, Sudarsanam S (2002) The protein kinase complement of the human genome. *Science* 298(5600):1912–1934.

3. Xue L, Tao WA (2013) Current technologies to identify protein kinase substrates in high throughput. *Front Biol (Beijing)* 8(2):216–227.

4. Mok J, Im H, Snyder M (2009) Global identification of protein kinase substrates by protein microarray analysis. *Nat Protoc* 4(12):1820–1827.

5. Houseman BT, Huh JH, Kron SJ, Mrksich M (2002) Peptide chips for the quantitative evaluation of protein kinase activity. *Nat Biotechnol* 20(3):270–274.

6. Amano M, et al. (2015) Kinase-interacting substrate screening is a novel method to identify kinase substrates. *The Journal of Cell Biology* 209(6):895–912.

7. Ong S-E, et al. (2002) Stable isotope labeling by amino acids in cell culture, SILAC, as a simple and accurate approach to expression proteomics. *Mol Cell Proteomics* 1(5):376–386.

8. Wiese S, Reidegeld KA, Meyer HE, Warscheid B (2007) Protein labeling by iTRAQ: a new tool for quantitative mass spectrometry in proteome research. *Proteomics* 7(3):340–350.

9. Li Z, et al. (2012) Systematic comparison of label-free, metabolic labeling, and

isobaric chemical labeling for quantitative proteomics on LTQ Orbitrap Velos. *J Proteome Res* 11(3):1582–1590.

10. Shah K, Liu Y, Deirmengian C, Shokat KM (1997) Engineering unnatural nucleotide specificity for Rous sarcoma virus tyrosine kinase to uniquely label its direct substrates. *Proc Natl Acad Sci USA* 94(8):3565–3570.

11. Liu Y, Shah K, Yang F, Witucki L, Shokat KM (1998) A molecular gate which controls unnatural ATP analogue recognition by the tyrosine kinase v-Src. *Bioorganic & Medicinal Chemistry* 6(8):1219–1226.

12. Blethrow JD, Glavy JS, Morgan DO, Shokat KM (2008) Covalent capture of kinase-specific phosphopeptides reveals Cdk1-cyclin B substrates. *Proc Natl Acad Sci USA* 105(5):1442–1447.

13. Allen JJ, et al. (2007) A semisynthetic epitope for kinase substrates. *Nat Meth* 4(6):511–516.

14. Hertz NT, et al. (2010) Chemical genetic approach for kinase-substrate mapping by covalent capture of thiophosphopeptides and analysis by mass spectrometry. *Curr Protoc Chem Biol* 2(1):15–36.

15. Horn L, et al. (2018) First-Line Atezolizumab plus Chemotherapy in Extensive-Stage Small-Cell Lung Cancer. *N Engl J Med* 379(23):2220–2229.

16. Pietanza MC, Byers LA, Minna JD, Rudin CM (2015) Small cell lung cancer: will recent progress lead to improved outcomes? *Clinical Cancer Research*

21(10):2244–2255.

17. Sabari JK, Lok BH, Laird JH, Poirier JT, Rudin CM (2017) Unravelling the biology of SCLC: implications for therapy. *Nat Rev Clin Oncol* 14(9):549–561.

18. Xia Y, et al. (2018) Targeting CREB Pathway Suppresses Small Cell Lung Cancer. *Mol Cancer Res* 16(5):825–832.

19. Baba A, et al. (2011) PKA-dependent regulation of the histone lysine demethylase complex PHF2-ARID5B. *Nat Cell Biol* 13(6):668–675.

20. Imamura H, Sugiyama N, Wakabayashi M, Ishihama Y (2014) Large-scale identification of phosphorylation sites for profiling protein kinase selectivity. *J Proteome Res* 13(7):3410–3419.

21. Isobe K, et al. (2017) Systems-level identification of PKA-dependent signaling in epithelial cells. *Proc Natl Acad Sci USA* 114(42):E8875–E8884.

22. Moore CEJ, Xie J, Gomez E, Herbert TP (2009) Identification of cAMP-dependent kinase as a third in vivo ribosomal protein S6 kinase in pancreatic beta-cells. *J Mol Biol* 389(3):480–494.

23. Nagai T, et al. (2016) Phosphoproteomics of the Dopamine Pathway Enables Discovery of Rap1 Activation as a Reward Signal In Vivo. *Neuron* 89(3):550–565.

24. Lipp JJ, Marvin MC, Shokat KM, Guthrie C (2015) SR protein kinases promote splicing of nonconsensus introns. *Nat Struct Mol Biol* 22(8):611–617.

25. Crooks GE, Hon G, Chandonia J-M, Brenner SE (2004) WebLogo: a sequence

logo generator. *Genome Res* 14(6):1188–1190.

Appendix 1

Substrates of PKA identified by covalent capture

Protein Name	Peptide	Peptide Mod	seq start	seq end	Cell Line
ATP-binding cassette sub-family A member 12	LAIMVNGKFQCIGSLQHIK	Phospho@2472	2459	2477	LX102
Apoptotic chromatin condensation inducer in the nucleus	KISVVSATK	Phospho@825=25	823	831	5b1
Apoptotic chromatin condensation inducer in the nucleus	KPSISITTESLK	Phospho@863=13	861	872	H29
Apoptotic chromatin condensation inducer in the nucleus	KISVVSATK	Phospho@825=30	823	831	H29
Apoptotic chromatin condensation inducer in the nucleus	RASHTLLPSHR	Phospho@561=12	559	569	H29
Apoptotic chromatin condensation inducer in the nucleus	RLSQPESAEK	Phospho@710=37	708	717	H82
Apoptotic chromatin condensation inducer in the nucleus	RASHTLLPSHR	Phospho@561|563	559	569	H82
Neuroblast differentiation-associated protein AHNAK	RVTAYTVDVTGR	Phospho@158=45	156	167	H29
Neuroblast differentiation-associated protein AHNAK	ISMPDIDLNLKGPK	Phospho@2708;Oxidation@2709	2707	2720	H29
Serum albumin	LSQTFPNADFAEITK	Phospho@244=10	243	257	5b1
Anosmin-1	LEVQVLTPGGEGPATIK	Phospho@638|646	632	648	H82
Arginine and glutamate-rich protein 1	SRPKLSFSLK	Phospho@264=7	259	268	5b1
Arginine and glutamate-rich protein 1	SRPKLSFSLK	Phospho@266=12	261	270	H29
Rho GTPase-activating protein 35	KVSIVSKPVLYR	Phospho@1150=24	1148	1159	H29
Armadillo repeat-containing X-linked protein 2	VTQSPGTVIPPLPPPSSVLPR	Phospho@282=6	266	286	5b1
cAMP-regulated phosphoprotein 19	QLPTAAPDKTEVTGDHIPTPQDLPQRKPSLVASK	Phospho@104|108	76	109	H29
ATPase family AAA domain-containing protein 2	KATVYYQAPLEKPR	Phospho@302=27	300	313	LX102
Sarcoplasmic/endoplasmic reticulum calcium ATPase 2	DIVPGDIVEIAVGDKVPADIRLTSIK	Phospho@166;Phospho@167	144	169	H29

Protein Name	Peptide	Peptide Mod	seq start	seq end	Cell Line
ATP synthase subunit alpha, mitochondrial	ISVREPMQTGIK	Phospho@184=35;Oxidation@189	183	194	5b1
ATP synthase subunit e, mitochondrial	RYSYLKPR	Phospho@31=31	29	36	5b1
Biorientation of chromosomes in cell division protein 1-like 1	RLSVLGR	Phospho@795	793	799	5b1
Biorientation of chromosomes in cell division protein 1-like 1	KLSVLGK	Phospho@800	798	804	H29
Peregrin	RTSVLFSK	Phospho@890|891	889	896	H82
Ashwin	SPPLSPVGTTPVK	Phospho@197|198	189	201	H82
CAD protein	RLSSFVTK	Phospho@1406=11	1404	1411	H82
Calcium-responsive transcription factor	VETNQTR	Phospho@536=38	531	537	H29
Calcium-regulated heat-stable protein 1	TFSATVR	Phospho@52=23	50	56	H29
Chromobox protein homolog 5	KSSFSNSADDIK	Phospho@93=14	91	102	5b1
Coiled-coil domain-containing protein 187	ASLSLRR	Phospho@233=37	232	238	5b1
Coiled-coil domain-containing protein 86	MDTPLRR	Acetyl+Oxidation@1;Phospho@3	1	7	H82
Coiled-coil domain-containing protein 86	RFSQMLQDKPLR	Phospho@255;Oxidation@257	253	264	LX102
Protein Daple	RFSLAPPKEER	Phospho@1887	1885	1895	H29
T-complex protein 1 subunit gamma	TAVETAVLLLRIDDIVSGHK	Phospho@512|524	508	527	LX102
DNA-directed RNA polymerase I subunit RPA34	QEQINTEPLEDTVLSPTK	Phospho@285|287	271	288	H82
Anaphase-promoting complex subunit CDC26	RKPTRLELK	Phospho@7	4	12	H29
Serine/threonine-protein kinase MRCK alpha	RYSFRVPEEER	Phospho@1545=34	1543	1553	H29
Centrosomal protein of 170 kDa	RRTLPQLPNEEK	Phospho@644	642	653	H29
Centrosomal protein of 170 kDa	RRTLPQLPNEEK	Phospho@644	642	653	H29
Centrosomal protein of 170 kDa	RKSFTSLYK	Phospho@958=19	956	964	H29
Cofilin-1	KSSTPEEVK	Phospho@24=12	22	30	H29
Chromatin assembly factor 1 subunit B	RVTLNTLQAWSK	Phospho@485=22	483	494	H29
Calcium homeostasis endoplasmic reticulum protein	NKSYSFIAR	Phospho@911|913	909	917	5b1
Calcium homeostasis endoplasmic reticulum protein	SYSFIAR	Phospho@913=25	911	917	5b1

Protein Name	Peptide	Peptide Mod	seq start	seq end	Cell Line
Calcium homeostasis endoplasmic reticulum protein	NKSYSFIAR	Phospho@902|904	900	908	H29
Calcium homeostasis endoplasmic reticulum protein	SYSFIAR	Phospho@904=24	902	908	LX102
Cytoskeleton-associated protein 2	RKTLFAYK	Phospho@39=82	37	44	H29
CAP-Gly domain-containing linker protein 1	KISGTTALQEALKEK	Phospho@347|349|350	345	359	5b1
CAP-Gly domain-containing linker protein 1	KISGTTALQEALKEK	Phospho@348|350|351	346	360	H29
Clathrin light chain A	MRSVLISLK	Oxidation@221;Phospho@223=47	221	229	5b1
Clathrin light chain A	MRSVLISLK	Oxidation@234;Phospho@236=36	234	242	LX102
Cordon-bleu protein-like 1	RVSGHYVTSAAAK	Phospho@952=28	950	962	H29
Dihydropyrimidinase-related protein 1	SIPHITSDR	Phospho@8=68	8	16	H29
CTP synthase 1	RRTLFQTK	Phospho@455=49	453	460	5b1
CTP synthase 1	RRTLFQTK	Phospho@455=52	453	460	H82
Cholesterol 7-alpha-monooxygenase	NPEAMKAATEEVK	Phospho@312	304	316	H29
Drebrin-like protein	AMSTTSISSPQPGK	Oxidation@268;Phospho@269=15	267	280	H29
Discoidin, CUB and LCCL domain-containing protein 1	LDLITSDMADYQQPLMIGTGTVAR	Phospho&Phospho@((326&(340|342))|(327&(340|342)))	322	345	5b1
Dynactin subunit 1	KTSQLLETLNQLSTHTHVVDITR	Phospho@1152|1153	1151	1173	H29
DET1- and DDB1-associated protein 1	RPSVYLPTR	Phospho@33=63	31	39	5b1
DET1- and DDB1-associated protein 1	RPSVYLPTR	Phospho@33=58	31	39	LX102
Probable ATP-dependent RNA helicase DDX4	CPVLVATSVAARGLDIENVQHVINFDLPSTIDEYVHR	Phospho&Phospho@((619&(620|624))|(620&624))	591	627	LX102
DENN domain-containing protein 4C	SSLYGIAK	Phospho@948=8	947	954	H29
Pre-mRNA-splicing factor ATP-dependent RNA helicase PRP16	APAPRPSLLGLDLLASLK	Phospho@47=71	41	58	H29
Digestive organ expansion factor homolog	SQSQLLNTLTK	Phospho@10=25	8	18	H82
Disks large homolog 2	KKSFIFSR	Phospho@635=36	633	640	H29

Protein Name	Peptide	Peptide Mod	seq start	seq end	Cell Line
Deoxynucleotidyltransferase terminal-interacting protein 2	QSLIPRTPK	Phospho@61=53	55	63	H82
Kinetochore-associated protein DSN1 homolog	RKSLHPIHQGITELSR	Phospho@109=52	107	122	H82
ELL-associated factor 1	ASFHTIR	Phospho@29=23	28	34	H29
Eukaryotic translation initiation factor 3 subunit A	RQTIEER	Phospho@574	572	578	H82
Eukaryotic translation initiation factor 3 subunit A	RITYYR	Phospho@805=41	803	808	H82
Eukaryotic translation initiation factor 3 subunit A	AARQSVYEEK	Phospho@770=16	766	775	LX102
Eukaryotic translation initiation factor 4B	AASIFGGAKPVDTAAR	Phospho@359=108	357	372	5b1
Eukaryotic translation initiation factor 4B	AASIFGGAKPVDTAAR	Phospho@359=116	357	372	H82
Protein 4.1	RLSTHSPFR	Phospho@703|704	701	709	5b1
Protein 4.1	RLSTHSPFR	Phospho@709|710	707	715	H29
Protein 4.1	RLSTHSPFR	Phospho@709|710|712	707	715	LX102
Band 4.1-like protein 3	RASALIDRPAPYFER	Phospho@420=100	418	432	H29
Electron transfer flavoprotein subunit alpha, mitochondrial	RAASLLR	Phospho@15	12	18	5b1
Electron transfer flavoprotein subunit alpha, mitochondrial	RAASLLR	Phospho@15	12	18	LX102
Erythroferrone	AGPAARPPEPTAER	Phospho@69	59	72	H29
Protein FAM207A	RATVVVGDLHPLR	Phospho@138	136	148	H82
rRNA 2'-O-methyltransferase fibrillarin	RVSISEGDDKIEYR	Phospho@130=11	128	141	5b1
rRNA 2'-O-methyltransferase fibrillarin	RVSISEGDDKIEYR	Phospho@130|132	128	141	5b1
rRNA 2'-O-methyltransferase fibrillarin	RVSISEGDDKIEYR	Phospho@124|126	122	135	H29
rRNA 2'-O-methyltransferase fibrillarin	RVSISEGDDKIEYR	Phospho@124=12	122	135	H82
Glucose-6-phosphate 1-dehydrogenase	KQSEPFFK	Phospho@84	82	89	LX102
G antigen 7	STYYWPRPR	Phospho@8=10	7	15	H82
Neutral alpha-glucosidase AB	RFSFSGNTLVSSSADPEGHFETPIWIER	Phospho@866|868|871	864	891	H29
Neutral alpha-glucosidase AB	LSFQHDPETSVLVLR	Phospho@916=50	915	929	H29
Neutral alpha-glucosidase AB	GSPESRLSFQHDPETSVLVLR	Phospho@913|916	909	929	H29

Protein Name	Peptide	Peptide Mod	seq start	seq end	Cell Line
Neutral alpha-glucosidase AB	RFSFSGNTLVSSSADPEGHFETPIWIER	Phospho@866|868	864	891	H29
Putative oxidoreductase GLYR1	KLSLSEGK	Phospho@130=14	128	135	H82
General transcription factor II-I	RPSTFGIPR	Phospho@784=11	782	790	5b1
General transcription factor II-I	RPSTFGIPR	Phospho@784=9	782	790	H29
HIRA-interacting protein 3	AVESTDEDHQTDLDAK	Phospho@141=68	131	146	5b1
HIRA-interacting protein 3	AVESTDEDHQTDLDAK	Phospho@141=80;Phospho@134|135	131	146	5b1
HIRA-interacting protein 3	KAVESTDEDHQTDLDAK	Phospho@134|135|141	130	146	5b1
Histone H1.3	MSETAPAAPAAPAPVEKTPVK	Met-loss+Acetyl@1;Phospho@18=122	1	21	5b1
Histone H1.4	KASGPPVSELITK	Phospho@36=45	34	46	H82
Histone H1.4	MSETAPAAPAAPAPAEKTPVKK	Met-loss+Acetyl@1;Phospho@18=116	1	22	LX102
Histone H2B type 1-F/J/L	KESYSVYVYK	Phospho@37|39	35	44	5b1
Histone H2B type 1-F/J/L	KESYSVYVYK	Phospho@37=13	35	44	5b1
Histone H2B type 1-K	KESYSVYVYK	Phospho@37=16	35	44	LX102
Histone H3.1t	VARKSAPATGGVK	Phospho@29=46	25	37	H82
Non-histone chromosomal protein HMG-14	KVSSAEGAAKEEPK	Phospho@7|8	5	18	H82
Non-histone chromosomal protein HMG-17	SARLSAKPAPPKPEPKPK	Phospho@25|29	25	42	5b1
Non-histone chromosomal protein HMG-17	SARLSAKPAPPKPEPKPK	Phospho@25|29	25	42	LX102
High mobility group nucleosome-binding domain-containing protein 5	SARLSAMLVPVTPEVKPK	Oxidation@26;Phospho@20|24	20	37	H82
High mobility group nucleosome-binding domain-containing protein 5	LSAMLVPVTPEVKPK	Phospho@24=44;Oxidation@26	23	37	H82
Heterogeneous nuclear ribonucleoprotein A1	SSGPYGGGGQYFAKPR	Phospho@285|286	285	300	5b1
Heterogeneous nuclear ribonucleoprotein A1	SSGPYGGGGQYFAKPR	Phospho@337|338	337	352	H29
Heat shock protein HSP 90-beta	KHSQFIGYPITLYLEK	Phospho@206=41	204	219	5b1

Protein Name	Peptide	Peptide Mod	seq start	seq end	Cell Line
Heat shock protein HSP 90-beta	RLSELLR	Phospho@452	450	456	5b1
Heat shock protein HSP 90-beta	KHSQFIGYPITLYLEK	Phospho@206=37	204	219	LX102
Heat shock protein HSP 90-beta	RLSELLR	Phospho@452	450	456	LX102
Endoplasmin	EEKEESDDEAAVEEEEEKKPK	Phospho@306	301	322	LX102
60 kDa heat shock protein, mitochondrial	GYISPYFINTSKGQKCEFQDAYVLLSEK	Phospho@243=14;Phospho@247=13	222	249	5b1
60 kDa heat shock protein, mitochondrial	TALLDAAGVASLLTTAEVVVTEIPKEEKDPGMGAMGGMGGGMGGGMF	Phospho@547=15	527	573	H29
Interphotoreceptor matrix proteoglycan 2	SILFPNGVK	Phospho@82	82	90	H82
Importin-7	ENIVEAIIHSPELIRVQLTTCIHHIIK	Phospho@111=29;Phospho@112=29	93	119	LX102
Ras GTPase-activating-like protein IQGAP1	FLSAIVSSVDK	Phospho@1151=24;Phospho@1152=24	1145	1155	LX102
Uncharacterized protein KIAA1211-like	SKSFLITPVKPAVDRK	Phospho@879|881	879	894	H29
Kinesin-like protein KIF2C	STRMSTVSELR	Oxidation@114;Phospho@115=13	111	121	H29
Leucine--tRNA ligase, cytoplasmic	RYTIYSPK	Phospho@238=21	236	243	H82
Ligand-dependent nuclear receptor corepressor-like protein	TEKSKLNLLETSEIK	Phospho@360=29;Phospho@370|371	360	374	LX102
DNA ligase 1	TLSSFFTPR	Phospho@232=74	226	234	5b1
LIM domain-containing protein 2	SKSFSLR	Phospho@30=23	28	34	5b1
Lamin-B1	ASAPATPLSPTRLSR	Phospho@26|29	16	30	5b1
Lamin-B1	AGGPTTPLSPTRLSR	Phospho@25|28	15	29	H82
Lamin-B1	AGGPTTPLSPTRLSR	Phospho@25=7	15	29	H82
Lamin-B1	MRIESLSSQLSNLQK	Phospho@302|304|305	298	312	H82
Lamin-B1	AGGPTTPLSPTRLSR	Phospho@28=11	15	29	LX102
U6 snRNA-associated Sm-like protein LSm7	KKESILDLSK	Phospho@11=42	8	17	H29
Lysosomal-trafficking regulator	GKEDAFISSCESAK	Phospho@2166|2167|2170	2159	2172	H29
Melanoma-associated antigen D2	RASRGPIAFWAR	Phospho@218	216	227	LX102

Protein Name	Peptide	Peptide Mod	seq start	seq end	Cell Line
Target of rapamycin complex 2 subunit MAPKAP1	RTSFSFQK	Phospho@510=7	508	515	H82
Myristoylated alanine-rich C-kinase substrate	RFSFKK	Phospho@152	150	155	5b1
Myristoylated alanine-rich C-kinase substrate	LSGFSFK	Phospho@170=33	166	172	H29
Myristoylated alanine-rich C-kinase substrate	FSFKK	Phospho@159	158	162	H29
MARCKS-related protein	LSGLSFK	Phospho@104=38	100	106	5b1
MARCKS-related protein	KFSFK	Phospho@93	91	95	5b1
MARCKS-related protein	KFSFKKPFK	Phospho@93	91	99	LX102
Matrin-3	RDSFDDRGPSLNPVLDYDHGSR	Phospho@188|195	186	207	5b1
Matrin-3	RRTEEGPTLSYGR	Phospho@150=74	148	160	H29
Matrin-3	RDSFDDRGPSLNPVLDYDHGSR	Phospho@188|195	186	207	LX102
Matrin-3	RDSFDDRGPSLNPVLDYDHGSR	Phospho@188=55	186	207	LX102
DNA replication licensing factor MCM2	GLLYDSDEEDEERPAR	Phospho@139=72	134	149	H82
DNA replication licensing factor MCM3	LTESINR	Phospho@771=29	768	774	H29
Major facilitator superfamily domain-containing protein 10	LSSLRR	Phospho@271=25	269	274	H82
Antigen KI-67	GINVFRETAK	Phospho@2163	2156	2165	H29
Antigen KI-67	RESVNLGK	Phospho@374	372	379	H82
Antigen KI-67	RKSLVMHTPPVLK	Phospho@538=17;Oxidation@541	536	548	H82
rRNA methyltransferase 3, mitochondrial	RLSSVMTIVK	Oxidation@108;Phospho@105|106	103	112	H82
28S ribosomal protein S9, mitochondrial	RETYTEDFIKK	Phospho@68=7	66	76	H82
DNA mismatch repair protein Msh6	MSRQSTLYSFFPK	Met-loss+Acetyl@1;Phospho@5=7	1	13	5b1
DNA mismatch repair protein Msh6	MSRQSTLYSFFPK	Met-loss+Acetyl@1;Phospho@2|5|6	1	13	5b1
DNA mismatch repair protein Msh6	MSRQSTLYSFFPK	Met-loss+Acetyl@1;Phospho@5=6	1	13	H29

Protein Name	Peptide	Peptide Mod	seq start	seq end	Cell Line
DNA mismatch repair protein Msh6	MSRQSTLYSFFPK	Met-loss+Acetyl@1;Phospho@5|6	1	13	H29
Metastasis-associated protein MTA1	SVSSVLSSLTPAK	Phospho@564=12	555	567	H82
C-1-tetrahydrofolate synthase, cytoplasmic	RFSDIQIR	Phospho@490	488	495	H29
Myb-binding protein 1A	ARLSLVSR	Phospho@1318=35	1315	1322	5b1
Myb-binding protein 1A	ARLSLVIR	Phospho@1303	1300	1307	H82
Nucleolin	VIPTPGKK	Phospho@106	103	110	5b1
Nance-Horan syndrome protein	RKTISGIPR	Phospho@401=16	399	407	H29
Nuclear ubiquitous casein and cyclin-dependent kinase substrate 1	ATVTPSPVKGK	Phospho@181=28	176	186	5b1
Nuclear ubiquitous casein and cyclin-dependent kinase substrate 1	LKATVTPSPVKGK	Phospho@179|181	174	186	5b1
Nuclear ubiquitous casein and cyclin-dependent kinase substrate 1	LKATVTPSPVKGK	Phospho@177=14;Phospho@179|181	174	186	5b1
Nuclear mitotic apparatus protein 1	RTTQIINITMTK	Oxidation@1819;Phospho@1811|1812	1810	1821	H29
Nuclear mitotic apparatus protein 1	RRTTQIINITMTK	Phospho@1811=12;Oxidation@1819	1809	1821	H29
Nuclear mitotic apparatus protein 1	RASMQPIQIAEGTGITTR	Phospho@1969=85;Oxidation@1970	1967	1984	H29
Nuclear mitotic apparatus protein 1	RQSMAFSILNTPK	Phospho@2047=49;Oxidation@2048	2045	2057	LX102
Oral-facial-digital syndrome 1 protein	RQSNLQEVLER	Phospho@899	897	907	H29
Oviduct-specific glycoprotein	EKFIASVISLLR	Phospho@123=20	118	129	H82
Palmdelphin	LSPRETIFGK	Phospho@374=29	369	378	H82
Poly(A) polymerase gamma	QGLAVTDEILQGK	Phospho@347	342	354	H29
Protein polybromo-1	RLSAIFLR	Phospho@681	679	686	LX102
PEST proteolytic signal-containing nuclear protein	TLSVAAAFNEDEDSEPEEMPPEAK	Oxidation@124;Phospho@108|119	106	129	5b1
PEST proteolytic signal-containing nuclear protein	KASAISIR	Phospho@84=29	82	89	5b1

Protein Name	Peptide	Peptide Mod	seq start	seq end	Cell Line
cAMP-specific 3',5'-cyclic phosphodiesterase 4A	RESFLYR	Phospho@140=61	138	144	5b1
cAMP-specific 3',5'-cyclic phosphodiesterase 4A	RESFLYR	Phospho@145=54	143	149	H82
Pyruvate dehydrogenase E1 component subunit alpha, somatic form, mitochondrial	YHGHSMSDPGVSYR	Oxidation@294;Phospho@293|295	289	302	H82
ATP-dependent 6-phosphofructokinase, platelet type	GRSFAGNLNTYKR	Phospho@386=91	384	396	H29
Phosphatase and actin regulator 2	KLSLRPTVAELQAR	Phospho@560=33	558	571	H29
Lysine-specific demethylase PHF2	DLSFLLDKK	Phospho@705	703	711	H29
Pirin	SIGRPELK	Phospho@27	27	34	LX102
Pleckstrin homology domain-containing family G member 3	RRESLSYIPK	Phospho@741=20	738	747	H29
Periphilin-1	RKSFYSSHYSR	Phospho@124=21	122	132	5b1
Periphilin-1	SFYSSHYAR	Phospho@110=34	110	118	H82
Protein phosphatase 1 regulatory subunit 11	RRATLGPTPTTPPQPPDPSQPPPGPMQH	Oxidation@124;Phospho@102|106|108|109	99	126	H29
Protein phosphatase 1 regulatory subunit 12A	STQGVTLTDLQEAEK	Phospho@695|696	695	709	LX102
Serine/threonine-protein phosphatase 2A 56 kDa regulatory subunit delta isoform	RKSELPQDVYTIK	Phospho@573=82	571	583	H29
Peroxiredoxin-2	RLSEDYGVLKTDEGIAYR	Phospho@112=46	110	127	LX102
Peroxiredoxin-5, mitochondrial	RFSMVVQDGIVK	Phospho@182;Oxidation@183	180	191	LX102
cAMP-dependent protein kinase catalytic subunit alpha	KGSEQESVKEFLAK	Phospho@11=32	9	22	5b1
DNA-dependent protein kinase catalytic subunit	RLSFAVPFR	Phospho@893	891	899	H82
Protein PRRC2A	KQSSSEISLAVER	Phospho@456=8	454	466	H29
Protein PRRC2A	RKQSSSEISLAVER	Phospho@456|457|458	453	466	H29
Pumilio homolog 2	RESLSTSSDLYKR	Phospho@587|589	585	597	H29
Glycogen phosphorylase, liver form	RMSLIEEEGGKR	Oxidation@429;Phospho@430	428	439	5b1
Glycogen phosphorylase, liver form	RMSLIEEEGSKR	Oxidation@429;Phospho@430=53	428	439	LX102

Protein Name	Peptide	Peptide Mod	seq start	seq end	Cell Line
Glycogen phosphorylase, muscle form	RMSLVEEGAVKR	Oxidation@429;Phospho@430	428	439	5b1
Glycogen phosphorylase, muscle form	RMSLVEEGAVKR	Oxidation@429;Phospho@430	428	439	H29
Ras-related protein Rab-36	ENEAGSCFIFLVGTKK	Phospho@237=35	224	239	H82
Rab-3A-interacting protein	LRSPSVLEVR	Phospho@165=9	161	170	H29
Ran-specific GTPase-activating protein	FASENDLPEWK	Phospho@60	58	68	5b1
Ran-specific GTPase-activating protein	FASENDLPEWK	Phospho@60	58	68	H82
Ras-associated and pleckstrin homology domains-containing protein 1	NPQNYLLGKK	Phospho@366	362	371	LX102
RNA-binding protein 14	RLSESQLSFR	Phospho@618=20	616	625	5b1
RNA-binding protein 14	RLSESQLSFR	Phospho@618=13	616	625	H82
Replication initiator 1	RFSQGSHLAAHR	Phospho@441=17	439	450	H29
Telomere-associated protein RIF1	RQTFITLEK	Phospho@1215=29	1213	1221	5b1
Telomere-associated protein RIF1	RQTFITLEK	Phospho@1220=30	1218	1226	H29
Telomere-associated protein RIF1	RVSFADPIYQAGLADDIDRR	Phospho@2205=41	2203	2222	H29
Telomere-associated protein RIF1	TLRRSSR	Phospho@1417|1418	1413	1419	H82
60S ribosomal protein L15	RRNTLQLHR	Phospho@197	194	202	H82
60S ribosomal protein L18	APGTPHSHTKPYVR	Phospho@158=28	155	168	H82
60S ribosomal protein L18a	AHSIQIMK	Phospho@123;Oxidation@127	121	128	H29
60S ribosomal protein L28	RASAILR	Phospho@115	113	119	H82
60S ribosomal protein L29	YESLKGVDPK	Phospho@31=64	29	38	5b1
60S ribosomal protein L29	YESLKGVDPK	Phospho@31=61	29	38	LX102
60S ribosomal protein L3	HGSLGFLPR	Phospho@13	11	19	LX102
60S ribosomal protein L34	RLSYNTASNK	Phospho@12|15	10	19	5b1
60S ribosomal protein L34	RRLSYNTASNK	Phospho@12=28	9	19	5b1
60S ribosomal protein L34	RRLSYNTASNK	Phospho@12|13	9	19	H29

Protein Name	Peptide	Peptide Mod	seq start	seq end	Cell Line
60S ribosomal protein L34	RRLSYNTASNK	Phospho@12=28	9	19	H82
60S ribosomal protein L34	RLSYNTASNK	Phospho@12|15	10	19	LX102
60S ribosomal protein L36a	KQSGYGGQTKPIFR	Phospho@46=24	44	57	LX102
60S ribosomal protein L4	RNTILR	Phospho@339	337	342	H82
60S ribosomal protein L5	KASFLR	Phospho@286	284	289	H82
60S ribosomal protein L7	VPAVPETLKK	Phospho@39	33	42	5b1
60S ribosomal protein L7	KVPAGPKTLK	Phospho@28	21	30	5b1
60S ribosomal protein L7	EVPAVPETLKKK	Phospho@17	10	21	H82
40S ribosomal protein S3a	KTSYAQHQQVR	Phospho@153|154	152	162	5b1
40S ribosomal protein S3a	KTSYAQHQQVR	Phospho@153|154	152	162	H29
40S ribosomal protein S3a	KTSYAQHQQVR	Phospho@154=8	152	162	H82
40S ribosomal protein S4, Y isoform 1	LTGVFAPRPSTGPHK	Phospho@32|33	23	37	LX102
40S ribosomal protein S4, Y isoform 2	LTGVFAPRPSTGPHK	Phospho@32|33	23	37	H29
40S ribosomal protein S6	RLSSLRASTSK	Phospho@235=52;Phospho@236=37	233	243	5b1
40S ribosomal protein S6	RLSSLR	Phospho@235=6	233	238	5b1
40S ribosomal protein S6	RLSSLR	Phospho@235=7	233	238	H82
40S ribosomal protein S6	RLSSLR	Phospho@235|236	233	238	H82
40S ribosomal protein S6	RLSSLRASTSK	Phospho@235=50;Phospho@236=39	233	243	LX102
40S ribosomal protein S7	SRTLTAVHDAILEDLVFPSEIVGK	Phospho@119|121|123	119	142	5b1
40S ribosomal protein S7	SRTLTAVHDAILEDLVFPSEIVGK	Phospho@119|121|123	119	142	H29
Ribonucleoside-diphosphate reductase subunit M2	VPLAPITDPQQLQLSPLKGLSLVDKENTPPALSGTR	Phospho@20=19	6	41	LX102
Retrotransposon-like protein 1	VGYVINHLSGLALEWAK	Phospho@246=6	238	254	H29
Protein S100-A13	KDSLSVNEFKELVTQQLPHLLK	Phospho@32|34	30	51	H29
Scaffold attachment factor B2	RLSELR	Phospho@31	29	34	H29
Protein scribble homolog	RVSLVGADDLRK	Phospho@1378	1376	1387	H29

Protein Name	Peptide	Peptide Mod	seq start	seq end	Cell Line
Protein scribble homolog	MKSLEQDALR	Oxidation@1506;Phospho@1508	1506	1515	H29
Protein transport protein Sec16A	RSSLSSHSHQSQIYR	Phospho@1190|1191|1193|1194	1189	1203	H29
Protein transport protein Sec16A	RSSLSSHSHQSQIYR	Phospho@1190|1191|1193	1189	1203	H29
Vesicle-trafficking protein SEC22b	NLGSINTELQDVQR	Phospho@137=19	134	147	H29
Septin-2	IYHLPDAESDEDEDFKEQTR	Phospho@218=73	210	229	LX102
Plasminogen activator inhibitor 1 RNA-binding protein	SSFSHYSGLKHEDKR	Phospho@203=9	202	216	5b1
Plasminogen activator inhibitor 1 RNA-binding protein	HSGSDRSSFSHYSGLK	Phospho@199|202|203	196	211	5b1
Plasminogen activator inhibitor 1 RNA-binding protein	HSGSDRSSFSHYSGLKHEDK	Phospho@197|199|202|203|205	196	215	5b1
Plasminogen activator inhibitor 1 RNA-binding protein	HSGSDRSSFSHYSGLK	Phospho@197|199|202|203	196	211	5b1
Plasminogen activator inhibitor 1 RNA-binding protein	SSFSHYSGLKHEDKR	Phospho@202|203	202	216	H29
Plasminogen activator inhibitor 1 RNA-binding protein	HSGSDRSSFSHYSGLKHEDK	Phospho@197|199|202|203|205	196	215	H29
Plasminogen activator inhibitor 1 RNA-binding protein	SSFSHYSGLK	Phospho@203=7	202	211	H82
Plasminogen activator inhibitor 1 RNA-binding protein	HSGSDRSSFSHYSGLK	Phospho@197|199|202|203	196	211	H82
Plasminogen activator inhibitor 1 RNA-binding protein	HSGSDRSSFSHYSGLK	Phospho@199|202|203	196	211	H82
Alpha-1-antitrypsin 1-4	RRSDAQIHIPR	Phospho@300	298	308	5b1
Protein SET	RQSAILPQPK	Phospho@7	5	14	5b1
Shootin-1	RQSHLLLQSSLPDQQLLK	Phospho@249=45	247	264	5b1
Shootin-1	RQSHLLLQSSIPDQQLLK	Phospho@249=59	247	264	LX102
Serine/threonine-protein kinase SIK3	RHTVGVADPR	Phospho@411	409	418	H82
Zinc transporter 4	LKSLLR	Phospho@12	10	15	5b1
SRA stem-loop-interacting RNA-binding protein, mitochondrial	SINQPVAFVR	Phospho@15	15	24	H29
SWI/SNF-related matrix-associated actin-dependent regulator of chromatin subfamily A containing DEAD/H box 1	KASISYFK	Phospho@79=22	77	84	H29

Protein Name	Peptide	Peptide Mod	seq start	seq end	Cell Line
SWI/SNF-related matrix-associated actin-dependent regulator of chromatin subfamily E member 1	LISEILSESVVPDVR	Phospho@204=48	202	216	5b1
SWI/SNF-related matrix-associated actin-dependent regulator of chromatin subfamily E member 1	LISEILSESVVPDVR	Phospho@204=57	202	216	H29
Structural maintenance of chromosomes protein 2	SLEDALAEAQRVNTKSQSAFDLK	Phospho@311|313|315	298	320	H29
Structural maintenance of chromosomes protein 4	IHEDTKEINEKSNILSNEMK	Phospho@355|359	344	363	H29
Msx2-interacting protein	ELQEAAAVPTTPR	Phospho@1946|1947	1937	1949	H82
Spectrin beta chain, non-erythrocytic 1	RFSLFGK	Phospho@2357	2355	2361	5b1
Spectrin beta chain, non-erythrocytic 1	RFSLFGK	Phospho@2358	2356	2362	LX102
Signal recognition particle 14 kDa protein	KISTVVSSK	Phospho@68=11	66	74	5b1
Signal recognition particle 14 kDa protein	KISTVVSSK	Phospho@68=9	66	74	LX102
Serine/arginine repetitive matrix protein 2	ALPQTPRPR	Phospho@1492	1488	1496	H82
Serrate RNA effector molecule homolog	MGDSDDEYDRR	Met-loss+Acetyl@1;Phospho@4=49	1	11	H82
Serine/arginine-rich splicing factor 7	SISLRR	Phospho@167=25	165	170	H82
Lupus La protein	TKFASDDEHDEHDENGATGPVKR	Phospho@366=23	362	384	LX102
Protein phosphatase Slingshot homolog 3	RQSFAVLR	Phospho@37	35	42	H29
Hsc70-interacting protein	RASVFVK	Phospho@155	153	159	5b1
Serine/threonine-protein kinase 11-interacting protein	RASISEPSDTDPEPR	Phospho@398|400	396	410	H82
Stathmin	SHEAEVLK	Phospho@63	63	70	5b1
Stathmin	RASGQAFELILSPR	Phospho@16=99	14	27	H29
Stathmin	SHEAEVLK	Phospho@63	63	70	H82
Syntaxin-16	RLTDAFLLLR	Phospho@7	5	14	LX102
Transforming acidic coiled-coil-containing protein 3	KQSLYLK	Phospho@558=44	556	562	H82
Tubulin-folding cofactor B	RGTVMYVGLTDFKPGYWIGVR	Phospho@178=34;Oxidation@180	176	196	H29
Transcription elongation factor B polypeptide 3	KLSELERPHK	Phospho@163	161	170	H29
Triosephosphate isomerase	KQSLGELIGTLNAAK	Phospho@58=72	56	70	LX102

Protein Name	Peptide	Peptide Mod	seq start	seq end	Cell Line
Nucleoprotein TPR	QTPQAPQSPR	Phospho@2141=60	2134	2143	5b1
Tubulin alpha-1A chain	LSVDYGKK	Phospho@158=53	157	164	5b1
Tubulin alpha-1A chain	LSVDYGKK	Phospho@158=52	157	164	H29
Tubulin alpha-1B chain	LSVDYGKK	Phospho@158=52	157	164	H82
Tubulin beta chain	ALTVPELTQQVFDAK	Phospho@285=36	283	297	H29
Tubulin beta chain	LHFFMPGFAPLTSRGSQQYR	Oxidation@267;Phospho@274|275|278	263	282	LX102
Tubulin beta-5 chain	ALTVPELTQQVFDAK	Phospho@285=48	283	297	5b1
Tubulin beta-5 chain	LHFFMPGFAPLTSRGSQQYR	Oxidation@267;Phospho@274|275|278	263	282	5b1
Ubiquitin-conjugating enzyme E2 T	KASQLVGIEK	Phospho@184	182	191	H82
E3 ubiquitin-protein ligase UBR5	RISQSQPVR	Phospho@1549=30	1547	1555	H82
Cytochrome b-c1 complex subunit 1, mitochondrial	RLSRTDLTDYLNR	Phospho@212=15	210	222	5b1
Putative cytochrome b-c1 complex subunit Rieske-like protein 1	RPFLSRESLSGQAVR	Phospho@63=18	56	70	H29
Vimentin	LRSSVPGVR	Phospho@73=11	70	78	5b1
Vimentin	LRSSVPGVR	Phospho@73=14	70	78	H29
Vimentin	LRSSVPGVR	Phospho@72|73	70	78	H82
WW domain-binding protein 11	AVSILPLLGHGVPR	Phospho@181	179	192	H29
WD repeat- and FYVE domain-containing protein 4	LASQAIEPDVLRQFLGLGIPSSLSATTK	Phospho@914=48;Phospho@932|933|935|937|938	912	939	H29
Y-box-binding protein 3	SRPLNAVSQDGK	Phospho@328=65	328	339	5b1
14-3-3 protein zeta/delta	EYREKIETELR	Phospho@88=26	81	91	H29
Zinc finger CCCH domain-containing protein 11A	KVEAPETNIDKTPK	Phospho@321=60	310	323	H82
Zinc finger CCCH-type antiviral protein 1	RKTVFSPTLPAAR	Phospho@375=14	373	385	H29
Zinc finger protein ZFPM2	SPEFPSVSEK	Phospho@581=25	581	590	LX102

Protein Name	Peptide	Peptide Mod	seq start	seq end	Cell Line
Zinc finger RNA-binding protein	DPFDTLATMTDQQR	Oxidation@1002;Phospho@1001|1003	994	1007	H29
Zinc finger MYM-type protein 4	KKSIVAVEPR	Phospho@1181	1179	1188	H82
Zinc finger protein 24	SSILVQHQR	Phospho@291|292	291	299	H29
Zinc finger protein 24	SSILVQHQR	Phospho@292=8	291	299	LX102

Publishing Agreement

It is the policy of the University to encourage the distribution of all theses, dissertations, and manuscripts. Copies of all UCSF theses, dissertations, and manuscripts will be routed to the library via the Graduate Division. The library will make all theses, dissertations, and manuscripts accessible to the public and will preserve these to the best of their abilities, in perpetuity.

Please sign the following statement:

I hereby grant permission to the Graduate Division of the University of California, San Francisco to release copies of my thesis, dissertation, or manuscript to the Campus Library to provide access and preservation, in whole or in part, in perpetuity.

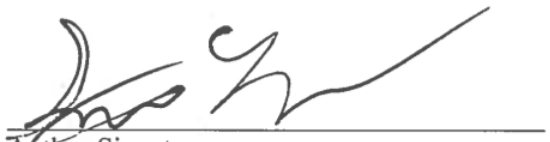

Author Signature

5/28/19

Date